

Validering av materialmodell for polypropylen (HDPE)

Tonje Hegni

Master i produktutvikling og produksjon

Innlevert: Juni 2012

Hovedveileder: Arild Holm Clausen, KT

Medveileder: Marius Andersen, KT

Norges teknisk-naturvitenskapelige universitet
Institutt for konstruksjonsteknikk



MASTER THESIS 2012

SUBJECT AREA: POLYMER ENGINEERING	DATE: 11 JUNE 2012	NO. OF PAGES: 72 + 45
--------------------------------------	-----------------------	--------------------------

TITLE:

Validation of material model for polyethylene (HDPE)

Validering av materialmodell for polyetylen (HDPE)

BY:

Tonje Hegni



SUMMARY:

This thesis is concerned with validation of a hyperelastic – viscoplastic material model, which previously has been implemented in the finite element code LS – Dyna. The material considered in this thesis is a high – density polyethylene (HDPE) produced by a German company SIMONA. The material parameters of the constitutive model are found from experimental testing and calibration.

The model is validated by comparing results from two types of well – defined experimental tests with numerical predictions. Firstly, tension tests on a plate with a hole have been performed. The reason for using a plate with a hole is that the geometry is more complex due to the hole which results in a more complex stress and strain state. It also has well – defined boundary conditions. There was also performed experimental testing of an impact problem. A real component used in the industry is stretched, compressed and subjected to different velocities, and an impact problem provides a realistic representation of real life circumstances.

The experimental and the simulated tests are evaluated and compared. The model captures the main features observed in the tests.

RESPONSIBLE TEACHER: Professor Arild H. Clausen

SUPERVISOR(S): Arild H. Haugen, Marius Andersen and Anne Serine Ognedal

CARRIED OUT AT: SIMLab, NTNU

MASTEROPPGAVE 2012

Tonje Hegni

Validation of material model for polyethylene (HDPE)

(Validering av materialmodell for polyetylen (HDPE))

As a part of the development of the finite element method, significant effort has been devoted to propose new material models which are able to represent the material behaviour at different conditions. Relevant parameters involve strain level, strain rate, temperature, and the material at hand may also exhibit anisotropy, viscoelasticity etc. Today, material models for metals are in general more accurate than models for e.g. polymers. This is a general tendency for all non-linear finite element programs, including Abaqus and LS-DYNA. SIMLab is involved in the development of improved models for thermoplastics. A model applicable for ductile polymers was ready in 2010, and the research work continues with other classes of models.

All new models need to be validated against experimental benchmark tests for different types of polymers. Validation involves also calibration, requiring material tests on the material at hand. This master thesis is concerned with a HDPE material produced by the German company SIMONA. The selected benchmark tests are tension of a plate with a hole and impact tests on small plates. Subsequently, the test results are to be compared with numerical predictions applying the material model for ductile thermoplastics.

Some keywords for activities related to this master thesis project are:

- Literature: Polymers in general, relevant test results, material models.
- Experimental tests: Material and component tests. Presentation of test results.
- Calibration: Identify the coefficients of the material model.
- Numerical modelling: Simulation of experimental tests. Evaluation of the model.

The candidate may agree with the supervisors to pay particular attention to specific parts of the investigation, or include other aspects than those already mentioned.

The thesis is to be organized as a research report, recognising the guidelines provided by Department of Structural Engineering.

Supervisors: Arild H. Clausen, Marius Andersen and Anne Serine Ognedal

The report is to be handed in at Department of Structural Engineering not later than 11 June 2012.

NTNU, 18 January 2012

Arild H. Clausen

faglærer

Acknowledgement

I wish to express my gratitude to supervisor Arild H. Clausen for outstanding guidance and support throughout the work. I would also like to thank co – supervisors PhD student Marius E. H. Andersen for facilitation and guidance. Thanks to Anne – Serine Ognedal for help with the software 7D and Matlab codes.

The experimental work was performed in cooperation with students Torgrim Østen, Kristin Sælen and Kjetil Vange. I would like to give them credits for being great supporters and sharing pictures and Matlab codes during the work. They have contributed both academically and socially throughout the work.

I would also like to thank Trond Auestad for support during testing in the laboratory at NTNU.

Sammendrag

Denne rapporten tar for seg validering av en hyperelastisk – viscoplastisk material modell som tidligere har blitt implementert i elementmetode koden LS – Dyna. Materialet som er evaluert er polyetylen (HDPE) som er levert av det tyske firmaet SIMONA. Material parameterne som er satt inn i den konstitutive material modellen er funnet fra eksperimentell testing og kalibrering.

Modellen er validert ved å sammenligne resultater av to veldefinerte eksperimentelle tester ved numeriske forutsigelser. Det har blitt utført tester på plate med hull. Platene har en mer kompleks geometri grunnet hullet i platen, og vil derfor gi mer komplekse spenning og tøyings tilstander. I tillegg har platene veldefinerte randbetingelser. Disse har en mer komplisert sammensetning av trykk og strekk og vil derfor være mer realistiske, da en virkelig komponent brukt i industrien vil bli utsatt for både trykk og strekk samt påført last av ulike hastigheter.

De eksperimentelle og simulerte testene er sammenlignet og evaluert i valideringskapittelet. Modellen fanger opp de viktigste egenskapene observert i testene.

Contents

Acknowledgement.....	I
Sammendrag	III
1. Introduction.....	1
2. Theory.....	2
2.1 High density polyethylene (HDPE).....	2
2.2 Mechanical behavior	2
2.3 Introduction to the constitutive model	3
2.4 Intermolecular resistance, Part A	3
2.5 Intramolecular resistance, Part B	5
3. Material testing	7
3.1 Introduction.....	7
3.2 Experimental program for tensile testing	7
3.3 Applying an optical technique to obtain stress and strain.....	8
3.4 Results obtained from the tensile tests.....	9
3.4.1 Comments on force – displacement curves of tensile tests of thickness 5 mm, T1 – T8.....	9
3.4.2 Comments on force – displacement curves of tensile tests of thickness 10 mm, T9 – T13.....	11
3.4.3 Comments on the true stress – strain curve, and determination of yield stress	11
3.4.4 Longitudinal versus transverse strain	14
3.5 Experimental program of compression tests, C1 – C5	15
3.6 Test results of compression tests	16
3.6.1 Comments on force – displacement curve of the compressions tests.....	16
3.6.2 Specimens with different extrusion directions.....	17
3.6.3 Comments on true stress – true strain curves of compression test C1 – C5.....	18
3.6.4 Poisson’s ratio from compression tests	19
3.7 Discussion	20
4. Calibration	21
4.1 Introduction	21
4.2 Calibration of parameters.....	21
4.2.2 Determination of parameters based on the stress – strain curve.....	22

4.2.3 Calibration of Part B	23
5. Validation	26
5.1 LS-Dyna simulations of the tensile tests.....	26
5.1.1 Modeling the tensile test in LS - Dyna	26
The Bridgman factor	28
5.1.2 Results from the simulation of tensile tests	29
5.1.3 Simulations of different elasticity modulus's	32
5.2 Simulation of the compression test.....	33
5.2.2 Results obtained from the simulation of the compression test.....	34
5.3 Plates with holes of diameter 30 mm and 20 mm.	35
5.3.1 Introduction	35
5.3.2 Procedure.....	35
5.3.3 Applying the DIC method.....	36
5.3.4 LS-Dyna simulations of the plates.....	37
5.4 Results obtained from the simulations of plate with a hole	38
5.4.2 Results obtained from the plate with a hole of test 02 through test 04	42
Force – displacement curves of all four tests	49
5.4.4 Young's modulus.....	49
5.5 Drop Tower testing	52
5.5.1 Introduction	52
5.5.2 Experimental program of drop tower testing.....	52
5.5.3 Simulation of drop tower.....	53
5.5.4 Results obtained from the drop tower tests	54
5.5.5 Stresses at the tip of the plate	58
5.6 Discussion and source of error	59
6. Conclusion	61
7. Reference	62
Appendix A	63
Appendix B	101

1. Introduction

This thesis is written in cooperation with Structural Impact Laboratory (SIMLab) which is located at the Department for Structural Engineering at NTNU. One of SIMLab's research areas is dedicated to polymers. They are cooperating with several industries to improve the existing models of polymers. The most important features that the material model for polymers should capture is strain rate, temperature change, pressure dependency and change in volume.

Polymers are becoming more of interest in the industries as there is a higher focus on more slender and lighter structures. This has led to a need for understanding how polymers work when exposed to different kinds of loading. The ductility and the low weight make thermoplastics ideal for energy absorption. This makes polymers a desirable material in car industries and as protection in impact incidents in the pipeline industry.

SIMLab has been developing a constitutive material model for thermoplastics which is built up of two parts; Part A is the hyperelastic – plastic model and Part B the entropic hyperelastic model. The model is built up of thirteen parameters which can be determined from uniaxial tensile and compression tests. The material that is considered is high density polyethylene (HDPE).

This thesis first presents some theory about the material and the material model that is implemented in LS – Dyna. Then, the experimental tests are described by explaining the procedure and illustrating the results obtained. The calibration method is presented with necessary equations and explanations. The final section contains the validation of plate with a hole and the impact tests performed in the drop tower with test results and discussion of source of error. The thesis is rounded off with a conclusion and a proposition for further work.

2. Theory

2.1 High density polyethylene (HDPE)

High density polyethylene is the polymerization of ethylene, and is built up of long molecule chains. The material is delivered by a German company SIMONA under the name PE-HWU, and was delivered as extruded sheets of 2000 x 1000 mm.

HDPE has a high chemical and corrosion resistance, good sliding properties, high UV-protection and has very good electrical isolation features. This means that the material is stabilized for outdoor use. The manufacturer SIMONA has not reported any use of fiber or particle reinforcement in the material. The mechanical properties of HDPE according to the manufacturer are given in Table 2.1 [1].

Table 2.1: Material properties of HDPE according to the manufacturer SIMONA

Density	0.950 g/cm ³
Yield stress	22.0 MPa
Elongation at yield stress	9 %
Elongation at tear	300 %
Tensile, E - modulus	800 MPa

This material is used in the building industry, machines, storage technology like boxes and pallets, as well as in the vehicle sector and where physiological safety is required. HDPE is tough at room temperatures, but not in elevated temperatures at approximately 100°C. The reason is that HDPE has a glass transition temperature T_g of approximately 120°C [1].

2.2 Mechanical behavior

The HDPE monomer has two carbon atoms and four hydrogen atoms linked together by covalent bonds. The monomers are linked together forming a polymer chain with a carbon backbone as shown in Figure 2.1. The chains are linked together by weak intermolecular bonds called van der Waals bonds. This gives the material a more flexible structure facilitating large plastic deformations caused by relative sliding between the chains. The weak van der Waals bonds may be overcome by thermal activation even at room temperature. This is because polymers are in the high temperature regime even at room temperature. The deformation is therefore time-dependent, and it is not always easy to distinguish between elastic and plastic deformations. These weak intermolecular bonds are what affect the elastic properties of the material. The bonds that link the monomers together are a lot stronger, for these bindings to break there has to be plastic deformation present [2-3].

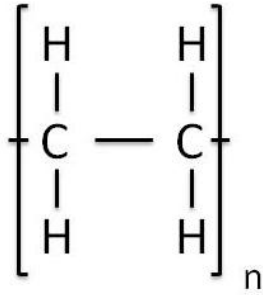


Figure 2.1: Molecule structure of HDPE

2.3 Introduction to the constitutive model

The material model has two parts. Part A is a hyperelastic-viscoplastic model representing intermolecular resistance. There are strong bonds in the longitudinal direction and weak bonds in the transversal direction. Part B is an entropic hyperelastic model representing re-orientation of molecular chains, which means that the molecules optimize the amount of entropy. This is intramolecular resistance. Both parts are kinematically described by the same deformation gradient, and the two parts will therefore have the same change of volume, expressed with the Jacobian determinant, $J = \det \mathbf{F} = J_A = J_B$. By summing the contribution from both Part A and Part B the Cauchy stress tensor, $\sigma = \sigma_A + \sigma_B$, is obtained. Figure 2.2 illustrates the material behavior [4-5].

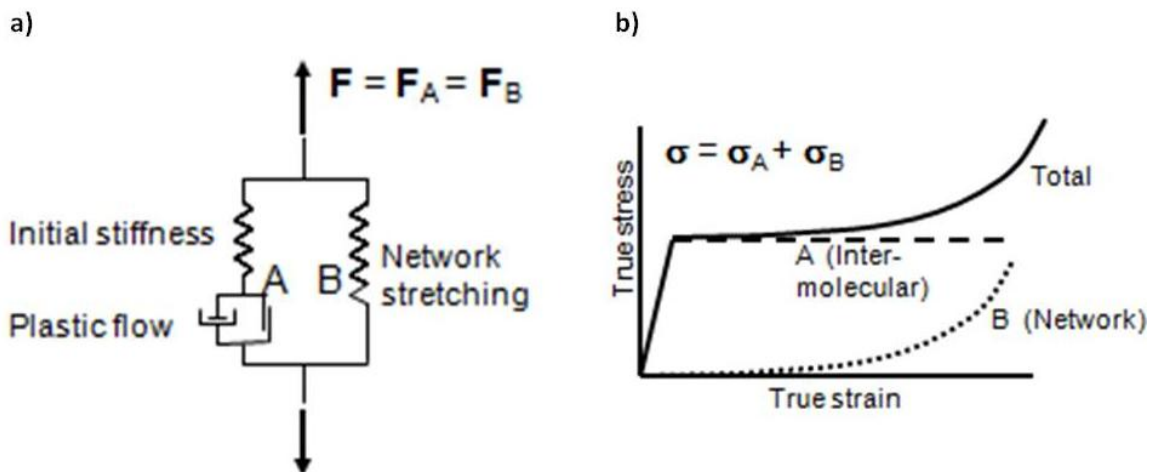


Figure 2.2: Hyperelastic-viscoplastic model with intermolecular (A) and network contributions (B), [6].

2.4 Intermolecular resistance, Part A

The Jacobian, which represents the volume change of Part A is decomposed as $J_A = J_A^e \cdot J_A^p$. Similarly, the deformation gradient F_A is decomposed into elastic and plastic parts, $F_A = F_A^e \cdot F_A^p$, where the plastic part defines an intermediate configuration which is invariant to rigid

body rotations of the current configuration. For allowing large elastic deformations a Neo – Hookean material is chosen for the spring of Part A. The Kirchhoff stress tensor, $\boldsymbol{\tau}_A = J_A^e \boldsymbol{\sigma}_A$, is the elastic stress tensor of Part A, and is written

$$\boldsymbol{\tau}_A = \lambda_0 \ln J_A^e \mathbf{I} + \mu_0 (\mathbf{B}_A^e - \mathbf{I}) \quad (2.1)$$

where \mathbf{B}_A^e is the elastic Cauchy – Green deformation tensor, and \mathbf{I} is the second order unit tensor. The coefficients λ_0 and μ_0 are the Lamé constants from linearized theory, and may be expressed as functions of Young’s modulus, E_0 , and Poisson’s ratio, ν_0 , [4].

For Part A to be isotropic-elastic the Mandel stress tensor $\bar{\boldsymbol{\Sigma}}_A$ is implied to be symmetric. This stress tensor applies to the viscoplastic contribution of Part A, which is represented in Figure 2.2 with the dashpot and friction element. The Mandel and the Kirchhoff stress tensors are related through $\boldsymbol{\tau}_A = (\mathbf{F}_A^e)^{-T} \bar{\boldsymbol{\Sigma}}_A (\mathbf{F}_A^e)^T$ and $\bar{\boldsymbol{\Sigma}}_A = (\mathbf{F}_A^e)^T \boldsymbol{\tau}_A (\mathbf{F}_A^e)^{-T}$ [4].

The pressure – sensitive behavior that is observed in polymeric materials is accounted for by the equivalent stress, $\bar{\sigma}_A$, and is defined as specified by Raghava,

$$\bar{\sigma}_A = \frac{(\alpha-1)I_{1A} + \sqrt{(\alpha-1)^2 I_{1A}^2 + 12\alpha J_{2A}}}{2\alpha} \quad (2.2)$$

Invariants of the Mandel stress tensor is represented in the Raghava equation as $I_{1A} = \text{tr } \bar{\boldsymbol{\Sigma}}_A$ and $J_{2A} = \frac{1}{2} \bar{\boldsymbol{\Sigma}}_A^{dev} : \bar{\boldsymbol{\Sigma}}_A^{dev}$, and the material parameter $\alpha = \sigma_c / \sigma_T \geq 1$ represents the pressure sensitivity, σ_c is the compressive yield stress. When $\alpha = 1$, the equivalent stress $\bar{\sigma}_A$ is equal to the von Mises equivalent stress, $\sigma_T = \sqrt{3J_2}$ [4].

The yield criterion is expressed as

$$f_A = \bar{\sigma}_A - \sigma_T - R = 0 \quad (2.3)$$

where σ_T is the yield stress in uniaxial tension and R is an isotropic variable defining hardening or softening of the material. The R is an expression for the accumulated plastic strain and is written as

$$R(\bar{\boldsymbol{\varepsilon}}_A^p) = (\sigma_s - \sigma_T)[1 - \exp(-H\bar{\boldsymbol{\varepsilon}}_A^p)] \quad (2.4)$$

σ_s represents the saturated stress level of Part A. By selecting $\sigma_s > \sigma_T$ hardening is obtained, and when $\sigma_s < \sigma_T$ softening is obtained, i. e. when $R(\bar{\epsilon}_A^p)$ is negative [4-5].

The flow rule is taken as non-associative to avoid potential unrealistic volumetric strains utilizing a plastic potential function similar to Raghava, the equation reads

$$g_A = \frac{(\beta-1)I_{1A} + \sqrt{(\beta-1)^2 I_{1A}^2 + 12\beta J_{2A}}}{2\beta} \geq 0 \quad (2.5)$$

where the volumetric plastic strain is controlled by the material parameter β , and isochoric plastic strain is obtained when $\beta = 1$. By differentiating the plastic potential function, g_A , with respect to the total stress invariant, I_{1A} , and the deviatoric stress invariant, J_{2A} , the functions f_1 and f_2 are obtained. They are written as

$$f_1 = \frac{\partial g_A}{\partial I_{1A}} = \frac{\beta-1}{2\beta} + \frac{(\beta-1)^2 I_{1A}}{2\beta \sqrt{(\beta-1)^2 I_{1A}^2 + 12\beta J_{2A}}} \quad (2.6)$$

$$f_2 = \frac{\partial g_A}{\partial J_{2A}} = \frac{3}{\sqrt{(\beta-1)^2 I_{1A}^2 + 12\beta J_{2A}}} \quad (2.7)$$

The gradient of the plastic potential is obtained by differentiating the plastic potential function with respect to Mandel stress tensor, given as

$$\frac{\partial g_A}{\partial \bar{\Sigma}_A} = f_1 \frac{\partial I_{1A}}{\partial \bar{\Sigma}_A} + f_2 \frac{\partial J_{2A}}{\partial \bar{\Sigma}_A} = f_1 \mathbf{I} + f_2 \bar{\Sigma}_A^{dev} \quad (2.8)$$

The plastic velocity can then be written as

$$\bar{L}_A^p = \dot{\bar{\epsilon}}_A^p \frac{\partial g_A}{\partial \bar{\Sigma}_A} \quad (2.9)$$

The $\dot{\bar{\epsilon}}_A^p$ is the viscoplastic multiplier defined as

$$\dot{\bar{\epsilon}}_A^p = \begin{cases} 0 & \text{if } f_A \leq 0 \\ \dot{\epsilon}_{0A} \left\{ \exp \left[\frac{1}{C} \left(\frac{\bar{\sigma}_A}{\sigma_T + R} - 1 \right) \right] - 1 \right\} & \text{if } f_A > 0 \end{cases} \quad (2.10)$$

where C and $\dot{\epsilon}_{0A}$ are constants [4-5].

2.5 Intramolecular resistance, Part B

In Part B the theory is built on the fact that the stretch resistance of the polymer network is of a hyper – elastic nature [4].

The Cauchy stress, σ_B , is given as

$$\sigma_B = \frac{1}{J} \frac{C_R \bar{\lambda}_L}{3 \bar{\lambda}} \mathcal{L}^{-1} \left(\frac{\bar{\lambda}}{\bar{\lambda}_L} \right) (\mathbf{B}_B^* - \bar{\lambda}^2 \mathbf{I}) \quad (2.11)$$

Where $\mathcal{L}^{-1}(x)$ is the inverse function of the Langevin function defined $\mathcal{L}(x) = \coth x - 1/x$. $\bar{\lambda}$ is the distortional effective stretch $\bar{\lambda} = \sqrt{\frac{1}{3} \text{tr}(\mathbf{B}_B^*)}$, where the distortional left Cauchy-Green deformation tensor is $\mathbf{B}_B^* = \mathbf{F}_B^* \cdot (\mathbf{F}_B^*)^\top$, and $\mathbf{F}_B^* = J_B^{-1/3} \cdot \mathbf{F}_B$ denotes the distortional part of \mathbf{F}_B . The two main parameters for the model of intramolecular resistance are the initial elastic modulus, C_R , and the locking stretch, $\bar{\lambda}_L$. When all polymer chains are directed in the stretching direction, the stretching is equal to the locking stretch. In addition the stretching is done on the chains themselves. When $\bar{\lambda}_L$ approaches $\bar{\lambda}$ the stresses proceed towards infinity [4, 6].

3. Material testing

3.1 Introduction

The quasi – static material tests were performed under displacement control in a servo-hydraulic Dartec machine. The capacity of the load cell was 20 kN. The HDPE material was delivered by SIMONA as extruded sheets of size 2000 x 1000 mm, and with two different thicknesses, 5 mm and 10 mm. All specimens for tensile testing and compression testing were machined in the laboratory at NTNU. The layout of the extrusion direction of the specimen is illustrated in Figure 3.1.

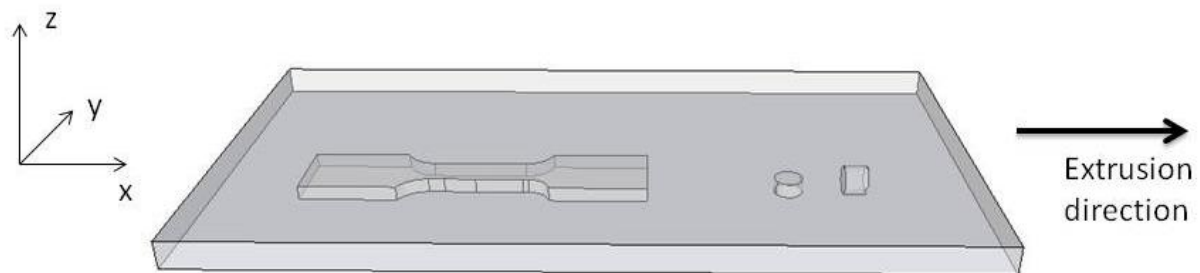


Figure 3.1: Layout of the specimen extrusion direction

3.2 Experimental program for tensile testing

The tensile specimens were made in the xy – plane of the extruded sheet. Altogether, 13 tensile tests were performed. The first eight tests had a thickness of 5 mm, Figure 3.2 a) illustrates the exact geometry of the specimen. A specimen of thickness 10 mm was applied in the last five tensile tests, the exact geometry is illustrated in Figure 3.2 b).

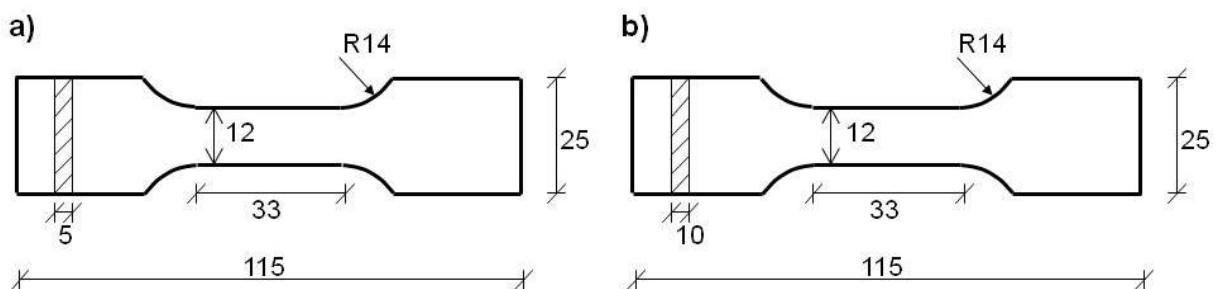


Figure 3.2: Nominal Geometry of tensile specimen; Specimen a) was used in test 1 - 8, specimen b) was applied in test 9 – 13 [7].

The main purpose of performing tensile tests was to determine true strain and true stress curves at different strain rates. Only two identical tests were performed at each strain rate to determine contingencies within the tests. If the force – displacement curves at each strain rate had a significant abnormal variation a third test was performed. Each specimen where placed into the servo - hydraulic Dartec machine by a wedge-mechanism in mechanical grips. All specimens had a gauge length of 33 mm. Each test was monitored with a Canon camera

placed close to the specimen, but in range to get the full displacement length in the xy – plane. The amount of pictures taken during the test was dependent on the strain rate subjected to each specimen. This was to ensure at least 100 photos of each test performed. There was only one camera taking photos from only one direction, this means that the displacement over the thickness was not measured during the test. However, each specimen was measured using a digital sliding caliper before and right after the test, this was to see the change in thickness in both x and z direction, calculating the ratio of these two values shows whether the material is isotropic or anisotropic. An overview of all tensile tests can be seen in Table 3.1 below.

Table 3.1: Overview of all tensile tests, T denotes tension specimen.

Test #	Strain rate [s ⁻¹]	Thickness, t ₀ [mm]	Width, w ₀ [mm]	Max load [N]	Yield stress [MPa]
T1	10 ⁻³	4.91	12.00	1218	22.7
T2	10 ⁻³	4.90	12.01	1218	22.9
T3	10 ⁻²	4.91	11.94	1475	27.8
T4	10 ⁻²	4.90	11.96	1425	26.6
T5	10 ⁻²	4.90	11.96	1409	26.6
T6	10 ⁻¹	4.89	11.95	1619	30.2
T7	10 ⁻¹	4.91	11.95	1621	29.9
T8	10 ⁻¹	4.90	11.95	1677	30.9
T9	10 ^{-2.5}	9.76	11.97	2750	26.2
T10	10 ^{-2.5}	9.76	11.95	2767	26.5
T11	10 ⁻²	9.76	11.96	2985	28.0
T12	10 ⁻¹	9.76	11.96	3307	30.5
T13	10 ⁻³	9.76	11.96	2552	24.2

3.3 Applying an optical technique to obtain stress and strain

Thermoplastics may experience volume change during plastic deformation, therefore the well known formula for true stress, $\sigma = S(1+e)$, relating nominal and true stress values cannot be used. This equation assumes that the material is incompressible, i.e. $A \cdot L = A_0 \cdot L_0$, which necessarily does not apply to plastics as HDPE. However, it is reasonable to assume that HDPE is an incompressible material, but due to the localization of stresses implying a non – homogenous strain field in the sample, a measurement of the full deformation field is needed. The formula for true strain, $\epsilon = \ln(1+e)$, on the other hand is applicable for HDPE [8].

Another aspect of thermoplastics is that necking occurs rather early in tension testing, this result in a non-homogeneous deformation field. A good way to avoid these problems is to measure the strains by using an optical technique [8].

Each specimen was first sprayed with white paint, and then a quick spray with black painting on top, see Figure 3.3. This made each specimen contain a black and white spotted appearance that would be visible on the images. The pattern deforms with the specimen,

and the deformation is captured by a camera with high resolution during the test. This optical technique for measuring displacement is called digital image correlation (DIC). A program called 7D processed the pictures by applying a mesh to the specimen, and calculating the displacements as it recognizes the positions of the mesh nodes when minimizing a DIC. Each picture was compared with the first one. From the displacements of each node the in-plane Green-Lagrange strain tensor, E , was determined [8].

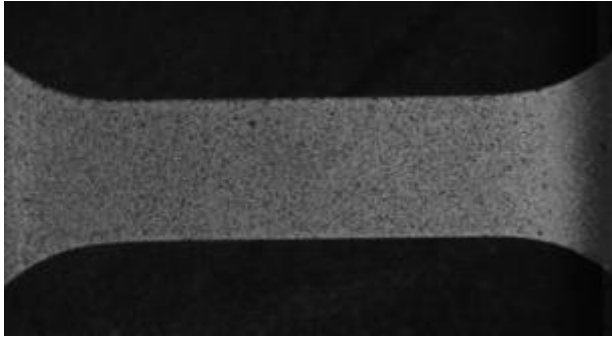


Figure 3.3: Black and white pattern of the tensile test.

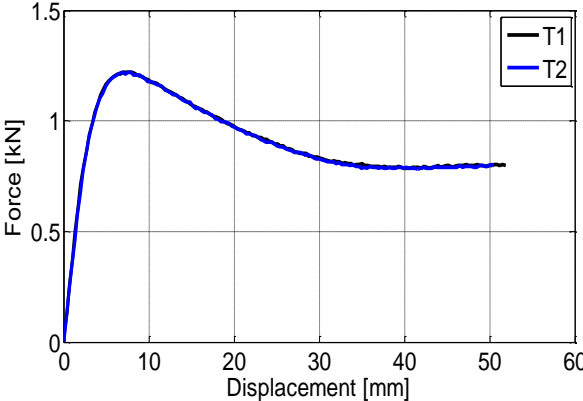
The longitudinal strains and the transverse strains were obtained from the software 7D through a Matlab script. By plotting an image of the specimen in Matlab it was easy to see where the necking had initiated and the area where the highest strains were. A Matlab script was written to find the exact section with the largest strains. These were then used to calculate the cross section area of the specimen in each picture by using the formula $A = A_0 e^{2\varepsilon_w}$, where ε_w is the transversal strains, and then calculating the true stress, $\sigma = F/A$. The transverse strains are assumed to be the same both in the thickness direction, z , and in the width direction, y . This has not been tested in this thesis, but in a previous master thesis [6].

3.4 Results obtained from the tensile tests

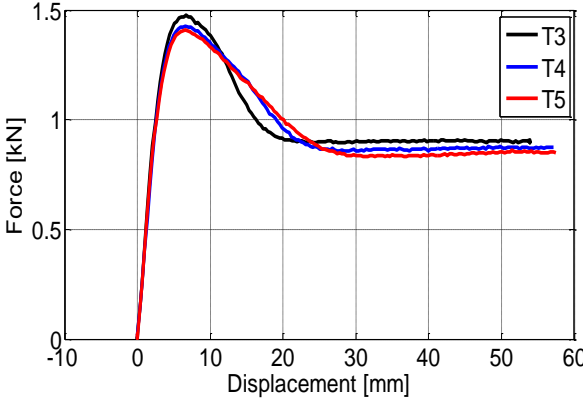
3.4.1 Comments on force – displacement curves of tensile tests of thickness 5 mm, T1 – T8

Figure 3.4 shows the force – displacement curves from all tensile tests with thickness 5 mm. By comparing the two first tests with strain rate 10^{-3} s^{-1} it can be seen that they are close to identical, thus a third test was not needed in this case. The strain rate is increased to 10^{-2} s^{-1} and it is seen that the force peak is elevated with approximately 200 N. Tensile test T3 and T4 turned out to have some variations; the two tests have different maximum force, and the falling part of the force – displacement curve is not in conformity like in test T1 and T2. A third test, T5, was necessary to reveal which one of them gave an abnormal force – displacement curve. By comparing all three of these curves it came clear that test T3 was the abnormal curve, it had a higher max force and the yield stress differs with 1 MPa from both test T4 and T5, this can be seen in Figure 3.4 (b). The strain rate was increased to 10^{-1} s^{-1} , this is quite fast, and it is clear that it affects the material behavior. The force peak increases with yet another 200 N, and also in this case a third test seemed reasonable. By comparing

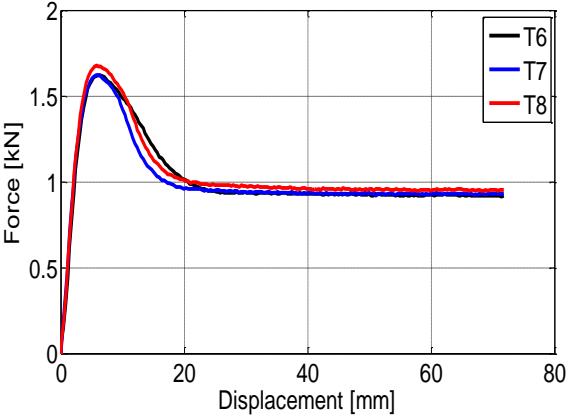
test T6 and T7 it is seen that T6 has a steeper declining than T7, and that the maximum force differ some. However, it appears that test T8 came in between test T6 and T7 in the falling part of the force – displacement curve, and in addition the maximum force increased with 50 N. This rate-dependent behavior is called viscoplasticity and this theory is applicable in structural impact problems, forming operations and creeps and stress relaxation. Quasi – static strain rate at yield stress is lower than the yield stress at elevated strain rate, this can be seen in Figure 3.7 [9]. Temperature may also be an effect to this phenomena, the melting temperature for HDPE is between 126 – 130 °C, this means that an elevation of 30 – 40 °C is quite significant for this material. An increased velocity leads to an increase in temperature in the material which changes the material behavior [10].



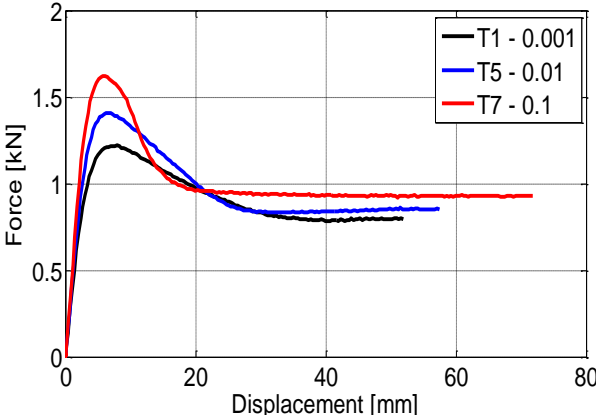
(a) Force – displacement at $\dot{\epsilon} = 10^{-3} s^{-1}$



(b) Force – displacement at $\dot{\epsilon} = 10^{-2} s^{-1}$



(c) Force – displacement curve at $\dot{\epsilon} = 10^{-1} s^{-1}$



(d) Comparison of the force – displacement curves, the strain rate is indicated in the figure.

Figure 3.4: Force - displacement of all tensile tests with strain rates ranging from $10^{-3} s^{-1}$ to $10^{-1} s^{-1}$

3.4.2 Comments on force – displacement curves of tensile tests of thickness 10 mm, T9 – T13

It was performed five tensile tests of thickness 10 mm. Tensile tests T9 and T10 were both subjected to a strain rate of $10^{-2.5} \text{ s}^{-1}$, and by illustrating Figure 3.7 the two curves are seen to be close to identical. Further on, test T11 was subjected to a strain rate of 10^{-2} s^{-1} , test T12 a strain rate of 10^{-1} s^{-1} and tensile test T13 was subjected to a strain rate of 10^{-3} s^{-1} . There was only performed one test at each strain rate. By comparing the five curves illustrated in Figure 3.5 it shows that HDPE is a strain rate dependent as seen for the tensile tests of thickness 5 mm. The maximal force is higher for these tests, but this is expected since the thickness of the specimen is twice as thick. The yield stress is not particularly influenced by the change in thickness.

HDPE is a ductile material, and it does not experience fracture. The tensile tests were therefore stopped when the force stabilized itself. This applies for all tensile tests, T1 – T13.

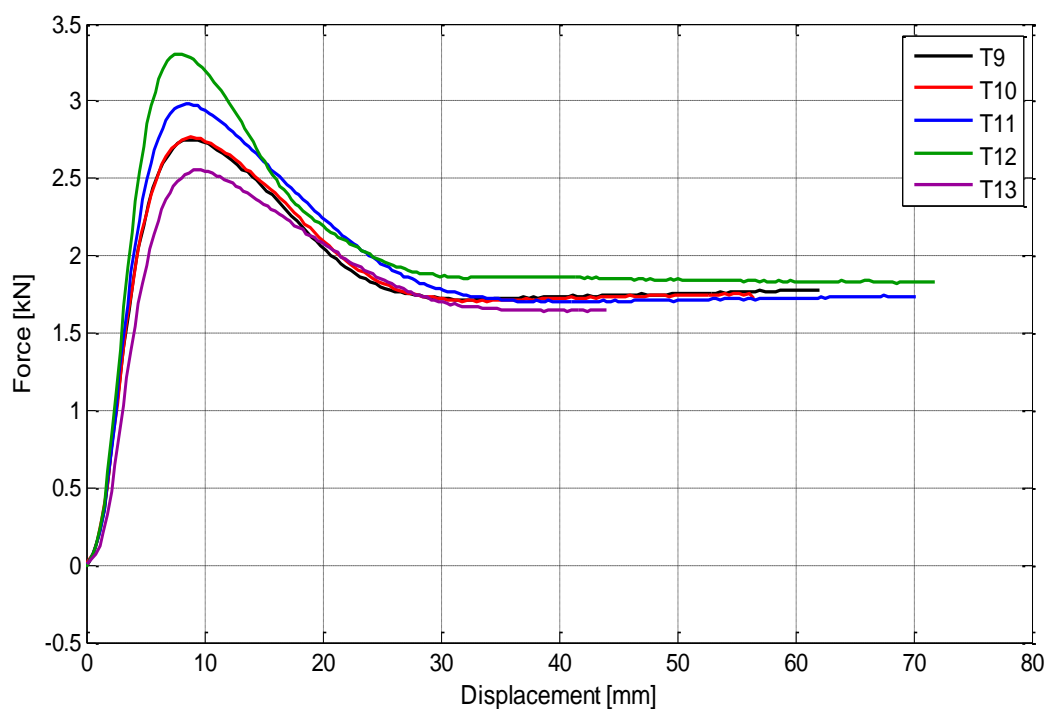
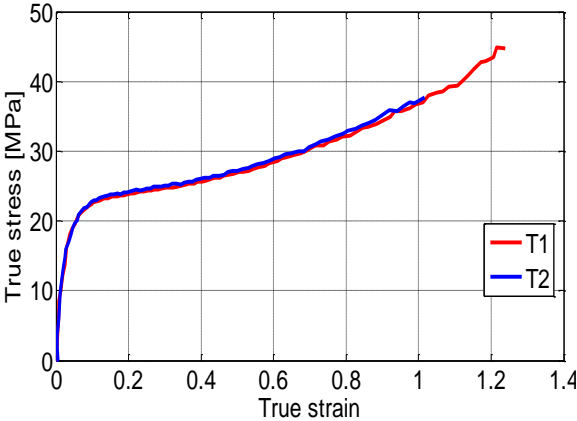


Figure 3.5: Force - displacement of tensile tests made from sheets of thickness 10 mm

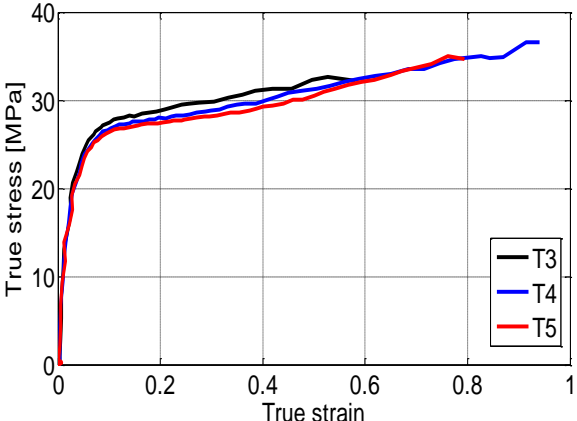
3.4.3 Comments on the true stress – strain curve, and determination of yield stress

Figure 3.6 show that the strain rate has a significant influence on the stress – strain curve as well as for the force – displacement curve. The reason why the stress – strain curve keeps rising is due to hardening in the material.

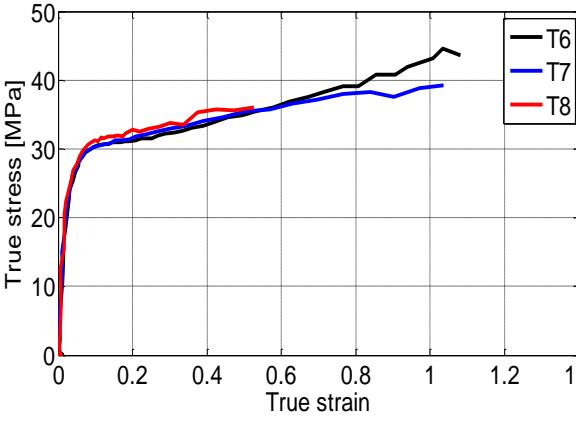
After the yield stress has been reached, the specimen starts to neck in some region due to local softening. If the deformation continues, more and more chain molecules are drawn and straightened in parallel. The more noticeable the drawings of the chains are the more loaded will the covalent bonds be, and this causes a local hardening. This will overcompensate for the reduction in cross section and prevents further necking in this area. The necking will continue to grow until the whole specimen consists of drawn molecule chains. The strains can be as high as 300 % [2].



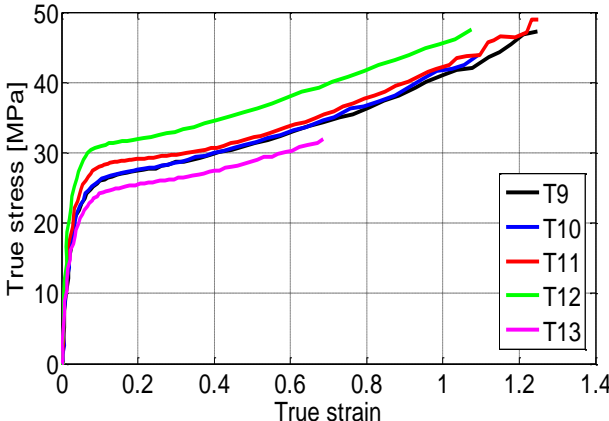
(a) True stress – strain at $\dot{\epsilon} = 10^{-3} \text{ s}^{-1}$



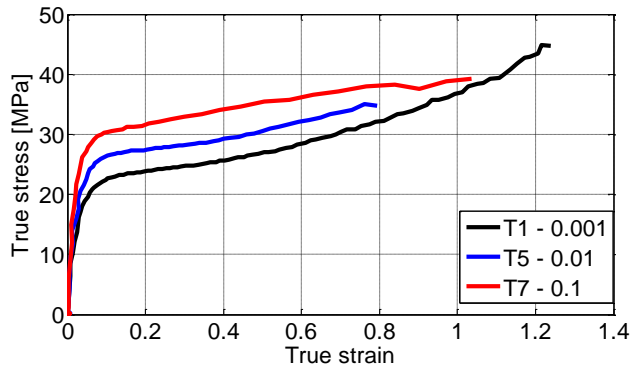
(b) True stress – strain at $\dot{\epsilon} = 10^{-2} \text{ s}^{-1}$



(c) True stress – strain at $\dot{\epsilon} = 10^{-1} \text{ s}^{-1}$



(d) True stress – strain at $\dot{\epsilon} = 10^{-3} \text{ s}^{-1} - 10^{-1} \text{ s}^{-1}$



**(e) Comparisson of true stress – strain curves
at strain rates indicated in the figure**

Figure 3.6: True stress - strain curves a – c tensile specimens of thickness 5 mm, d tensile specimens of thickness 10 mm.

The true stress – true strain curves in Figure 3.6 show that the curves do not have a distinct stress peak. The reason for this is that the material is experiencing hardening rather than softening. This means that the stress curve continues to rise, and it therefore makes it hard to see where the yield stress is. If the material were experiencing softening, there would have been a distinct stress peak, and calculations would not have been necessary. Anyway, the yield stress is calculated by plotting the true stress and the differentiated stress against the true strain. By plotting both of these curves in the same plot a point of intersection is obtained, this point is the yield stress for the test [10]. The equation for the differentiated stress for discrete data points reads

$$\frac{d\sigma}{d\varepsilon} = \frac{\sigma_{i+1} - \sigma_{i-1}}{\varepsilon_{i+1} - \varepsilon_{i-1}} \quad (3.1)$$

An overview of the yield stresses for all tensile tests are given in Figure 3.7.

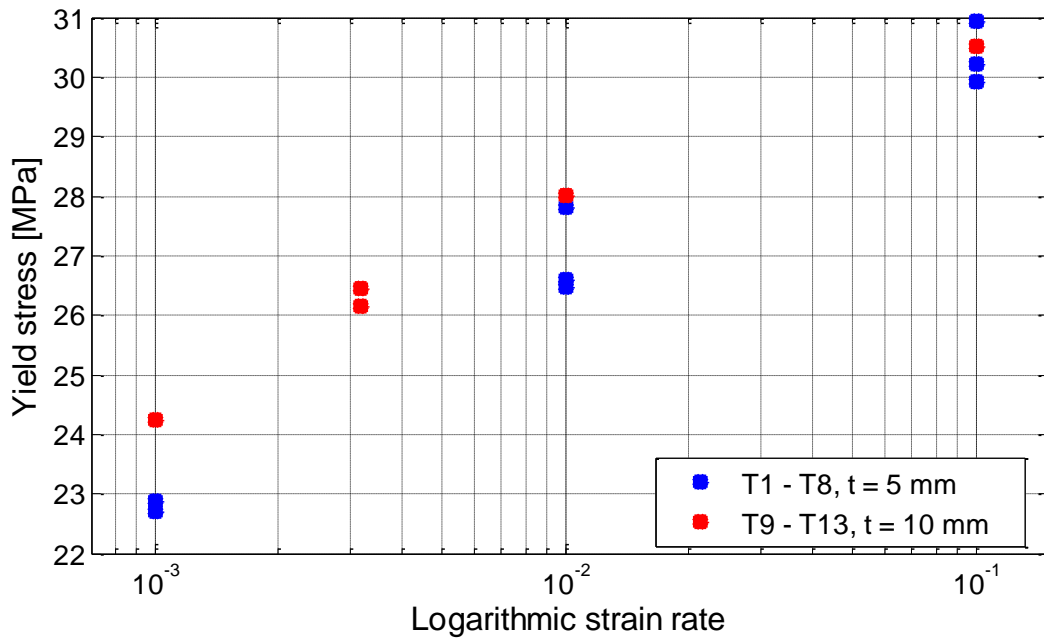


Figure 3.7: Yield stress for all tensile tests, T1 - T13

3.4.4 Longitudinal versus transverse strain

Figure 3.8 shows the longitudinal and absolute value of transverse strain as a function of time for test T1. An important observation of this is that the transverse strains are close to half the longitudinal strains, this result in a Poisson's ratio, ν , equal to 0.47. The strains through the thickness and over the width are considered equal, as mentioned in Section 2.2, and both of them are negative and multiplied with the Poisson's ratio, while the longitudinal strains are not multiplied with the Poisson's ratio. By adding together the strains, ϵ_x , ϵ_y and ϵ_z , it can easily be seen that HDPE has a volume change of 6 %. This is not a significant amount for the material, and HDPE is considered an isochoric material.

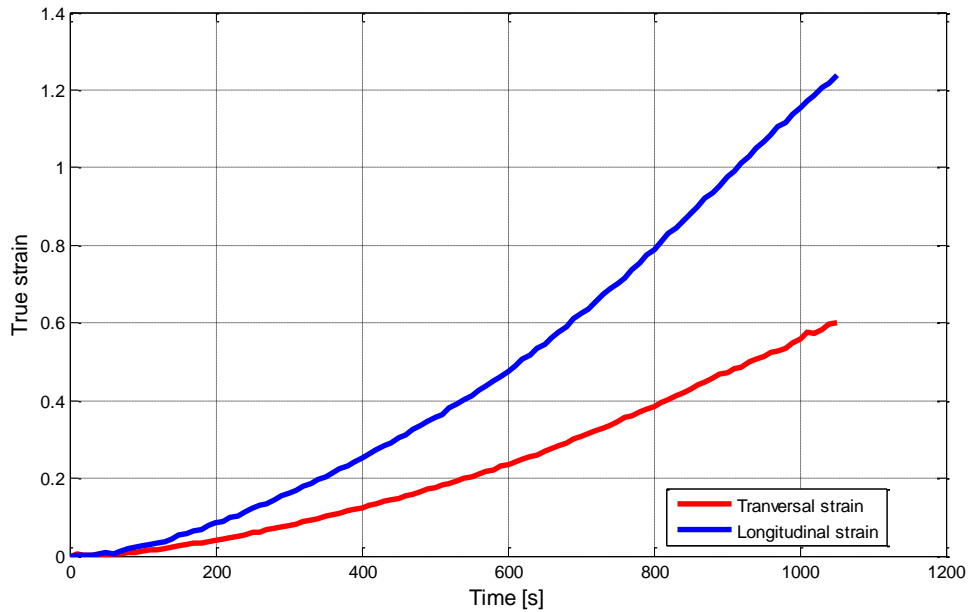


Figure 3.8: True stress - time curve of tensile test 1

3.5 Experimental program of compression tests, C1 – C5

Five compression tests were performed, four of them with height 8 mm and the last had a height of 5 mm. The compression specimens of height 5 mm was made in the xy – plane from the plate of thickness 5 mm, while the specimen of height 8 mm was made in the yz – plane from the plate of thickness 10 mm. The geometry illustrated in Figure 3.9 a) and b) shows the exact geometry of the test specimens.

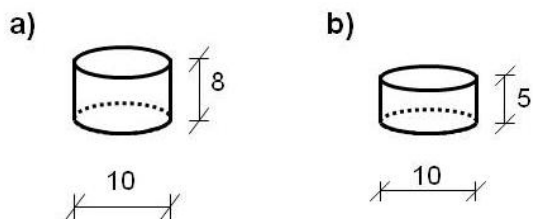


Figure 3.9: Exact geometry of compression specimen.

The axisymmetric compression specimen was inserted into the servo – hydraulic Dartec Machine, and three different strain rates were used on the five tests. The first two tests, C1 and C2, was subjected to a strain rate of 10^{-3} s^{-1} , the third, C3, and the fifth, C5, tests were subjected to a strain rate of 10^{-2} s^{-1} , these two tests is made out of two different extrusion sheets with two different thicknesses of respectively 5 mm and 10 mm. Only compression test four, C4, was subjected to a strain rate of 10^{-1} s^{-1} . The main purpose of testing the specimens at different strain rates is to see how the material behaves, if the yield stress will differ from one test to another by only changing the velocity of compressing.

Grease was applied to each specimen to avoid as much friction as possible. This facilitates free movement of the bottom and the top surface in radial direction, which contributes to keep the edges straight. The formula for true stress, $\sigma = F/A$, and true strain, $\epsilon = \ln(H/H_0)$, is not applicable when the specimen has a barrel shape because the stresses varies over the height of the specimen as the area is changing. It was therefore important to avoid friction to retain straight edges. Figure 3.10 illustrates the set up of a compression test.



Figure 3.10: Setup of a compression test

Although the camera was used on the compression tests as well as the tension tests, digital image correlation was not performed on the compression tests. The displacements were obtained by using Matlab since the black and white pattern could not be applied to the small compression specimen. A Matlab script was then written to obtain the change in diameter and height, since Matlab does not operate with units all lengths were given in pixels. True strain and true stress was calculated from the lengths obtained. The diameter was measured at the middle of the sample, where the strains evolve most in the beginning of the test. The cross section area of the specimen was calculated by using $A = (\pi/4)d^2$. The diameter was possible to calculate since d_0 was measured before placing the specimen into the servo – hydraulic machine, and the Matlab script gave the diameter in pixels at every photo.

3.6 Test results of compression tests

3.6.1 Comments on force – displacement curve of the compressions tests

The force – displacement curve for all five of the compression tests are shown in Figure 3.11. The two first tests, C1 and C2, were subjected to a strain rate of 10^{-3} s^{-1} . These two tests are as similar as one can hope for. Further on test 3, C3, is subjected to an increased strain rate of 10^{-2} s^{-1} . Test C5 was also subjected to the same strain rate, but as the height was only 5 mm, the force – displacement curve is quite different from the other tests. The deviation is due to the height which is 3 mm shorter than the other test specimens. Finally, test C4 was subjected to a strain rate of 10^{-1} s^{-1} . Similar to the tension tests, the compression tests also experience an elevation in forces when the strain rate is increased. Clearly, the material behaves quite similar both in tension and compression. An overview of the five compression tests are given in Table 3.2.

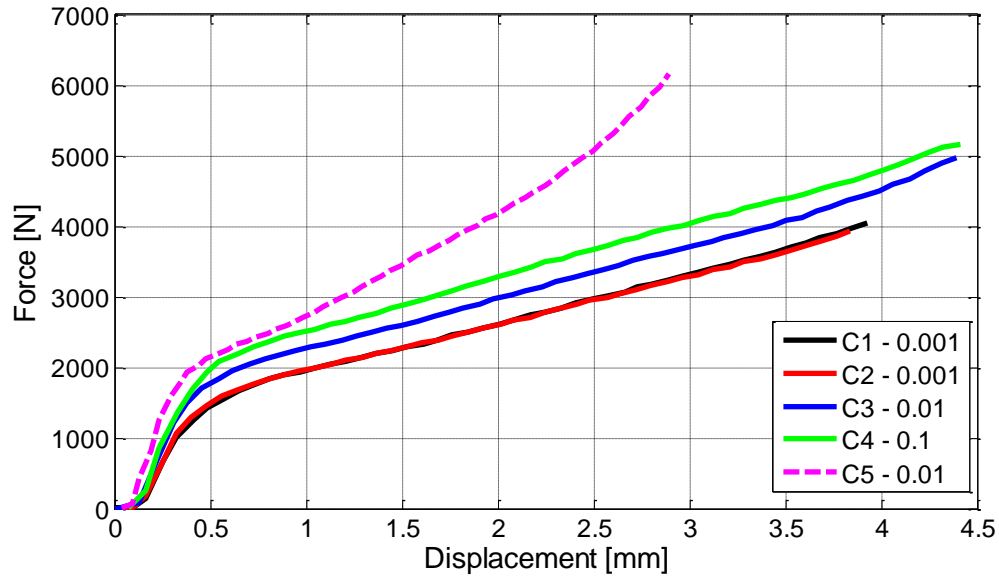


Figure 3.11: Force - displacement curves of compression specimens, the strain rate is indicated in the figure.

Table 3.2: Overview of compression tests, C denotes compression specimen.

Test #	Strain rate [s^{-1}]	Height, h_0 [mm]	Yield stress [MPa]
C1	10^{-3}	8.02	25.1
C2	10^{-3}	8.01	24.3
C3	10^{-2}	8.02	28.0
C4	10^{-1}	8.02	31.2
C5	10^{-2}	4.94	27.0

3.6.2 Specimens with different extrusion directions

The longitudinal axis of the C3 compression specimen was parallel with the extrusion direction of the plate, while specimen C5 was directed in the thickness direction of the extruded sheet. In addition the C5 specimen has a height of 5 mm instead of 8 mm. Both test specimen C3 and C5 was subjected to a strain rate of $10^{-2} s^{-1}$, and therefore it is reasonable to compare these two tests. Figure 3.12 illustrates the longitudinal strains in x and z direction of respectively compression test 3 and 5. The two curves are close to parallel. This means that there are no significant differences in the longitudinal strains when the specimen is machined from a different direction of the extruded sheet. The true stress – true strain curve, see Figure 3.13, illustrate no significant difference between compression test 3 and 5.

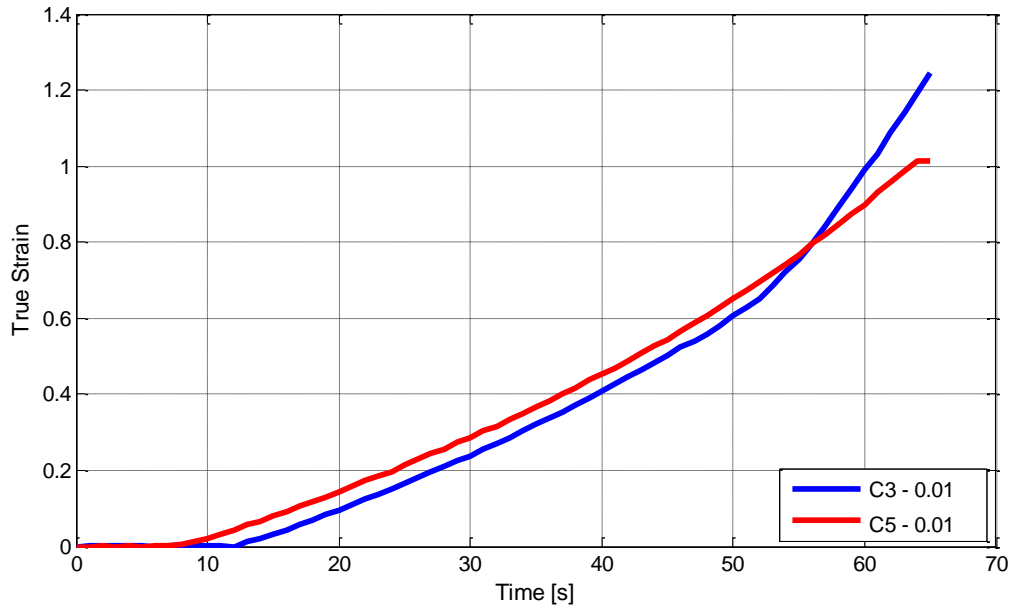


Figure 3.12: Comparing longitudinal strains in x and z direction

3.6.3 Comments on true stress – true strain curves of compression test C1 – C5

Figure 3.13 illustrates the true stress – strain curves of all compression tests performed. These curves show that hardening is present in compression similar as for tension. Although, the stress hardening is larger in compression than in tension, and therefore makes the two stress – strain curves different in the two loading modes. This means that the shape of the curve is pressure dependent.

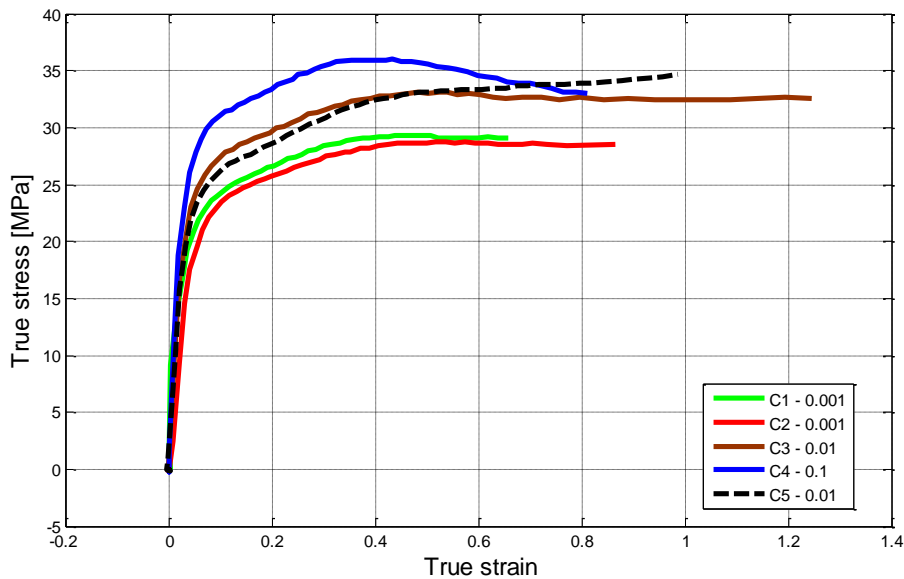


Figure 3.13: True stress - strain of all compression tests, the strain rate is indicated in the figure.

The yield stress must be calculated by plotting the stress and the differentiated stress as a function of the true strains. The point of intersection that is obtained is the yield stress for the test. This is the same procedure as used in tension, Section 3.4.3. Figure 3.14 illustrates the yield stress for the five different compression tests performed. As seen in tension, the yield stress increases when the strain rate is elevated due to hardening and elevated temperature during the compression test.

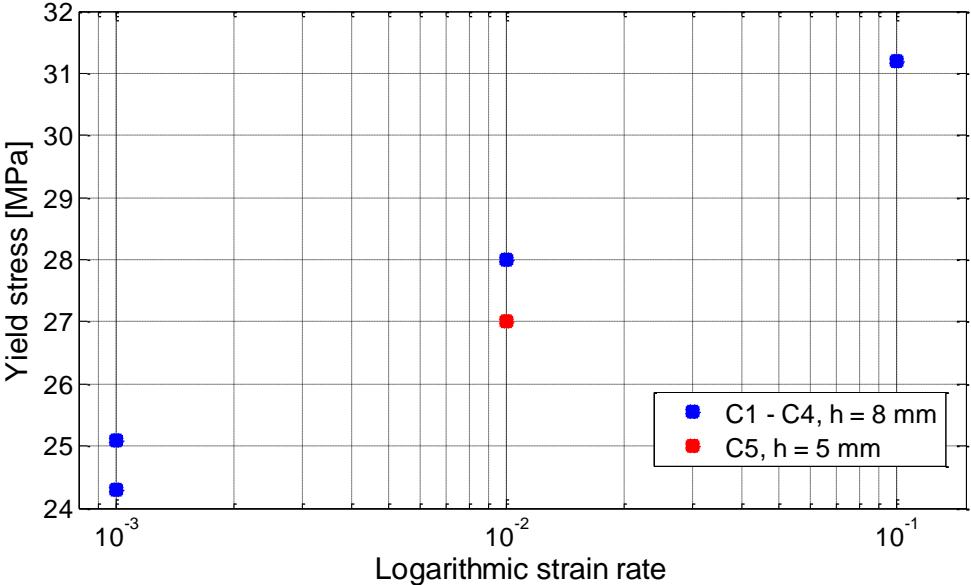


Figure 3.14: Yield stress of all five compression tests, the height is indicated as h in the figure.

3.6.4 Poisson’s ratio from compression tests

Figure 3.15 illustrates the transverse strains and the longitudinal strains. The transversal strains are half the longitudinal strains, resulting in no change of volume when the material is subjected to compression. This was seen during tension testing as well, since the material has no significant change in volume neither in compression nor in tension, the material is isochoric.

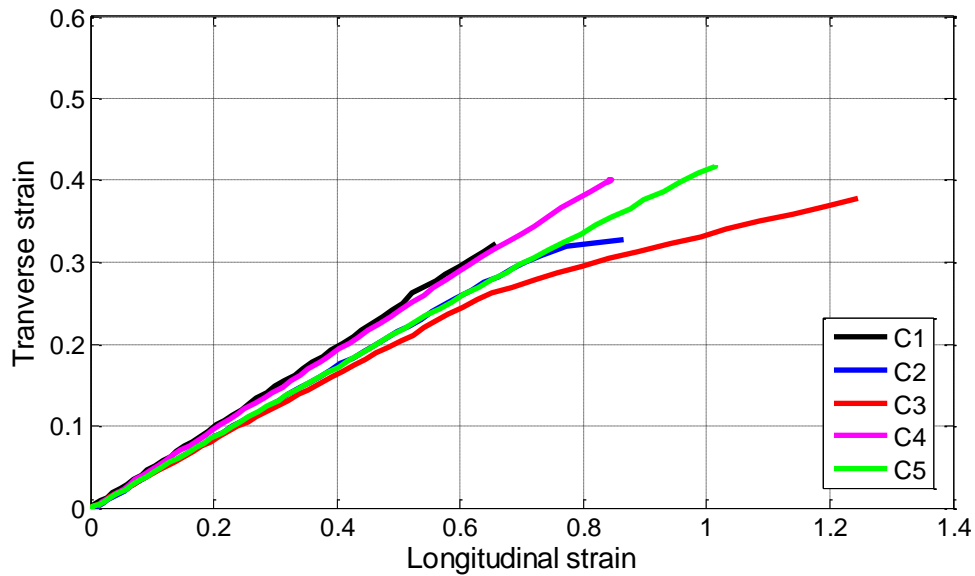


Figure 3.15: Transversal strains versus longitudinal strains of all compression tests

3.7 Discussion

The temperature within the material increases due to increased strain rates. As seen in Figure 3.6 (e) the tensile test of strain rate 10^{-3} s^{-1} is intersecting with the two curves of a higher strain rate due to elevated temperature within the material. The temperature can rise as much as 20 – 40 °C this is a lot for a material with a transition temperature of approximately 120 °C. [10]

The yield stress also increases due to increased strain rate, and one of the reasons is viscosity due to plastic flow. The material model is compared to a spring with a damping effect. The forces working on a stretched spring is the displacement multiplied with the spring stiffness, $F = k \cdot x$. The force working on a damper is calculated by multiplying the viscosity factor, c , with the velocity, $F = c \cdot \dot{x}$ [10].

Though, the velocity is constant throughout the test the strain rate however will change as the length of the sample extends. Another aspect of this matter is the localization of the strains, as the diffuse necking forms the strains are accelerating in the cross section. As the localized neck approaches the cross section the strain rate will decrease again. The cross section is depicted from the DIC measurements.

4. Calibration

4.1 Introduction

The material testing has now been done, and it is time to evaluate the results obtained from the experiments. The yield stress and Poisson's ratio have already been determined in Section 3.4.3 and 3.6.3 respectively. When performing the calibration the test results from a tensile test of strain rate 10^{-3} s^{-1} is used as a baseline case. The results from the first tensile test, T1, were selected. There are also needed results from a tensile test of a different strain rate as well as results from a compression test. The second compression test C2 was chosen. This test also had a strain rate of 10^{-3} s^{-1} .

4.2 Calibration of parameters

First the strain rate dependency has to be determined because of the accurate calibration based on the baseline tension test. The strain rate that is used corresponds to the yield stress found in tensile test T1. The parameters v_0 and β are related to the strain rate, and the slope of the curve in the elastic domain gives the Poisson's ratio, by plotting the contraction ratio, $\rho = -\epsilon_t / \epsilon_l$, and the true longitudinal strains the curve will converge toward a value. This contraction ratio applies to the plastic area.

The volumetric change is controlled by the material constant β . The coefficient can be calculated from the following equation

$$\beta = \frac{2-\rho}{1+\rho} \quad (4.1)$$

The value of ρ is close to 0.5, and $\beta = 1$, this means that the isochoric plastic behavior is obtained [4,6].

In the strain rate sensitivity part of the model the following three coefficients are involved σ_T , $\dot{\epsilon}_{0A}$ and C . The equation for the yield stress, $\bar{\sigma}_A$, reads

$$\bar{\sigma}_A = \sigma_T \left(1 + C \cdot \ln \left(\frac{\dot{\epsilon}_A^p}{\dot{\epsilon}_{0A}} + 1 \right) \right) \quad (4.2)$$

It is obvious that the expressions in the parentheses are equal to one, this means that equation 4.2 will predict a yield stress, $\bar{\sigma}_A$, higher than σ_{yield} . To avoid this problem the yield stress σ_T is replaced by the static yield stress σ_{T0} by extrapolating back to a fictitious strain rate $\dot{\epsilon} = 0$. Further on, the reference strain rate, $\dot{\epsilon}_{0A}$, is fetched from the section where the specimen experienced the onset of necking, and thereby the initial yielding. According to the results given from 7D the strain rate at yielding is $\dot{\epsilon} \cdot 0.7$ in the tension tests. The baseline case is tensile test T1 with the lowest strain rate, this means that the nominal strain rate $\dot{\epsilon} = 10^{-3} \text{ s}^{-1}$. This gives a reference strain of $\dot{\epsilon}_{0A} = 0.0007 \text{ s}^{-1}$. The logarithmic strain rate, $\dot{\epsilon}_A^p$, are determined from the DIC measurements [4, 10].

The parameters C and σ_s can now be determined as the yield stress and the corresponding strain rate is found. By plotting the yield stresses from all tension tests of thickness 5 mm against the logarithmic strain rate and making a logarithmic curve fit, the C is obtained.

$$y = abx + b \quad (4.3)$$

where $a = C$, b is the yield stress σ_T , y is the yield stress at the reference strain rate and $x = \ln\left(\frac{\dot{\epsilon}_A^p}{\dot{\epsilon}_{0A}} + 1\right)$. The abscissa value is observed to be $\ln(2) = 0.693$ for the slowest tests, the reason for this is that the strain rate is selected as $\dot{\epsilon}_{0A}$. By the linear curve fit the $C = 1.873/21.94 = 0.0854$ [4, 6].

4.2.2 Determination of parameters based on the stress – strain curve

The parameters still remaining from Part A are E_0 , σ_T , σ_s and H . These parameters have to be determined from a stress – strain curve. Again the test with strain rate 10^{-3} s^{-1} was selected as the baseline case.

The response of the material is strongly non-linear in the elastic domain, and it is therefore complicated to calculate the Young's modulus. In addition the DIC measurements are inaccurate for small strains. Therefore the Young's modulus is taken from the manufacturer SIMONA, where $E_0 = 800 \text{ MPa}$. The linear Young's modulus was plotted in the stress - strain curve to see if this seemed like a suitable value. Figure 4.1 illustrates that this value is reasonable.

As previously mentioned the material experience hardening which means that $\sigma_s > \sigma_T$.

$$R(\bar{\epsilon}_A^p) = (\sigma_s - \sigma_T)[1 - \exp(-H\bar{\epsilon}_A^p)] \quad (4.4)$$

The best curve fit is to choose a rather low yield stress for σ_T , and let equation 4.4 above represent the gradual reduction of stiffness towards the saturated stress, σ_s . By plotting the Young's modulus and the true stress – true strain curve, the σ_T is the interception point between the straight line, E_0 , and the test data. The σ_s is equal to the yield stress of strain rate $\dot{\epsilon} = 0$, this means that $\sigma_s = 21.9 \text{ MPa}$. According to equation 4.4 the hardening is strain rate dependent. This means that a similar adjustment have to be done for σ_T . The difference between σ_s and σ_T has to be the same for the fully static conditions, thus $(\sigma_s - \sigma_T) = 12.2 \text{ MPa}$. A curve fit between these two test data finds the rate – independent hardening parameter $H = 55.3$. Figure 4.1 shows Part A from the observed test data, the analytical method and the Young's modulus [4]

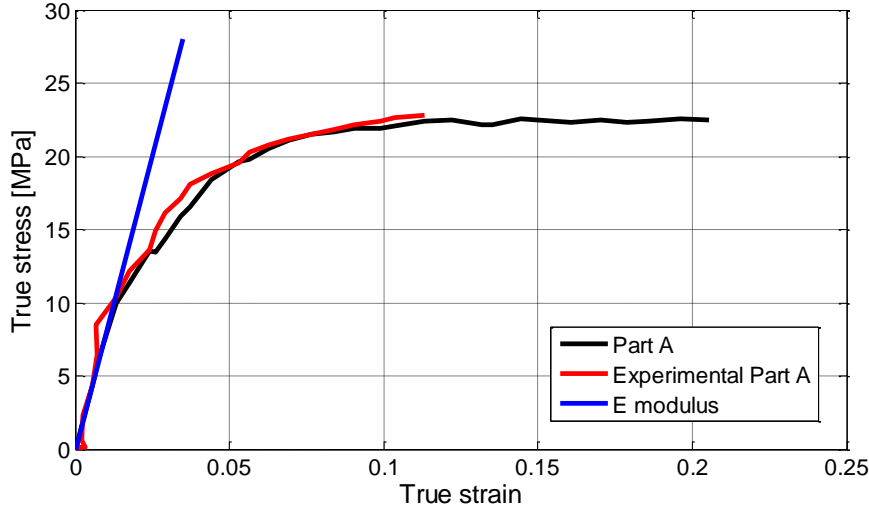


Figure 4.1: Comparison of analytical stress and experimental data of Part A, including the Young's modulus $E_0 = 800$ MPa.

4.2.3 Calibration of Part B

The remaining parameters are C_R and $\bar{\lambda}_L$ related to Part B. This identification part has to be performed with some care due to the factor $(\mathbf{B}_B^* - \bar{\lambda}^2 \mathbf{I})$. The transverse deformation is assumed isotropic, $\varepsilon_2 = \varepsilon_3$, and the stretches are defined as $\lambda_1 = \exp(\varepsilon_1)$ and $\lambda_2 = \exp(\varepsilon_2)$, where the logarithmic strains were obtained from the DIC measurements [4, 6]. The deformation gradient of a uniaxial tension test reads

$$\mathbf{F} = \mathbf{F}_B = \begin{pmatrix} \lambda_1 & \mathbf{0} & \mathbf{0} \\ \mathbf{0} & \lambda_2 & \mathbf{0} \\ \mathbf{0} & \mathbf{0} & \lambda_3 \end{pmatrix} \quad (4.5)$$

The stress of Part A is assumed to saturate at σ_s because Part B is most important at large deformations [4].

The parameter $\alpha = 1.07$, and is close to obeying the Mises' yield criterion. This means that Part A in the plastic domain, σ_{eq} , is corresponding to the uniaxial Part A, $\sigma_{A,ua}$. Both Part A and Part B observed from the uniaxial tension test is allocated as

$$\sigma_{test} = \sigma_{A,ua} + \frac{3}{2}\sigma_{B1} \quad (4.6)$$

The longitudinal stress of Part B from the test data can be isolated as follows

$$\sigma_{B1,target} = \frac{2}{3}(\sigma_{test} - \sigma_{A,ua}) \quad (4.7)$$

The stress component σ_{B1} has to be fitted to the stress of target Part B, $\sigma_{B1,target}$. The Langevin function has no inverse function which is complicating the regression fit of $\sigma_{B1,target}$. By introducing a Padé approximation to $\mathcal{L}^{-1}(\circ)$ proposed by Cohen. [4, 6]

$$\mathcal{L}^{-1}(x) = x \cdot \frac{3-x^2}{1-x^2} \quad (4.8)$$

The following expression for the stress component σ_{B1} is given as

$$\sigma_{B1} = \frac{2}{9} C_R J^{-5/3} \frac{3\bar{\lambda}_L^2 - \bar{\lambda}^2}{\bar{\lambda}_L^2 - \bar{\lambda}^2} (\lambda_1^2 - \lambda_2^2) \quad (4.9)$$

The numerical values $C_R = 1.932$ MPa and $\bar{\lambda}_L = 6.095$ were obtained by a regression fit of Equation 4.9 to the target stress of equation 4.7. The total uniaxial stress was found from equation 4.6. The first part $\sigma_{A,ua}$ is sensitive to the strain rate, while σ_{B1} is independent of the strain rate [4].

In addition the bulk modulus and the shear modulus had to be calculated, and inserted in the material card of LS-Dyna. The following equations are used

$$K = \frac{E}{3(1-2\nu)} \quad (4.10)$$

$$G = \frac{E}{2(1+\nu)} \quad (4.11)$$

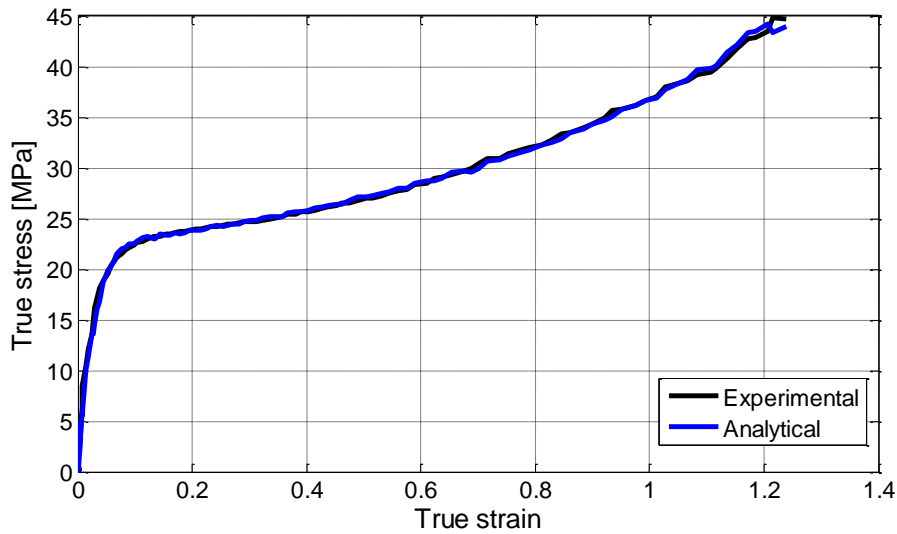


Figure 4.2: True stress – strain of experimental data and analytical test.

Figure 4.2 illustrates both Part A and Part B. It can be seen that the curves are almost identical. An overview of all parameters that are calculated is given in Table 4.1 below.

Table 4.1: An overview over the parameters calculated in the calibration

Parameter	Value	Unit
E_0	800	MPa
ρ_0	0.47	
v_0	0.47	
σ_s	21.9	MPa
σ_T	10.5	MPa
$(\sigma_s - \sigma_T)$	12.2	MPa
α	1.07	
H	55.3	
β	1.0	
$\dot{\epsilon}_{0A}$	0.0007	s^{-1}
C	0.0854	
C_R	1.93	MPa
$\bar{\lambda}_L$	6.095	

5. Validation

In this section the experimental tests are modeled and simulated in the non – linear finite element program LS – Dyna. The models are evaluated by using an explicit dynamic calculation method. A material model for ductile plastic materials has been developed, the material model for elastic – viscoplastic materials is implemented. The main purpose of modeling and simulating the experimental tests is to see how this implemented material model works for HDPE. All necessary material properties were calculated in Section 4, and are being implemented in the material model in Ls – Dyna. The simulations are supposed to be as similar to the experimental tests as possible. All tests are not simulated, but a variety of tests subjected to different strain rates are chosen.

5.1 LS-Dyna simulations of the tensile tests

There were simulated three tensile tests in LS – Dyna at nominal different strain rates of respectively 10^{-3} s^{-1} , 10^{-2} s^{-1} and 10^{-1} s^{-1} . There was not simulated any tensile tests of thickness 10 mm since there was no significant differences.

5.1.1 Modeling the tensile test in LS - Dyna

The whole tensile specimen was modeled in LS – Dyna by using solid elements. There was not used any symmetry planes on this model, although it would have been possible to have two symmetry planes; one in the thickness direction and one in the width direction. During the test the specimen was clamped at each end and pulled upwards by one of the mechanical grips. The model is therefore fixed at one end, and subjected to a displacement controlled loading in the positive x – direction. It was necessary to restrict the rotation around the loading direction because the end of the plate started to rotate around the x – axis. This would never have happened in the experimental test since the mechanical grips would not have allowed this. Figure 5.1 illustrates the model.

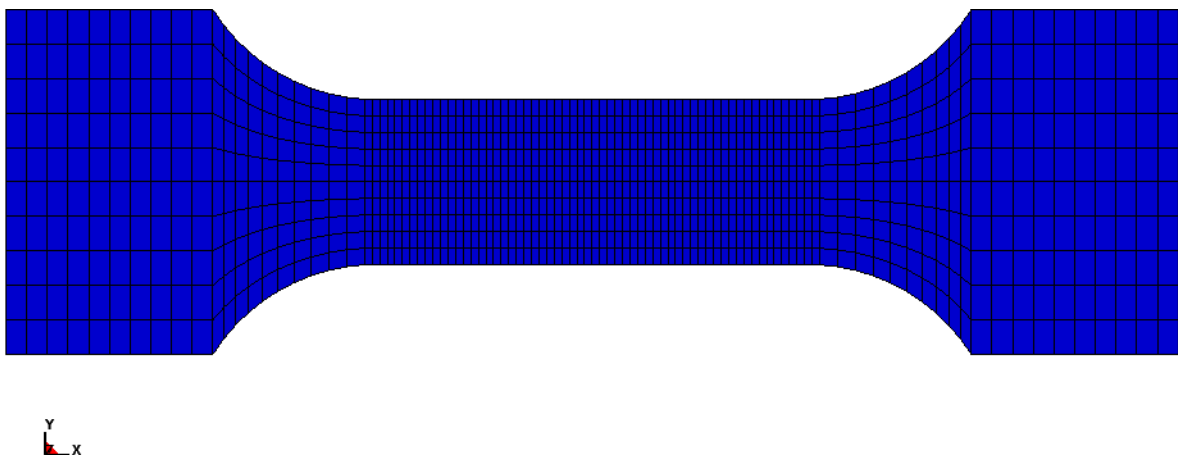


Figure 5.1: Mesh of tensile test

The tensile test of strain rate 10^{-3} s^{-1} was the first test that was modeled in LS – Dyna. All necessary parameters have been determined. The material model explained in Section 2.3

was implemented in LS – Dyna as a user-defined material model working for shell and brick elements. A fracture criterion is not implemented in the model [4].

As seen in Figure 5.1 the elements are longer in the width direction than in the longitudinal direction. This is to avoid that the elements get too drawn out in the necking zone. When this happens the accuracy is poor, and the force – displacement curve gets rough. There are four elements through the thickness of the tensile specimen. The element formulation was set to -1 for fully integrated solid elements. This formulation is efficient and intended for elements with poor aspect ratio [11]. In addition, the hourglass effect is avoided when applying full integration. The model is quite big and contains many elements, to reduce the simulation time the model has been mass scaled. This means that the density is increased to make the time step larger and less iterations are performed [12]. The density of the material was reduced from $0.950 \cdot 10^{-9} \text{ ton/mm}^3$ to 0.950 ton/mm^3 . The reduction of the density is large, and it may cause error. Therefore it has been simulated tests specimens with a lower density, but this does not have any particular influence on the simulations, except longer simulation time. This applies for the tests of a nominal strain rate of 10^{-3} s^{-1} . When the nominal strain rates have been increased to 10^{-2} s^{-1} and 10^{-1} s^{-1} the density have been reduced to 0.0950 ton/mm^3 and 0.00950 ton/mm^3 respectively. The equation for the critical time step reads

$$\Delta t_{cr} = \frac{L_e}{\sqrt{\frac{E}{\rho}}} \tag{5.1}$$

During tensile testing there has to be accounted for two types of necking; diffuse and localized necking. When the material reaches its maximum force the test specimen starts to neck, this can barely or not at all be seen on the test specimen. As the neck keeps growing the thickness and width of the specimen will be reduced and a clear notch will be visible as illustrated in Figure 5.2. This necking condition is called localized necking. [13, 14]

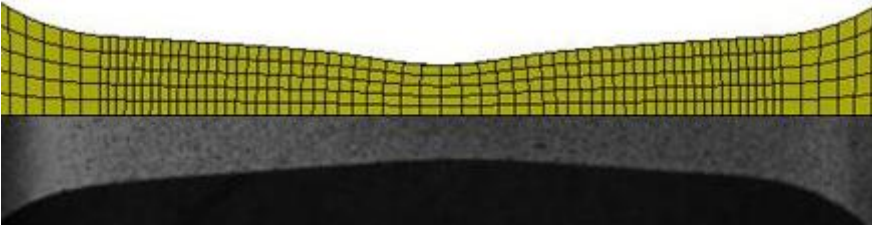


Figure 5.2: Localized necking in tensile specimen T1.

As the neck keeps growing the necking area gets harder due to part B. The deformations will then come to an halt, and the neighboring areas of the neck will start to neck as well, this is called propagating or drawing, this is illustrated in Figure 5.3 [13, 14].



Figure 5.3: Propagated necking in tensile specimen T1, comparing experimental and simulated neck.

By comparing the simulated and experimental necking it is clear that they are similar. The neck in the simulation is more distinct. Figure 5.2 is taken from the middle of the experimental test and simulation, and Figure 5.3 is taken from the last picture in the experimental test, and in the end of the simulation.

The Bridgman factor

The stress state in a test specimen will change from uniaxial to triaxial after the onset of diffuse necking. To account for this triaxial behavior Bridgman developed a correction to the average stress based on the geometry of the neck. Bridgman examined the triaxial stress state for circular cylindrical test specimens with parameters a and R , where a is the radius of the test specimen during necking and R is the curvature of the neck. The parameters are defined in Figure 5.4 [6, 13]

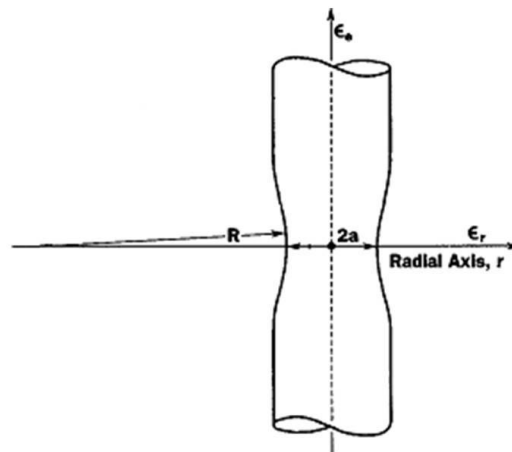


Figure 5.4: Defining the constants R and a in the Bridgeman correction.

The Bridgman corrector factor is expressed as

$$F_T = \frac{\sigma_e}{\bar{\sigma}_z} \quad (5.2)$$

where $\bar{\sigma}_z$ is the average longitudinal stress and the σ_e is the equivalent uniaxial stress [Hovden + Diffuse necking]. The Bridgeman corrector was accounted for in the master thesis of Martin T. Hovden [6], but did not have any significant outcome on the stress – strain curve and is not accounted for in this thesis.

5.1.2 Results from the simulation of tensile tests

The force – displacement of the experimental and simulated results of T1 is compared in Figure 5.5. There are three main characteristics of importance; the initiation of the curve up to the force peak, the force peak itself and the stabilized force at the end of the simulation. The force – displacement curves illustrated in Figure 5.5 shows that the initiation of the experimental curve is too stiff compared to the simulation done in LS – Dyna. The force peak of the simulated curve is slightly higher than the experimental force peak. For the experimental test the force stabilizes at 800 N. The simulated test reaches approximately 900 N, however, the force does not stabilize but continues to rise slowly due to a secondary hardening. Altogether the overall shape of the curves is similar.

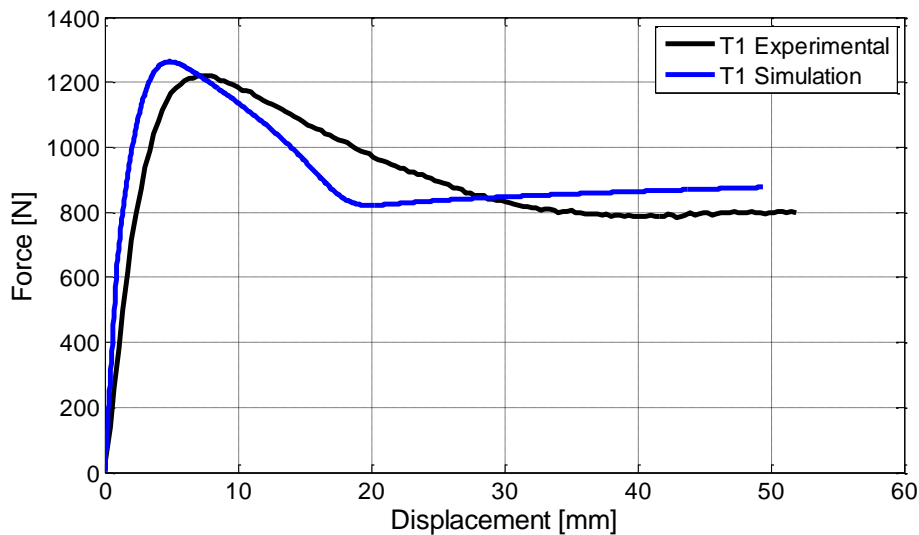


Figure 5.5: Force – displacement curve of tensile specimen T1

The true stress – strain curve illustrated in Figure 5.6 shows the similarities between the simulated stress – strain curve and the experimental. The simulated curve is slightly higher from about yield stress, but other than that they are approximately similar. It can be seen from the curves that the experimental curve does not go all the way up due to large deformations. The black and white pattern could not be recognized by the 7D program any longer.

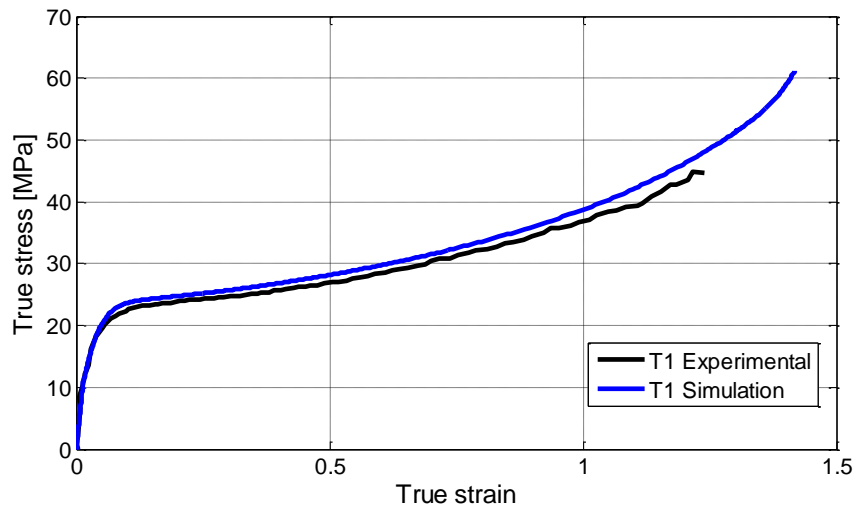


Figure 5.6: True stress – true strain curve of tensile specimen T1

Tensile test T5 is subjected to a nominal strain rate of 10^{-2} s^{-1} . By comparing the two curves in Figure 5.6 it can be seen that the overall shape of the two curves are approximately similar. The force peak is shown to be slightly higher for the simulated curve. As seen in tensile test T1 the simulated curve is stiffer for the simulated curve. The overall shape of the simulated curve is a good approximation. The force stabilizes at approximately 800 N. Again, the analysis is seen to experience a second hardening towards the end of the analysis.

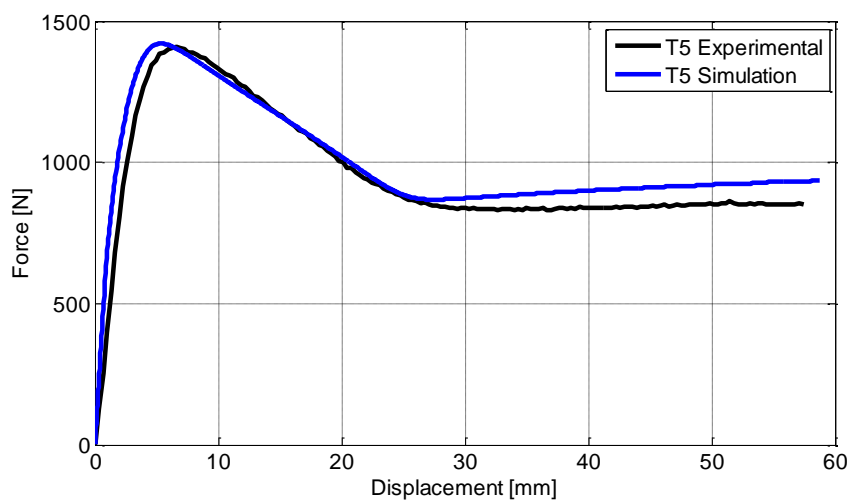


Figure 5.7: Force – displacement curve of tensile specimen T5

Comparison between the true stress – strain curve in Figure 5.8 shows that the experimental results and the simulation is close to identical.

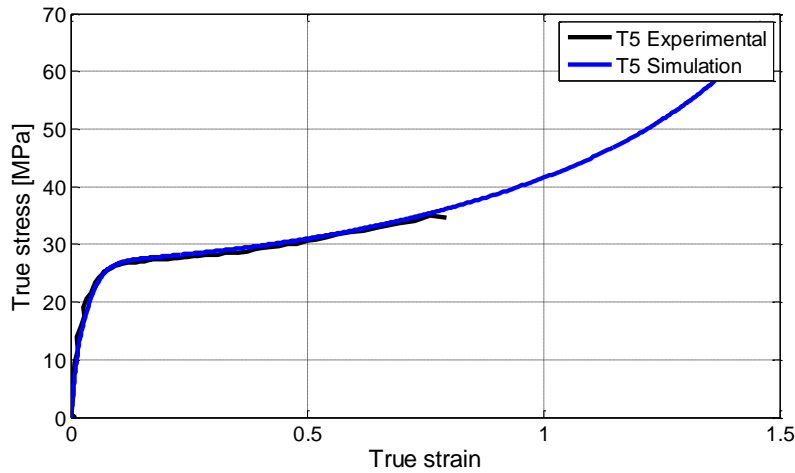


Figure 5.8: True stress – strain curve of tensile specimen T5

There were three tensile tests subjected to a nominal strain rate of 10^{-1} s^{-1} , and test T7 was selected to be simulated. The force – displacement curve, shown in Figure 5.9 (a), of tensile specimen T7 is similar from the start and up to peak force, the stabilized force is a little higher as for all other tensile tests. There is a difference in the descending part of the two curves.

The true stress – strain curve illustrated in Figure 5.9 (b) shows that the experimental and the simulated curves are close to identical up to approximately 40 MPa, after that the experimental values of the stress are constant. When the neck starts to propagate the stress and strains may be approximately constant.

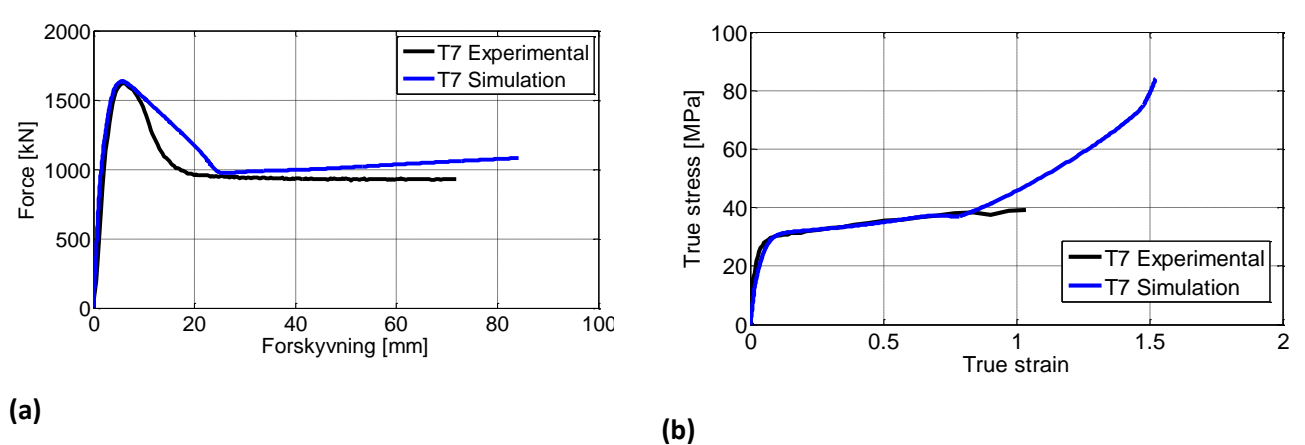


Figure 5.9: (a) Force – displacement curve and (b) True stress – true strain curve of tensile test T7

Figure 5.10 shows the true stress – true strain curve of the three tensile tests that was simulated in LS – Dyna. The nominal strain rate subjected to each of the three specimens is indicated in the figure. By comparing the three curves it is seen that tensile specimen T7 subjected to a nominal strain rate of 10^{-1} s^{-1} is experiencing higher stresses than the other tests. The experimental true stress – strain curves in Section 3.4.3 illustrated in Figure 3.6 (e) shows that the curves of a nominal strain rate of 10^{-3} s^{-1} crosses the curves subjected to a

nominal strain rate of 10^{-1} s^{-1} . The reason for this is that a specimen subjected to a nominal strain rate of 10^{-1} s^{-1} is experiencing an increased temperature which makes the material softer. The true stress – strain curve will then flatten. LS – Dyna does not take the temperature changes into account, and the tensile specimen subjected to a nominal strain rate of 10^{-1} s^{-1} will give a higher true stress – strain curve for the simulated results [10]. This means that the simulated tensile tests subjected to a nominal strain rate of 10^{-3} s^{-1} will not cross a simulated tensile test subjected to a nominal strain rate of 10^{-1} s^{-1} as seen for the experimental results. This presupposes that the tensile test subjected to a nominal strain rate of 10^{-3} s^{-1} is used in the calibration.

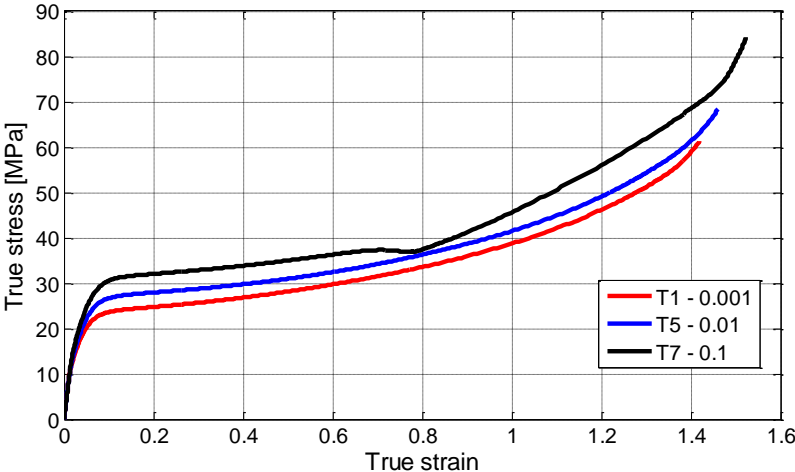


Figure 5.10: Comparison of stress – strain curve of tensile specimen T1, T5 and T7.

5.1.3 Simulations of different elasticity modulus’s

In some of the force – displacement curves the elastic part of the curve is seen to be slightly stiffer. It has therefore been performed a variation of simulation with elasticity modulus ranging from 400 MPa to 800 MPa, where 800 MPa is the value found in the calibration. Figure 5.11 illustrates test T1 applied to the various elasticity modulus’s mentioned.

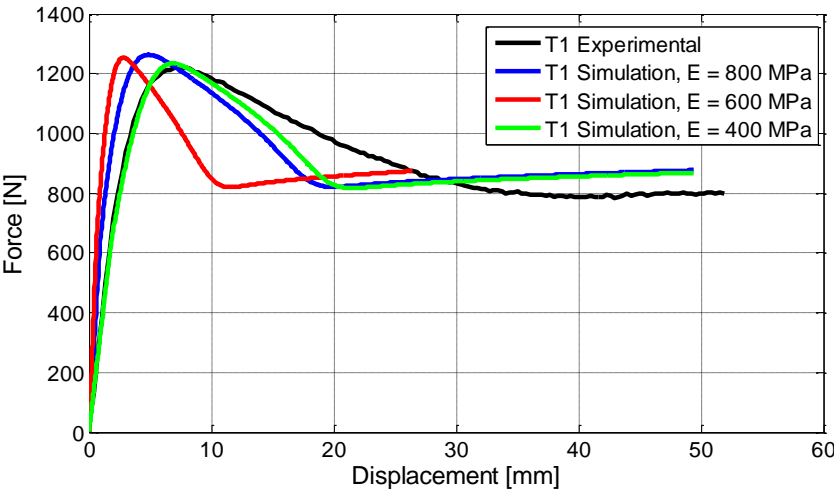


Figure 5.11: Comparison of Young’s modulus of tensile test T1.

By looking at the force – displacement curves it is clear that the elasticity modulus of 400 MPa is the best fit for the uniaxial quasi – static tensile test T1. Both tensile test T5 and T7 are simulated, and an overview of which elasticity modulus that makes the best fit is illustrated in Table 5.1.

Table 5.1: An overview of elasticity modulus for each tensile test

Test #	Strain rate [s^{-1}]	E modulus [MPa]
T1	10^{-3}	400
T5	10^{-2}	600
T7	10^{-1}	800

5.2 Simulation of the compression test

The compression test subjected to a strain rate of $10^{-3} s^{-1}$ was modeled in LS – Dyna. As this was the only test that was used in the calibration of the material model this was the only compression test that was modeled. The compression test was modeled after the dimensions that were measured with the sliding caliper before inserting the test specimen into the Dartec machine. There were used eight node solid elements in the model, and ten elements through the height of the specimen. The element formulation that was selected was fully integrated solid elements that are intended for elements with poor aspect ratio [11]. The same method as used in the tensile simulations. This method is an efficient formulation.

The only constraint applied is for displacement in the z – direction of the model to prevent it from moving downwards when the specimen is compressed. In addition there is applied a prescribed motion in the negative z – direction, and a smooth curve is defined to prevent the velocity to initiate abruptly which can lead to incorrect simulation results. In the laboratory each compression specimen was applied a layer of grease in between the specimen and the metal plates to avoid friction. The friction coefficient was therefore neglected in the simulations.

The mesh has a distance of 0.5 mm, and is illustrated in Figure 5.12 below.

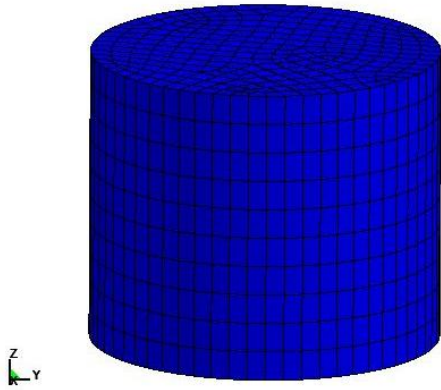


Figure 5.12: The simulation model of the compression specimen C1.

5.2.2 Results obtained from the simulation of the compression test

The force – displacement curve from the experimental and the simulated tests are approximately very similar. As mentioned in Section 3.6.2 the DIC method was not used in the compression test. All results from the compression test are therefore determined from a Matlab script. By comparing the experimental results with the simulated results it can be seen from Figure 5.13 that the force is slightly higher in the beginning of the ascending part of the curve. The overall shape is similar.

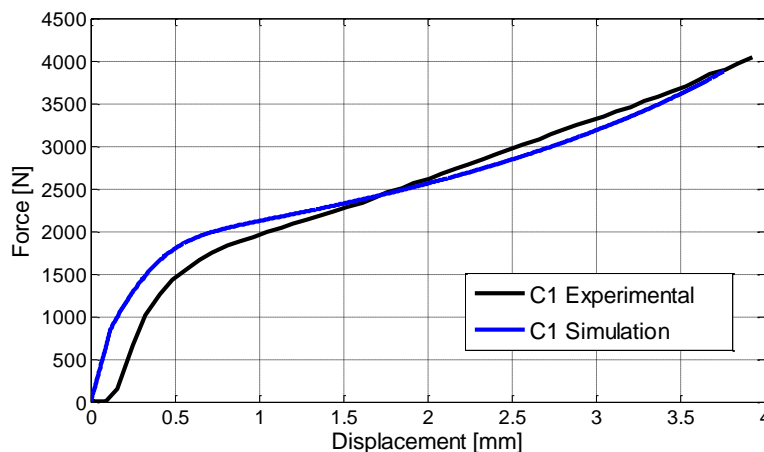


Figure 5.13: Force – displacement curve of compression test C1.

Figure 5.14 illustrates the stress – strain curves obtained from the experimental results and the simulation. The stress and strains from the simulation are taken from selected elements in the centre of the compression specimen where the strains are supposed to be at its largest. The average value of the strains and the stresses are plotted into Matlab. The two curves have a similar overall shape, and the test is in consistency with the simulation. The force peak seems to be slightly higher for the simulated curve, and the hardening is not as distinct in the simulation as it is for the experimental curve.

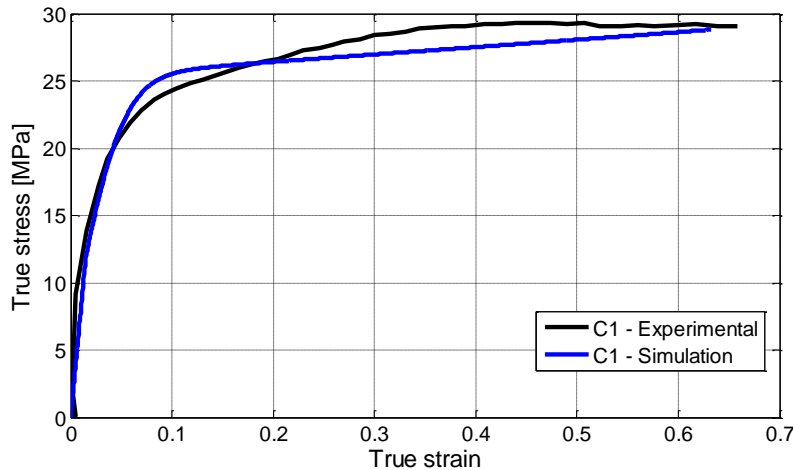


Figure 5.14: True stress – true strain of compression specimen C1.

5.3 Plates with holes of diameter 30 mm and 20 mm.

5.3.1 Introduction

The main purpose of performing the tests on plates with a hole is that the geometry is more complex than a uniaxial tensile test due to the hole. This results in a more complex stress and strain state. In addition the boundary conditions and loading conditions are well defined which is important to make it a good validation object for the material model. The test can be evaluated both globally and locally. The force – displacement comparison as well as geometrical considerations as diameter and lateral faces are the global aspects of the validation. The comparison between the strains close to the hole obtained from the pictures and the simulated results obtained through the analysis is the local responses of the plate with a hole tests [10].

5.3.2 Procedure

There were performed four tests on plates with a hole in the centre. The holes had two different diameters of 30 mm and 20 mm respectively. All plates were dimensioned as 160 x 60 x 5 mm. Each specimen was measured to make sure that the geometries were exact. It was, however, noted that the holes were not placed perfectly in the centre of the specimen. A line was drawn 50 mm from centre across the test specimen. This was to place the specimen correctly into the Dartec machine with the same distance from the hole in both ends. After the specimen had been measured the specimen was inserted into the Dartec machine using a load cell with a maximum capacity of 20 kN.

The DIC method was applied on these tests as well as the tensile tests, and the specimens were sprayed with white and black painting to obtain a black and white spotted pattern. The specimen was painted on the top side of the specimen covering both lateral faces as well as the parts over and below the hole. During these tests there were placed to cameras in two different directions to obtain the change in thickness. As the DIC method was not applied to the thickness of the specimen the lateral side turned towards the camera was marked with

two points 35 mm from centre on each side of the hole. These marks were visible on both cameras. Figure 5.15 illustrates the two lateral faces w_1 and w_2 .

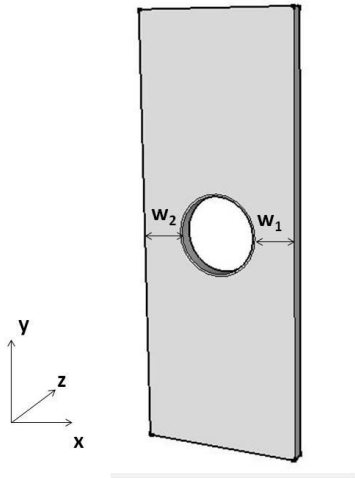


Figure 5.15: Geometry of the plate with indications of lateral faces and diameter

Two different nominal strain rates were applied to four test specimens. They were estimated so that the strain rate in the necking area would correspond to $10^{-3} \text{ s}^{-1} - 10^{-2} \text{ s}^{-1}$. Since the distance between the mechanical grips and the centre of the hole, where the necking area is assumed to develop, is approximately 50 mm the velocity will be 0.05 mm/s and 0.5 mm/s. The first test, 01, and the second test, 02, are subjected to a strain rate of approximately 10^{-3} s^{-1} , where the diameter is 30 mm and 20 mm respectively. The two last tests, 03 and 04, are subjected to a nominal strain rate of about 10^{-2} s^{-1} . An overview of all plates with a hole tests performed is illustrated in Table 5.2 with their respective measurements.

Table 5.2: An overview of all plates with a hole tests performed.

Test #	Estimated strain rate [s^{-1}]	Velocity [mm/s]	Width [mm]		Diameter [mm]	Thickness [mm]
			Lateral face, w_1	Lateral face, w_2		
01	10^{-3}	0.05	15.69	15.29	30.09	4.89
02	10^{-3}	0.05	20.21	20.16	20.06	4.92
03	10^{-2}	0.5	15.12	15.56	29.87	4.89
04	10^{-2}	0.5	20.33	20.11	20.02	4.92

5.3.3 Applying the DIC method

The displacement were obtained by using the DIC method, but to be able to compare the test results and the simulations the displacement would have to come from the exact same cross section of the plate. It was chosen to take out the displacements 40 mm from the centre of the hole. It was necessary to choose a cross section placed high enough so that the

displacements had stabilized. In the program 7D it was important that the first row in the mesh was 40 mm from the centre, if not it would be impossible to find the right row in the matrix. A Matlab script was then written to obtain only the first row of displacements in every picture taken. The test setup is illustrated in Figure 5.16, the two marks placed 35 mm from the centre is clearly seen on the test specimen.

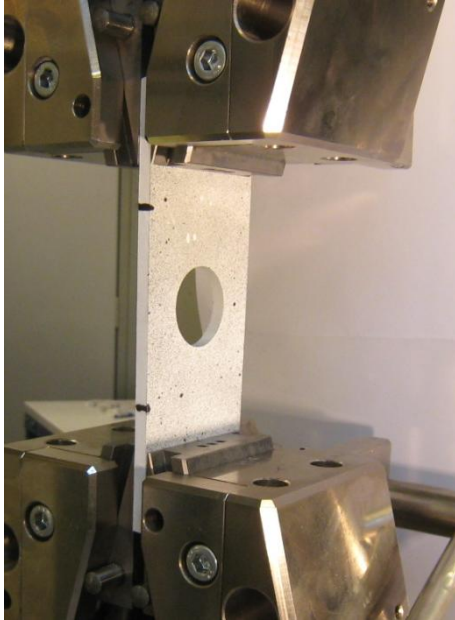


Figure 5.16: Test setup of plate with a hole

The change in diameter and the change of the lateral faces were determined by a Matlab script. The contrast between the white painted plate and the black background makes it possible for Matlab to distinguish the width of the lateral faces. Black color is defined as zero and white as one, by summing the value over the face the width is obtained. Unfortunately there was not used a perfectly black background this made it difficult for Matlab to distinguish the background from the plate. The grey color scale from the background have affected the results, this can be seen from the results obtained as the width suddenly increases during the experiment. This was not a problem for the compression test as the background was perfectly white.

5.3.4 LS-Dyna simulations of the plates

The plates were simulated by using a symmetry plane across the length direction. Since it turned out that the plates was not symmetrically placed over the width a symmetry plane could not be used in the x - direction. This means that half the model was sketched up in LS – Dyna, and simulated. By using a symmetry plane in the y - direction the simulation time will be reduced due to fewer nodes and therefore less iterations. Mass scaling is applied in this model, and the equation for the critical time step is given in Section 5.1.1 equation (5.1). The density is set from $0.95 \cdot 10^{-9} \text{ ton/mm}^3$ to 0.095 ton/mm^3 , though this is a lot there is no particular difference when applying a lower density except increased running time of the

simulation. The element formulation is set to -1 for fully integrated solid elements. This formulation is efficient and intended for elements with poor aspect ratio [11].

In the symmetry plane the edges are detained in the y direction and all rotations are fixed. In addition the middle row of nodes on the edges in the symmetry plane is detained in the z – direction. This way the thickness can vary through the simulation but not the whole specimen. The top of the model is prescribed a motion in the positive y – direction to stretch the plate as done in the testing. A smooth curve is defined to prevent abrupt initiation of the velocity which can lead to incorrect results. The velocity will then reach constant speed after approximately 10 % of full running time.

Solid elements with eight nodes are chosen for the model. The lower part of the model has elements that are wider in the x – direction than in the y – direction. The reason for this is that the material experience large strains due to tensile loading which makes the simulation inaccurate if not the elements are rectangular before the test is initiated. The mesh is illustrated in Figure 5.17.

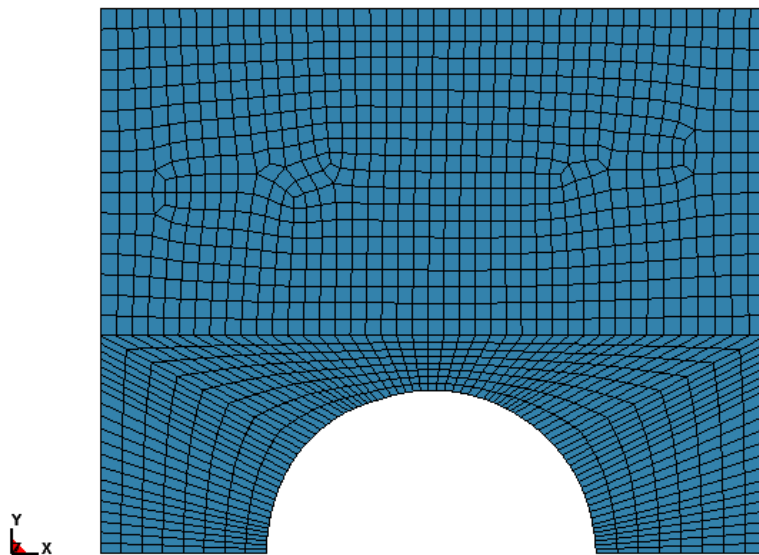


Figure 5.17: The mesh of the plate with a hole.

5.4 Results obtained from the simulations of plate with a hole

All plates with hole have been simulated in LS – Dyna with the correct geometry for each and every plate since the thickness, diameter and the lateral faces differ some for each test. The four different plates are applied to two different velocities and two diameters of respectively 20 mm and 30 mm. All four tests are presented as either the velocity or the diameter is different for all four tests.

5.4.1 Plate with hole of diameter 30 mm, test 01.

The first test performed in the laboratory had a diameter of 30 mm and was subjected to a velocity of 0.05 mm/s. A comparison of the force – displacement curves of the experimental

and simulated data is illustrated in Figure 5.18. There are three main characteristics that are taken into consideration; the peak force, the stabilized force and the overall shape of the curve. By looking at Figure 5.18 it is seen that the force peak is close to identical, but that the simulated curve is slightly stiffer. In addition the simulated force – displacement curve is experiencing secondary hardening. The overall shape of the simulated force – displacement curve is satisfying.

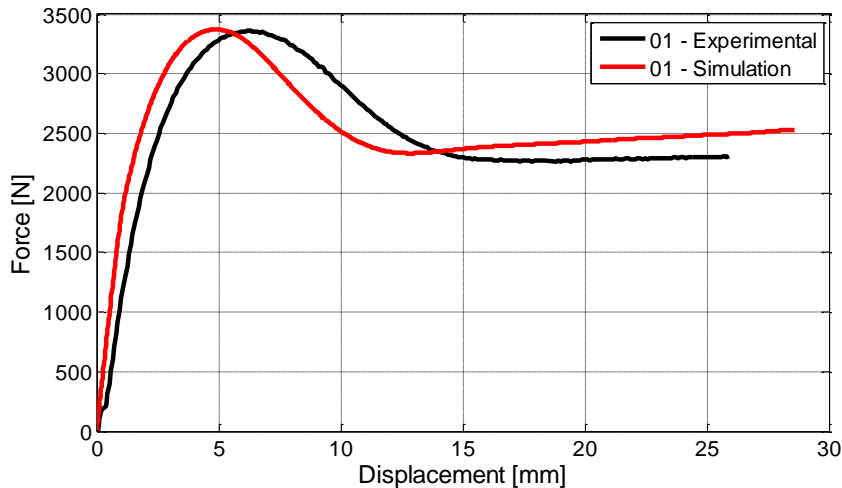


Figure 5.18: Force - displacement curves of plate with hole, $d = 30$ mm

The change in lateral faces, diameter in both directions and thickness

The lateral faces and the diameter of the plate have been determined by a Matlab script, where the contrast between the black test specimen and the white background gives the width of the lateral faces and the dimensions of the diameter in both x – and y – directions. The main reason for measuring this is to see how the material deforms during tensile loading of a plate with a hole. By considering the displacement – time curve of lateral face w_1 in Figure 5.19 it is seen that the two curves have the same initial value and ending value. The overall shape is similar, and the experimental and simulated curves give a good approximation for the validation. The lateral face w_1 stabilizes itself after approximately 300 s. Lateral face w_2 , on the other hand, is not quite as similar. There was a mark at the outer side of the lateral face which made the width incorrect. This curve is therefore not illustrated as there is no reason to compare with the simulation.

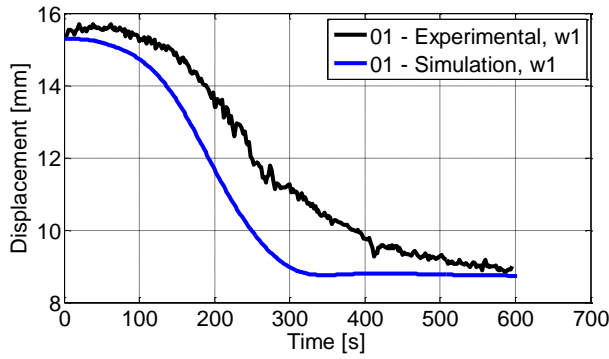


Figure 5.19: Width of lateral face w_1 .

The same procedure was used to determine the thickness of the specimen. Figure 5.20 illustrates the change in thickness during both the simulation and the experimental testing. It is seen that the shape and the ending value are very similar to the experimental curve. By comparing the curve shape to the lateral faces it can be seen that neither the thickness nor the lateral faces are decreasing from approximately 400 s and throughout the test. This is because the specimen has propagated in the necking area which is illustrated in the figure. The reduction of the thickness is happening further away from the cross section. The ratio of the change in thickness is 0.38 while the ratio for the width is 0.56. It is seen that the plate deforms more in the width direction than in the thickness direction. The thickness of the test specimen was measured right after testing on the inner and outer sides of each lateral face. This showed that the inner thickness was thinner than the outer. This was not possible to measure during the test as only the widest part of the lateral face will be visible on the pictures.

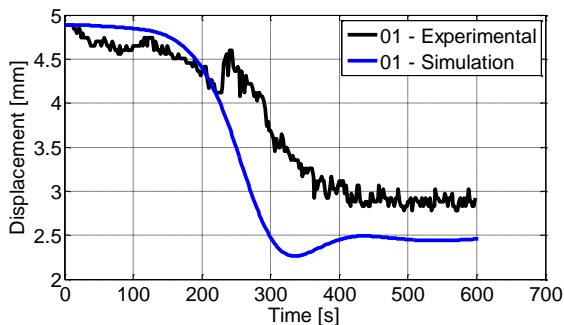


Figure 5.20: Thickness of specimen plate with hole 01.

By studying Figure 5.21 it is seen that the diameter in the x – direction first contracts slightly due to the tensile loading. As the mechanical grips is clamped around the specimen the width of the upper specimen will not change this makes the specimen wider in the upper part which pulls the lateral faces out to each side, and the diameter expands. This happens after approximately 150 s. [10] The two curves are similar in the beginning but differ more during the analysis. The final diameter is quite alike.

The change in the diameter in the y direction is illustrated in Figure 5.22. The experimental test and the simulated test are both parallel through the test. They start off at the same value, but differ slightly as the test continues.

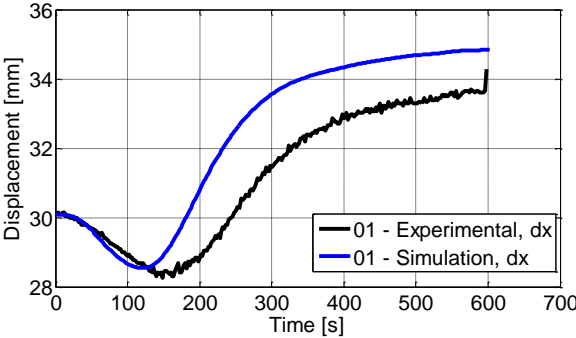


Figure 5.21: Displacement – time curve of diameter in the x – direction.

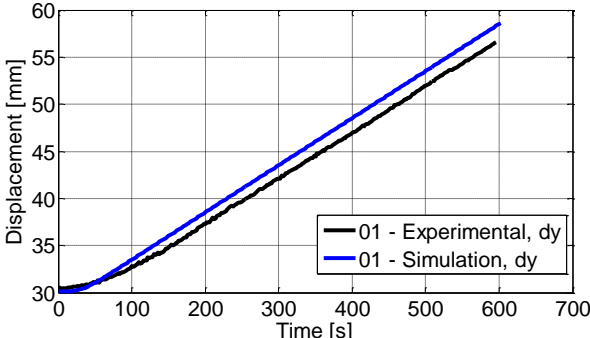


Figure 5.22: Displacement – time curve of the diameter in y – direction.

Strain rate

The strains are plotted against time during the simulation as shown in Figure 5.23. As necking initiates the strains will increase rapidly in the necking area until the specimen experiences propagation. The strains will be largest where the necking initiates which is approximately at the middle of the lateral faces. The strains are therefore taken from a cross section in that area and plotted against simulated time. By differentiating with respect to time the strain rate is obtained. This is illustrated in Figure 5.24. Although the strain rate was estimated to be quasi – static the strain rate will vary locally. The strain rate increases as the necking progresses. When the specimen reaches localized necking the strain rate in the necking area is close to zero, this is logical as the change in strains is very small. The experimental values of the strains obtained are very poor because the 7D program is not able to recognize the black and white pattern due to large strains in the area. There is not much to compare other than the initiation of the strains in the experimental test and simulated model is alike. The experimental test values for the other three tests are not plotted and compared to the simulation as the strains cannot be evaluated when the necking develops.

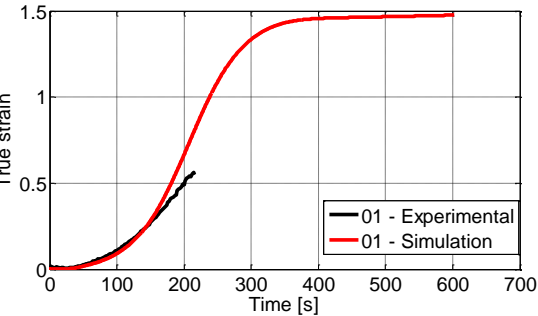


Figure 5.24: True strain – time curve of test specimen 01.

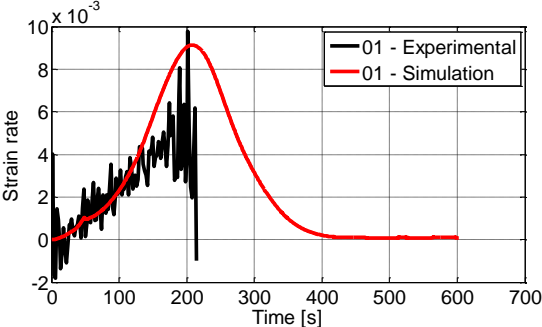


Figure 5.25: Strain rate – time curve of specimen 01.

5.4.2 Results obtained from the plate with a hole of test 02 through test 04

The test results from tests 02, 03 and 04 are represented under the same section as the procedure is identical to the first test described above.

Test 02, plate with a hole of 20 mm

The plate with hole of diameter 20 mm has been simulated in LS – Dyna to see if there are any significant differences from the plate with hole of diameter equal to 30 mm. The force – displacement curves from the experimental results and the simulated results are illustrated in Figure 5.25, and shows that the simulated curve is stiffer than the experimental curve. The displacements for both the curves are taken from the same node and at the same distance from the centre of the hole which is 40 mm. The force peak is slightly higher for the simulated curve, and as seen earlier it is experiencing a second hardening. This is seen from the elevation in force at the end of the simulation. The experimental curve stabilizes at a force of approximately 3000 N. The overall shape of the two curves is satisfactory equal. The experimental curve is a little shorter than the simulated curve due to invalid pictures in that area. As it is clear at which value the force stabilizes it was chosen not to add experimental values measured by the machine.

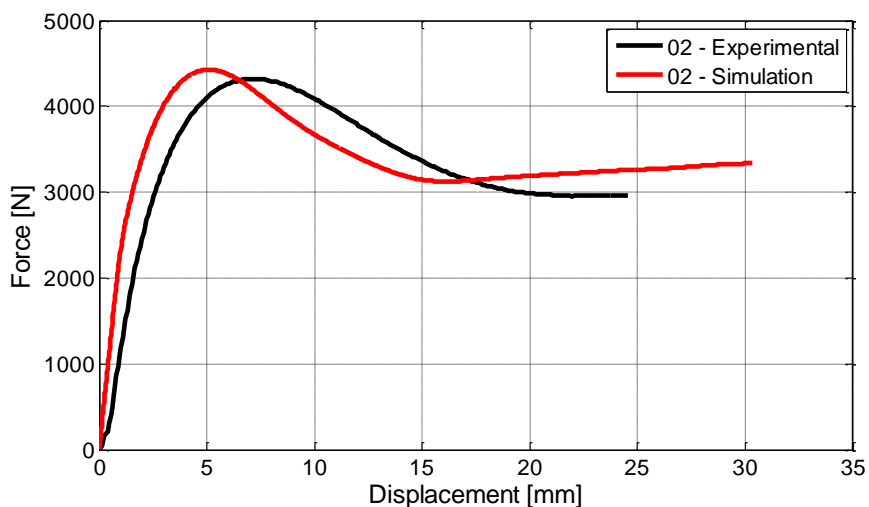
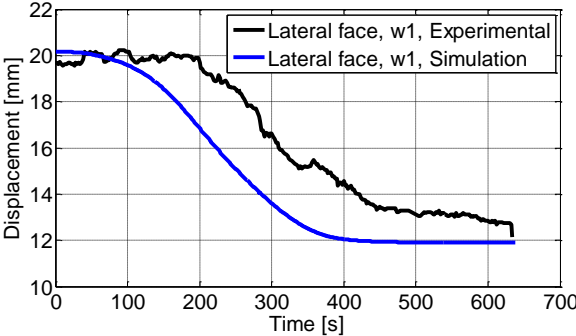


Figure 5.25: Force – displacement curve of plate with a hole test 02.

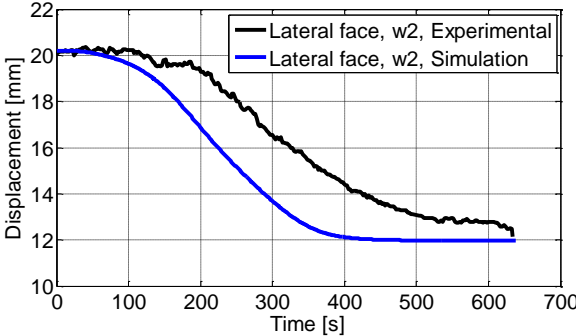
Dimensions of the lateral faces and the diameters of test 02

The lateral faces and the diameter of the hole in both directions are found from the experimental results and from the simulation in LS – Dyna. First, by comparing the changes in lateral faces during testing and simulation it is seen that the initial values and the end values of both curves are close to identical; this can be seen in Figure 5.26 (a) and (b). Though there are differences during the analysis. The ending value is larger for the simulated curves in both x and y directions due to error in the Matlab calculations. This can be said as the test specimen was measured right after the test was performed, and the diameter was measured to be $d = 27.76$ mm which is similar to the analysis. Though, these results cannot be fully trusted as the plate contracts slightly when the test specimen is removed from the

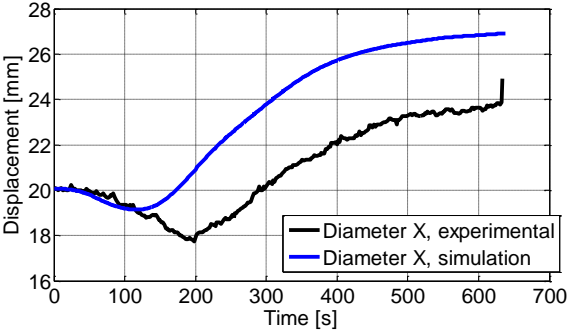
test machine, but it does however give an indication of the value. The diameter in the y – direction was neither measured before nor after testing, and it is therefore difficult to say which one of the values that is most correct. The diameters are illustrated in Figure 5.26 (c) and (d). Figure 5.26 (e) shows the experimental and simulated curves of the thickness of the specimen. The two curves start off at the same point and follow the same shape during the first 300 s. In the end the displacements differ with about 1 mm which is quite a lot when the thickness was 5 mm in the first place. Nevertheless, the overall shape of all five of the curves is similar and comparable.



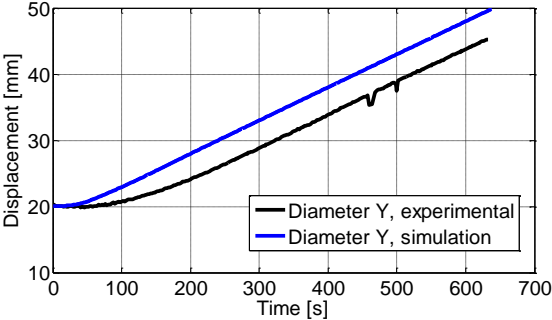
(a) Displacement – time of lateral face w_1



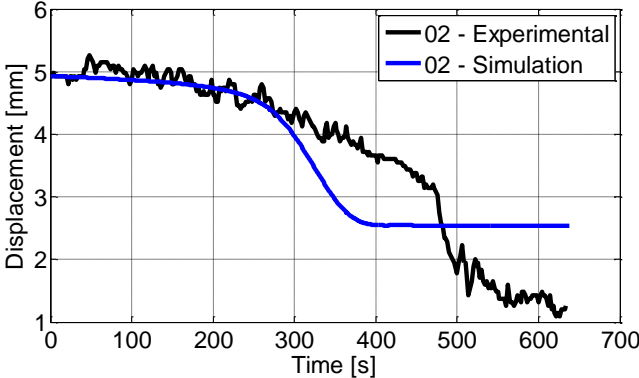
(b) Displacement – time of lateral face w_2



(c) Displacement – time curve of the diameter in the x - direction



(d) Displacement – time curve of the diameter in the y - direction



(e) Displacement – time curve of the thickness

Figure 5.26: Comparison between the experimental and the simulated curves of changes in lateral faces and diameter

Strain rate

Test 02 was applied the same velocity as test 01, but the diameter of the hole is 10 mm wider. The strains and the strain rate are plotted against time and compared to test 01 to see if there will be changes as the lateral faces are wider for test 02. By considering Figure 5.27 and Figure 5.28 it is seen that the strains in test 01 is slightly higher which leads to a difference in strain rate. The reason for this difference is due to more localized necking in test 01. As the plate from test 02 has wider lateral faces the necking will be less localized which leads to less strains in the necking area i.e. the strain rate will be lower for test 02 [10].

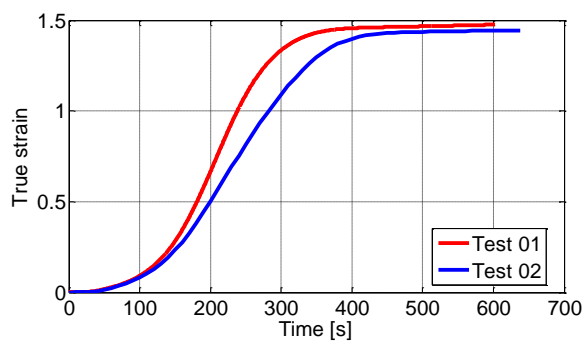


Figure 5.27: True strain – time curve of tests 01 and 02.

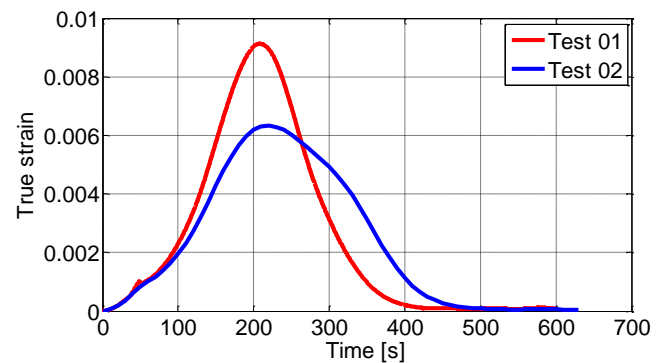


Figure 5.28: Strain rate – time curve of tests 01 and 02.

Plate with hole of 30 mm, test 03

The third test, 03, was applied a velocity of 0.5 mm/s, and had the same diameter as test 01 that is 30 mm. As seen in Figure 5.29 the force – displacement curve of the two curves are close to identical. The force peak hits exactly the same point as well as the declining part of the curves. The model is experiencing secondary hardening and does not follow the stabilizing force, at approximately 2400 N. During the test the camera was placed too close to the specimen which means that the cross section 40 mm from the centre is not in the picture. Therefore the test data obtained from the machine is inserted from the dot marked in Figure 5.29.

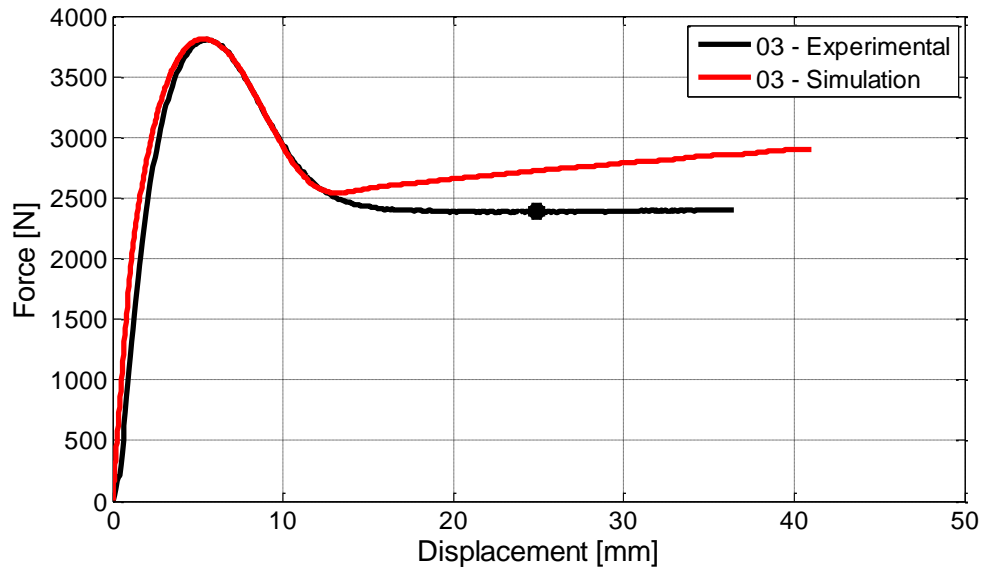
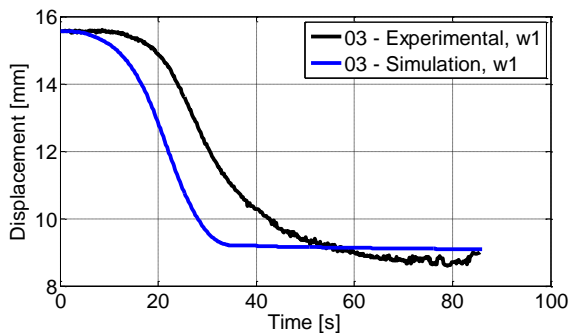


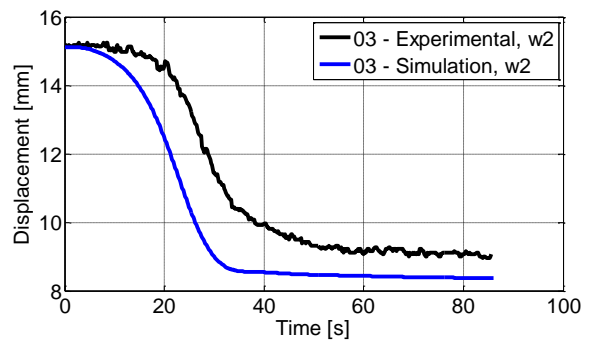
Figure 1.29: Force – displacement curve of plate with a hole of diameter 30 mm, test 03.

Change in lateral faces, thickness and diameter, test 03

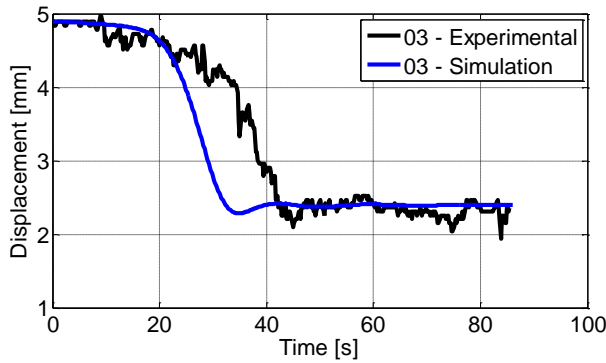
The change in the width of the lateral faces and the diameter is shown in Figure 5.30 (a), (b) and (c). The overall shape between the experimental and simulated curves is more similar for this test as the pictures obtained during testing had fewer disturbances. By comparing the displacements in the thickness direction and in the transverse direction it is seen that there is a slightly difference, taking the ratio for the transverse displacement gives 0.58 and the ratio for the thickness direction gives 0.5. This means that the material HDPE is not perfectly isotropic but close to. This ratio is not calculated for the other tests as there was too much insecurity in the experimental tests due to background noise in the pictures taken.



(a)



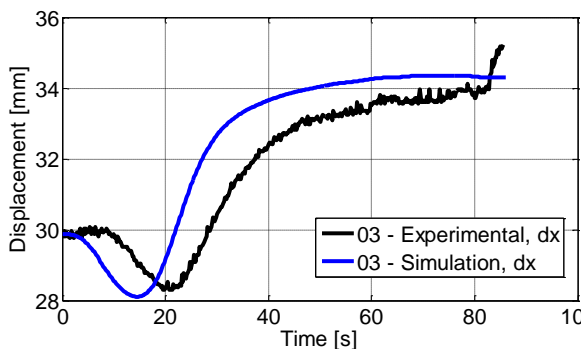
(b)



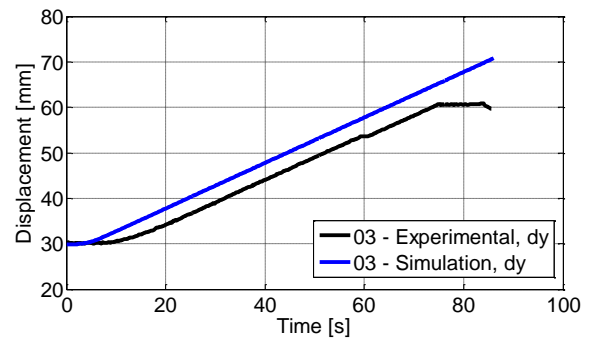
(c)

Figure 5.30: (a) Displacement – time curve of lateral face w_1 , (b) displacement – time curve of lateral face w_2 and (c) displacement – time curve of the thickness.

The diameter in the x – direction is illustrated in Figure 5.31 (a) and shows how it first is pulled together and then pulled out again due to the wider upper part of the test specimen. It can also be seen that the displacements are approximately constant during the localized necking condition at the end of the test. Figure 5.31 (b) illustrated the displacement of the diameter in the y – direction follows the displacement controlled tensile loading that the specimen was subjected to.



(a)

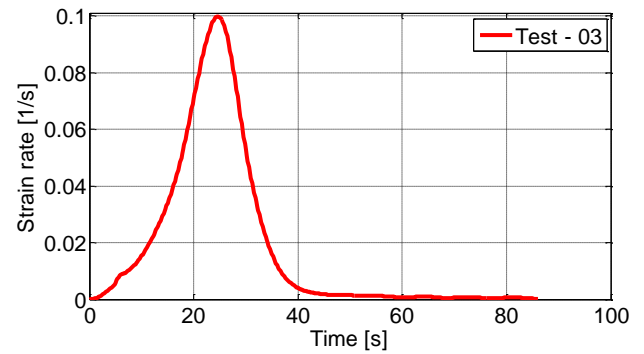
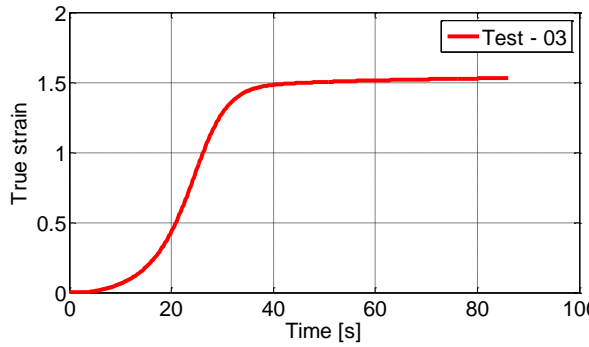


(b)

Figure 5.31: (a) Displacement – time curve of the diameter in the x – direction and (b) displacement – time curve of the diameter in the y – direction.

Strain rate

As the third test, 03, was applied a velocity of 0.5 mm/s the strain rate was determined to see the changes of the strains through the test. The diameter of the hole is 30 mm as for test 01. The strains and the strain rate are both plotted against time, and illustrated in Figure 5.32 (a) and (b) where the simulated and the experimental curves are both represented. It is seen from the curve that the strain rate is 10^{-2} s^{-1} in the beginning of the test, but as the necking progresses the strain rate increases up to 10^{-1} s^{-1} .



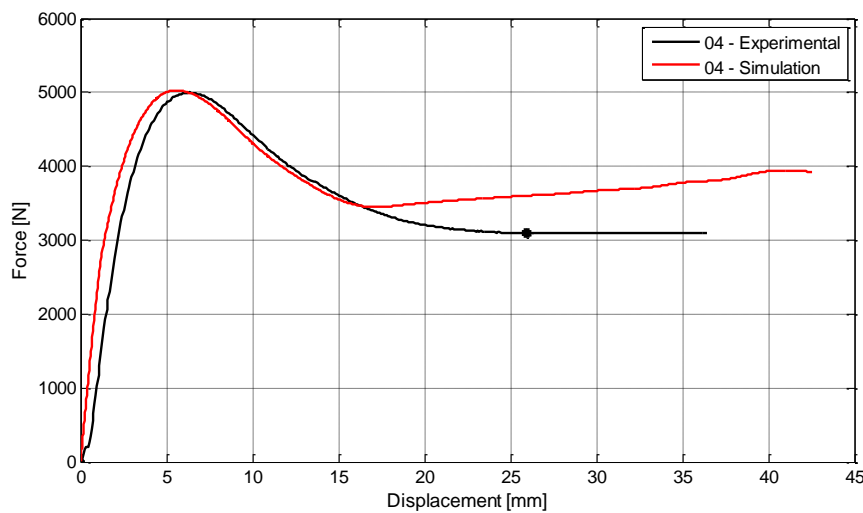
(a)

(b)

Figure 5.32: (a) True strain – time curve of test 03 and (b) strain rate – time curve of test 03.

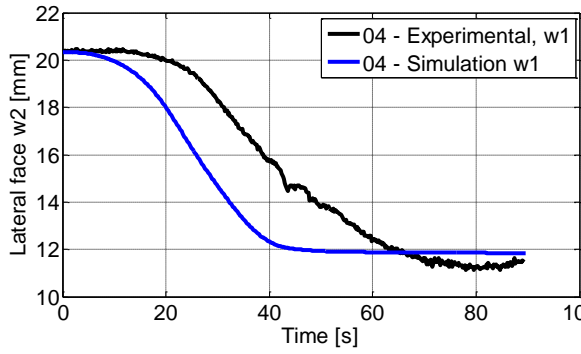
Plate with hole of 20 mm, test 04

The last test had a diameter of 20 mm, and was applied a velocity of 0.5 mm/s. The force – displacement curve illustrated in Figure 5.33 shows that the ascending part of the curve, the force peak itself and the declining part is very similar. The difference is the stabilizing force which starts off a lot earlier and experiences a second hardening in the simulated curve. Also in this case the cross section taken 40 mm from the centre is not captured in the picture after approximately 60 s of the running time. Therefore experimental data obtained from the machine is inserted from the dot marked in the figure.

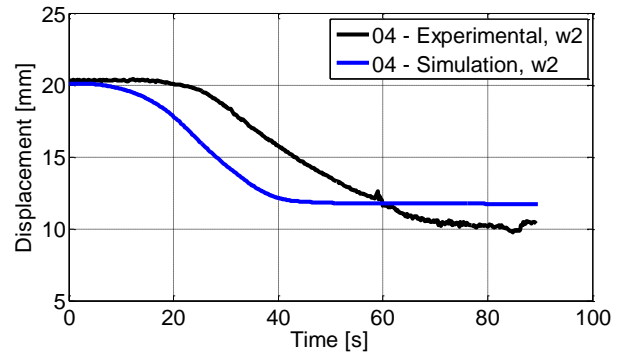


Change in lateral faces, thickness and diameter

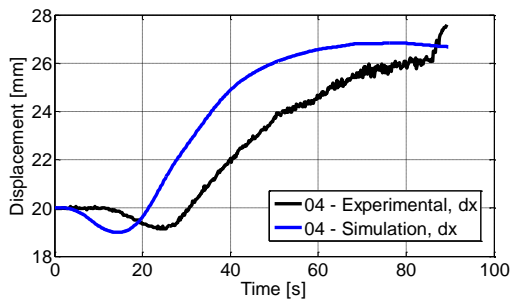
Further on, the lateral faces and diameters are following the overall shape nicely as seen in Figure 5.34 (a) through (d).



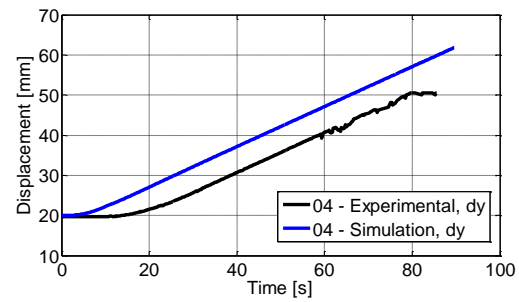
(a) Lateral face w_1



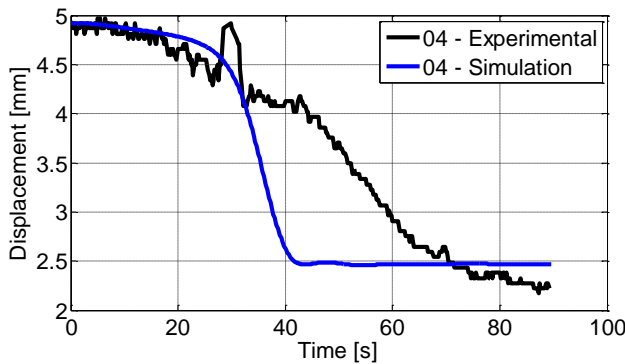
(b) Lateral face w_2



(c) Diameter in x - direction



(d) Diameter in y - direction



(e) Thickness

Figure 5.34: Displacement – time curves of (a) lateral faces w_1 , (b) lateral face w_2 , (c) diameter in x – direction, (d) diameter in y - direction and (e) thickness.

Strain rate

The true strain – time curve is illustrated in Figure 5.35 and maximum strains are 1.5 while for test 03 the maximum strains are 1.53. The difference due to a smaller diameter in test 04, although the difference is very small compared to each other. The strain rate – time curve is illustrated in Figure 5.36.

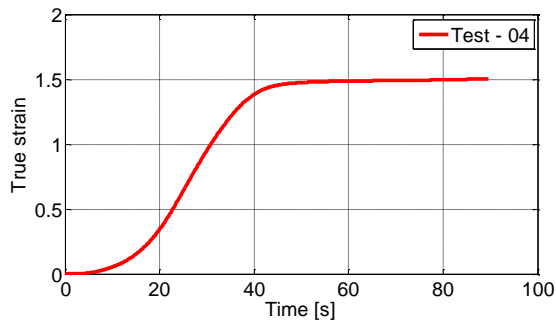


Figure 5.35 True strain – time curve

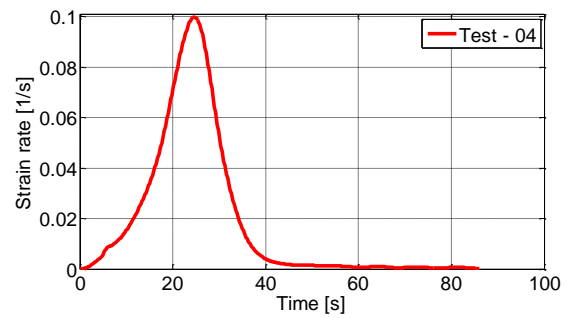


Figure 5.36 Strain rate – time curve

Force – displacement curves of all four tests

Figure 5.37 illustrates the force – displacement curves of all plate with a hole tests performed, and it is seen that the force – displacement curves varies depending on both the diameter of the specimen and the velocity applied. A higher velocity and a wider diameter results in a higher force peak.

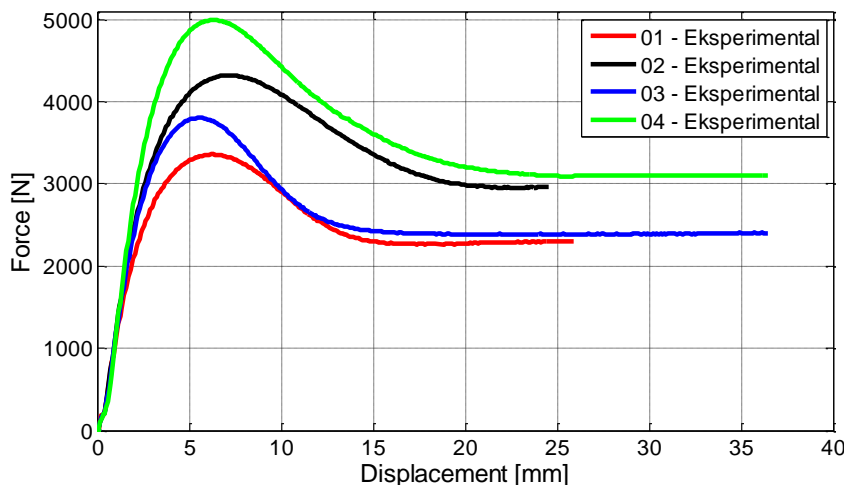


Figure 5.37: Force – displacement curves are illustrated for all plate with a hole tests performed.

5.4.4 Young's modulus

It is seen in the force – displacement curves that the elasticity modulus is too stiff in some occasions. Therefore a variety of simulations were performed to see which Young's modulus that would fit each test the best. The reason for wanting to try this out is that polymers as HDPE is experiencing viscoelasticity, and the material model in LS – Dyna does not account for this, the material model implemented in LS – Dyna is elastic – viscoplastic.

Figure 5.38 below shows the first test of plate with a hole applied to different elasticity modulus'. By studying the curves it is seen that a Young's modulus of $E = 600 \text{ MPa}$ is a much better fit. The force peak is closer as well as the initiation of the curve up to force peak.

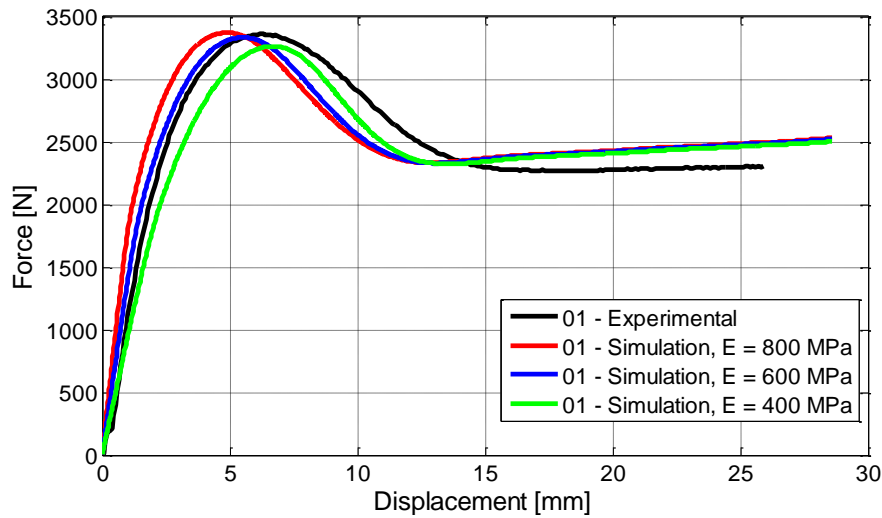
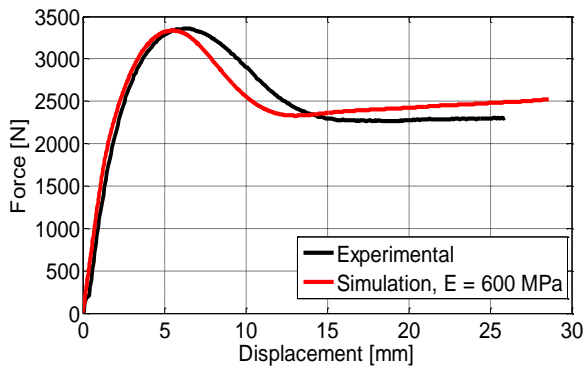
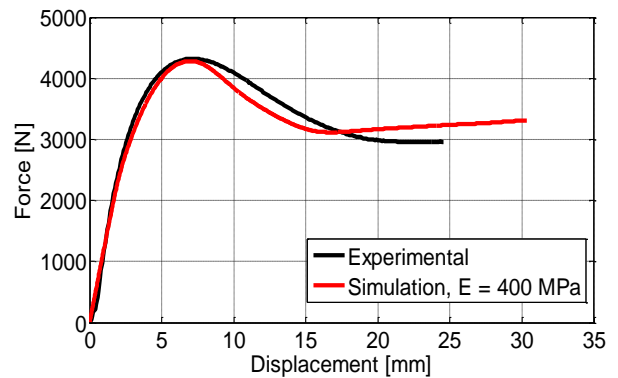


Figure 5.38: Force – displacement curves of plate with a hole test 01 applied different Young’s modulus’s.

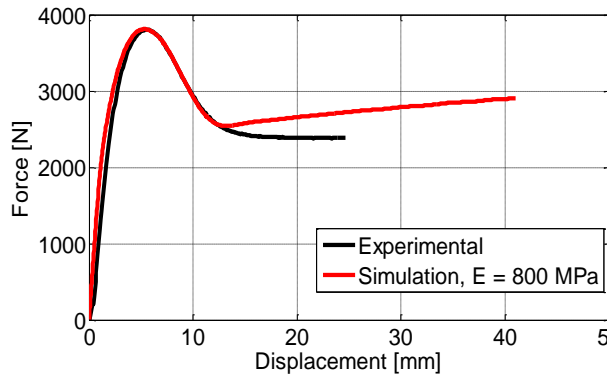
All the plates with hole have been applied different Young’s modulus’ to see which one of them would make the best fit. The Young’s modulus have been seen to differ quite a lot depending on if the test have been applied a high strain rate or if the test performed is quasi-static. The quasi-static tests shows that the Young’s modulus is lower for these tests, as the strain rate increases the Young’s modulus increases as well. In addition the diameter of the plate is significant. A wider diameter leads to more localization of strains. This leads to a higher local strain rate and the Young’s modulus will therefore be higher [10]. The Young’s modulus that results in the best fit for each test is illustrated in Figure 5.39 below.



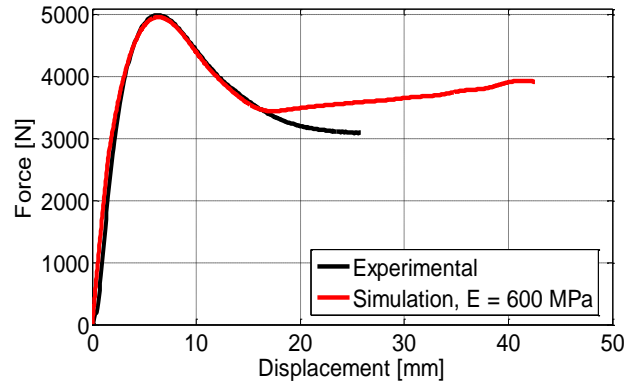
(a) Force – displacement curve of plate 01 of diameter 30mm and applied a velocity of 0.05 mm/s.



(b) Force – displacement of plate 02 of diameter 20 mm and applied a velocity of 0.05 mm/s.



(c) Force – displacement of plate 03 of diameter 30 mm and applied a velocity of 0.5 mm/s.



(d) Force – displacement of plate 04 of diameter 20 mm and applied a velocity of 0.5 mm/s.

Figure 5.39: Force – displacement curves of all tests of plate with hole (a through d) applied the Young's modulus which makes the best fit for each test.

5.5 Drop Tower testing

5.5.1 Introduction

To evaluate the material model it is important that the validation model is subjected to more complex situations according to stresses and strains. A real component will be stretched, compressed and undergo different velocities when applied in the industry. In addition it is important that the boundary conditions and loading condition are well defined to minimize the uncertainty in the validation process. The friction between the sphere and the plate will make some uncertainties in the model and will be a source of error in this testing [10].

5.5.2 Experimental program of drop tower testing

There were performed six drop tower tests all of different magnitudes. A plate of about 100 mm in both length and width was placed into the Instron CEAST 9350 machine. The specimen was lying on top of a hollow cylinder with a 15 mm wide edge. A long shaft made of metal was lifted up, and let fall. The tip of the shaft was shaped like half a sphere of radius 10 mm. There was applied different amount of weights, velocities and fall height dependent on how much the material would endure. Two tests led to fracture and that was test DT – 4 and DT – 5. An overview of all tests performed in the drop tower is given in Table 5.3.

Table 5.3: Drop tower testing

Test #	Weight [kg]	Velocity [m/s]	Fall height [m]	Energy [J]	Maximum force [N]	Maximum displacement [mm]
DT - 1	5.045	4.4	1	50	5499	16.92
DT - 2	5.045	6.263	2	100	6303	23.89
DT - 3	10.045	4.4	1	100	6276	15.95
DT - 4	10.045	6.263	2	200	6469	24.17
DT - 5	10.045	5.4	1.5	150	6336	20.06
DT - 6	10.045	4.85	1.2	120	6114	18.17

The shaft was dropped, and the fall height was adjusted by a spring that is attached to the shaft. The fall height differed from between one and two meter. There were added weight on top of the plate attached to the shaft, and the two first tests had an additional weight of 5.045 kg, while the four last ones had 10.045 additional kilos. Figure 5.40 illustrates the setup of the plate right after the specimen has been hit by the sphere.



Figure 5.40: The plate and the shaft right after impact.

5.5.3 Simulation of drop tower

The drop tower tests were simulated by using axisymmetry where only one thin section was sketched and simulated both for the plate and the sphere. The right end is fixed, see Figure 5.41 for illustration. Since this end was clamped between two metal grips the model could have been modeled with the clamps by adding contact definitions. However, this method was not chosen. Further on, the left side is detained in the x – direction so as to prevent any displacements other than in the y direction. The sphere is only constrained in the x – direction on the left side. Both the sphere and the plate was modeled by shell elements, and is applied a shell thickness of $1/2\pi$. There was applied a mass of respectively 5.045 kg and 10.045 kg that was implemented by calculating the density of half a sphere including a cylinder of height and radius equal to 10 mm. The density was then implemented in the LS – Dyna material card. The material used for the sphere was chosen as 001 – Elastic and the properties for steel were inserted. Figure 5.41 below illustrates the simulated model of the drop tower test.

The sphere was dropped in the experimental tests, and this was modeled in LS – Dyna by adding an initial velocity to the sphere.

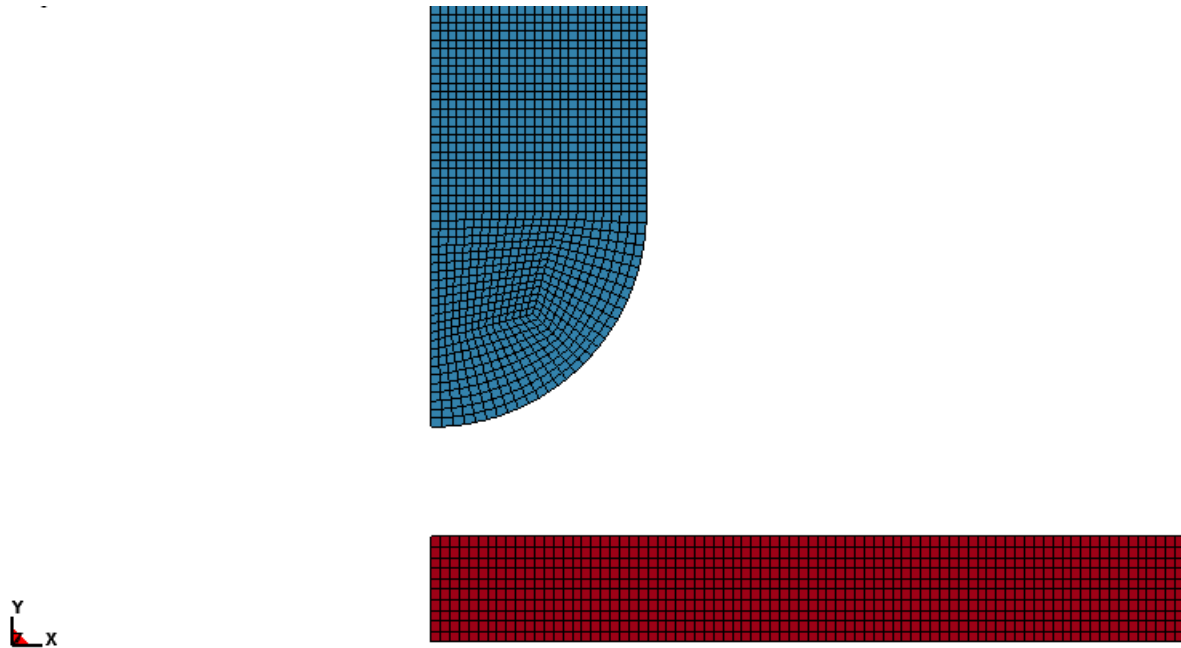


Figure 5.41: The mesh of the simulated model of the drop tower test.

The mesh shown in Figure 5.41 is 0.6 mm in both x and y directions making the elements quadratic. This applies to both the plate and the sphere. A four node axisymmetric solid element formulation is chosen for the model. The elements have a symmetry around the y – axis and are volume weighted [11].

In these models there have not been necessary to use mass scaling as the running time is set to approximately 16 milliseconds which was the running time of the experiments performed. The critical time step is then kept small which is important to avoid information to propagate more than the distance between adjacent nodes during a single time step [12].

The contact definitions are important in this analysis, and the most common type for crash analyses is 2D automatic single surface. The slave surface is typically defined as a list of part ID s, and the master surface is not defined. This contact definition includes self – contact in addition the contact is considered between all the parts in the slave list [15].

Friction is another important parameter during this test, and will also be an important source of error. It has therefore been performed several simulations with different friction coefficients ranging from 0.1 - 0.3. The first simulation was run with no friction at all [16].

5.5.4 Results obtained from the drop tower tests

The first test, DT – 1, was applied a kinetic energy of 50 J and a mass of 5.045 kg which makes the velocity equal to 4400 mm/s. A drop tower test is a lot more complicated, and there are more factors involved. Figure 5.42 illustrates the force – displacement where the experimental and the simulated curves are compared. It is seen that the force peak is close to identical but the simulated curve is stiffer than the experimental curve. The initial part of the curve is a good approximation, and fits nicely. As viscoelastic parameters are not

implemented in LS – Dyna the unloading of the simulated test will not match the experimental test. However, the first part of the declining is quite parallel to the experimental curve.

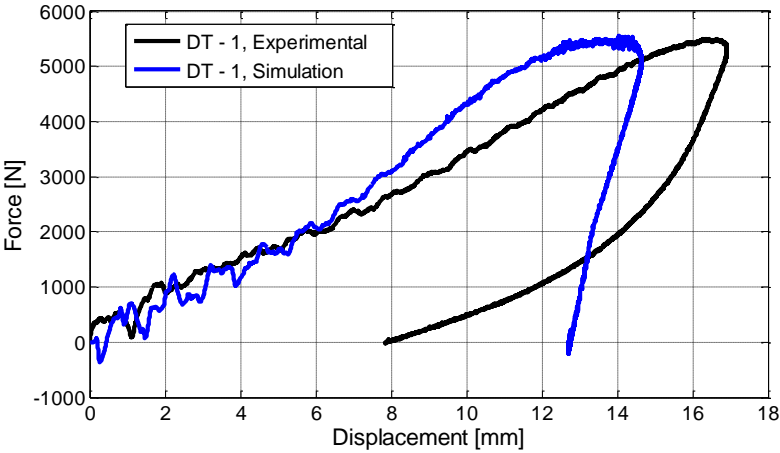


Figure 5.42: Force – displacement curves of drop tower test 1

When the test specimen is hit by the falling sphere the specimen is pushed downwards into the cylinder making a plug where the sphere hit. As the specimen is fixed, due to the mechanical grips clamping around the plate, the plate has no ability to contract and the plate is forced to stretch. This means that the plate gets slightly longer, and a membrane effect is obtained. The specimen will in particular experience a lot of strains near the plug.

Drop tower test 2 is applied the same mass, but the energy is increased to 100 J since the first plate did not experience much deformation. The force – displacement curve of test 2 is illustrated in Figure 5.43 and shows that the force peak is not very similar in this test. The beginning of the ascending part of the curve is however similar. The force – displacement curve does not match quite as good in this test as the first test, DT – 1.

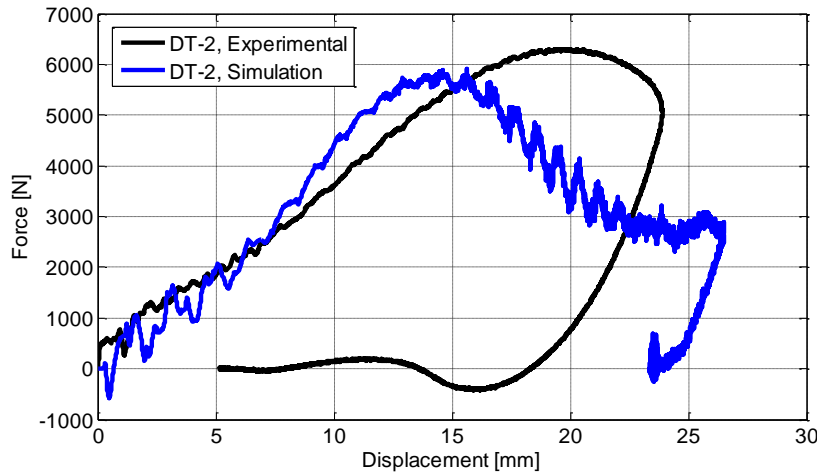


Figure 5.43: Force – displacement curves of drop tower test 2.

The tests DT – 4 and DT – 5 both experienced fracture, the specimens where added a mass of 10.045 kg and kinetic energy of 200 J and 150 J respectively. In test DT – 4 the cap of the plug was flung open, it was clear that there had been large forces working on the specimen. It was desired to see how much displacement the material could hold before it fractured, and therefore another test was performed of lower energy to hope for it to hold. It did not. The cap of the plug on test DT – 5 was barely torn open which means that the plate could almost hold the impact. Therefore a sixth test, DT – 6, was performed hoping that the sphere would not penetrate the plate, but make a big plug. The specimen withheld the impact forming a huge plug in the test specimen. The color of the material is black, but the plug had changed to a grayish color. The grayish layer can be removed by scratching on it with a sharp instance.

In the drop tower test the friction will be of major influence, and it has therefore been performed several analysis of different coefficients of friction ranging from 0.1 to 0.3. Figure 5.44 illustrates that a friction coefficient of 0.1 fits best to the experimental curve.

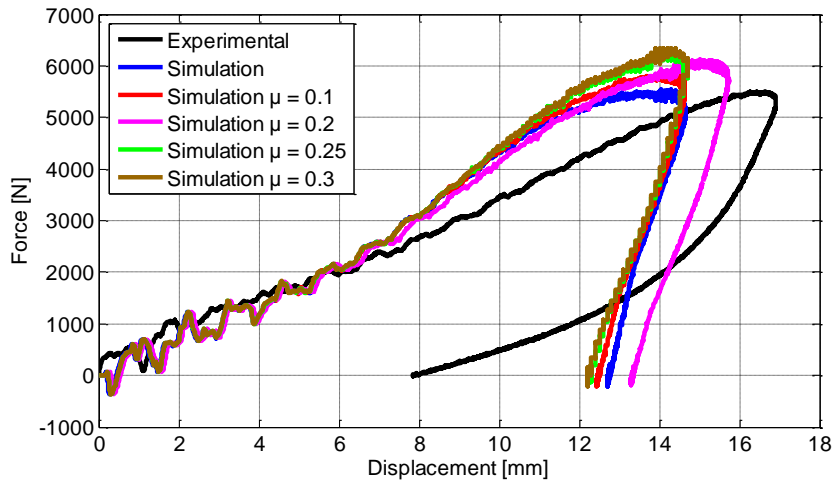


Figure 5.44: Force – displacement curves of drop tower test 1 applied different coefficients of friction.

When considering the force – displacement curve it is clear that the simulated curves are stiffer than the experimental ones. Various simulations with different modulus' of elasticity were run to see if there would be any significant outcomes, both near the force peak and the unloading. Figure 5.45 illustrates the force – displacement curves of test DT – 1 applied different Young's modulus'. By applying a Young's modulus of 400 MPa it is seen that the initiation of the curve makes a poorer fit, but the unloading part is more parallel. The curves shows that there are two different elasticity modulus' for the drop tower test; one for the loading and another for the unloading. The reason for this occurrence is that the specimen is applied a high velocity leading to large strains and this makes the elasticity modulus higher. When the projectile stops and reverses the velocity will be lower than the incoming velocity. This makes the strain rates lower during unloading which leads to a lower elasticity modulus in the descending part of the curve.

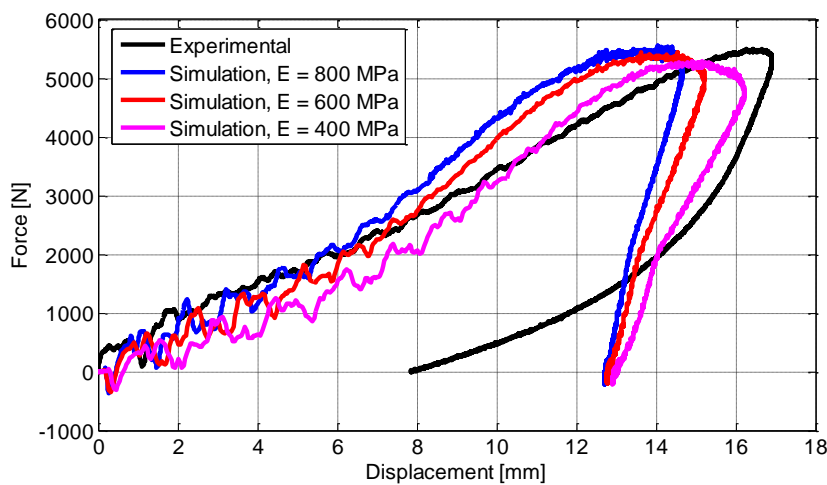


Figure 5.46: Force – displacement curves of drop tower tests applied various Young's modulus'

The force – displacement curves of four of the tests performed is illustrated in Figure 5.46 to compare the shapes of the tests. It is seen that the initiating part of the force – displacement curve is similar for all the tests. The difference lies in the force – peak and the unloading. The two first tests, DT – 1 and DT – 2, is applied the same amount of weights, but the velocity is increased in the second test. Neither of these tests provided more than a dent in the plate. The fourth and the sixth tests are both applied weights of 10.045 kg, and a velocity of 6263 mm/s and 4850 mm/ s respectively. Test DT – 4 went right through, and the cap of the plug was flung open. The sixth and last test did not fracture, but it was close. The displacements were not measured manually after the testing as it was very difficult to get the height of the cap. For this to be done it would have been necessary to cut the specimen in two pieces. This way both the displacements and the thickness of the specimen could have been measured.

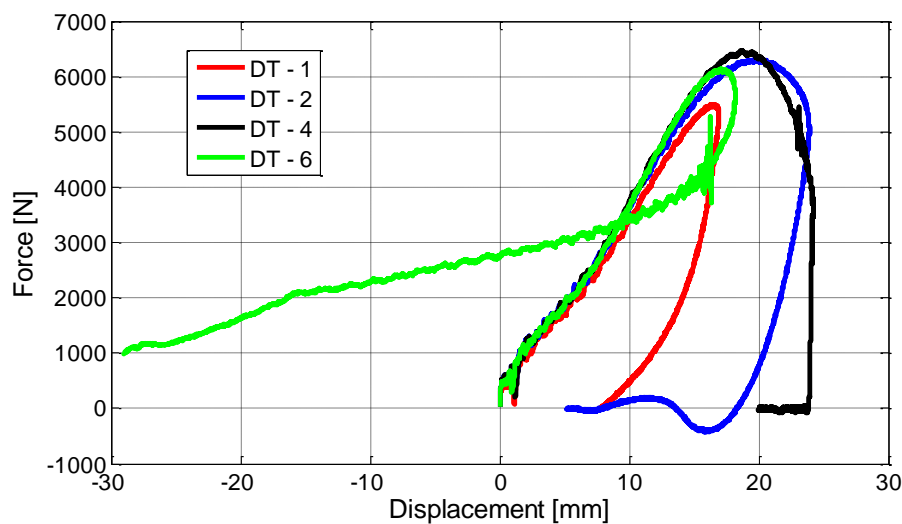


Figure 5.46: Force – displacement curves of drop tower tests 1, 2, 4 and 6.

5.5.5 Stresses at the tip of the plate

The plate experiences a lot of stresses during the impact between the plate and the sphere. There are both tensile and compression stresses present during the test. First the plate will endure compression stresses as the sphere hits the plate, and they will be as large as approximately 50 MPa. As the plate is bent further down the upper side of the plate experience tensile stresses up to about 90 MPa. This is quite a lot, but the deformations close to the projectile are large. Figure 5.47 illustrates the stress – time curve from the simulation. As there was not used a camera during the drop tower test it is not possible to compare the stresses and strains to the experimental results.

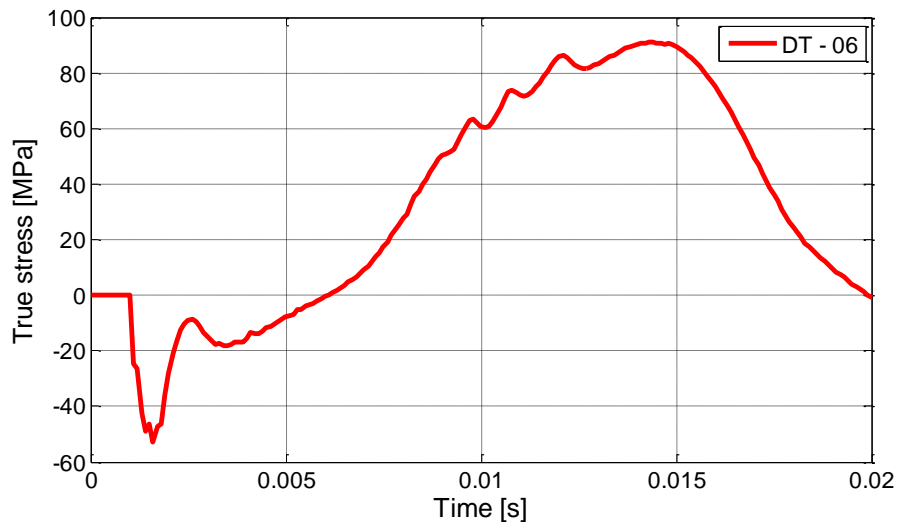


Figure 5.47: True stress – time curve of drop tower test 6.

5.6 Discussion and source of error

The experimental tensile tests are experiencing an increase in temperature due to elevated strain rates in the true stress – strain curves this is illustrated in Figure 3.6 (e). This makes the material behavior more soft which leads to less steeper curve. LS – Dyna does not consider temperature changes during an analysis. The material model is calibrated from the tensile test of low strain rate which has a steeper curve. When the model is applied a higher velocity the curve is just elevated without any softening effect present.

There are performed a variety of simulations of different elasticity modulus of both tensile tests and plate with a hole. The reason for performing these analyses is to determine how important the viscoelastic effect is, since this is not accounted for in the material model in LS – Dyna. The simulations shows that the viscoelasticity has an influence on how the force – displacement responds, and that there are some misleading results as this is not considered. On the other hand, the viscoelasticity effect is not suppose to be that significant for large deformations, and all tests performed in this thesis are applied to large deformations and stress – strain relations. Another aspect of not implementing the viscoelastic effect into the material card in LS – Dyna is that the simulations would have been a lot more complicated.

The plate with a hole has a slightly more complex geometry than the uniaxial tensile test, and that was also the purpose of validating these specimens. To be able to make an appropriate validation of the material model it was necessary to use a more complex stress – strain response than the uniaxial tensile test. The inside of the hole is experiencing large strains; it was not even possible to get out any strains after 200 s as the mesh was completely ruined in 7D. This makes it very difficult to compare local variations in the specimens. Therefore the experimental strains have not been taken into much consideration.

As not all pictures have had a perfect solid – colored background this have affected the results obtained from Matlab. When the thickness, diameters and the lateral faces was measured there will be some errors due to background noise. The grayscale was adjusted to the utmost ability, but there are some inaccuracies present. When the compression tests was performed a solid – colored background was used which makes these results more reliable. There is less inaccuracy during these tests.

When performing experiments and simulations of impact problems as the drop tower testing there is many aspects to take in consideration such as complex stress – strain responses. During these tests friction was an important factor to considerate, and it is room for error when simulating these tests. It was seen by Figure 5.x that by applying different coefficients of friction there was variations in forces. The friction is considered a “dark horse” in the impact simulations [10].

The coefficient C is determined in the quasi – static tensile test at a strain rate of 10^{-3} s^{-1} , in the impact simulation the strain rate is experienced to be roughly 100 s^{-1} to 1000 s^{-1} , the yield stress is therefore extrapolated to a satisfactory value as this is unknown. This will be a source of error during the simulation of the drop tower.

The flow criteria in the model determine how the plastic strains develop in the model. β affects the change in thickness during the analysis, and was determined in the calibration to be equal to 1. If this constant is incorrect this may lead to error in the plastic strains as well as for the necking [10].

6. Conclusion

The experimental tests were subjected to nominal strain rates ranging from 10^{-3} s^{-1} to 10^{-1} s^{-1} . It was seen that the stress – strain curves subjected to a nominal strain rate of 10^{-3} s^{-1} crossed the curves subjected to a nominal strain rate of 10^{-1} s^{-1} . The reason is that when the material is subjected to high strain rates the temperature increases which makes the material softer. This shows that HDPE is strain rate dependent due to elevated temperatures that leads to changes in the material behavior.

The tensile tests, plate with a hole tests and the drop tower tests were all simulated with different Young's modulus'. As the results of the force – displacement curves was more similar to the experimental results in some of the occasions, it showed that there are viscoelasticity that is not taken in consideration during the simulations, and that this affects the results.

During the material testing of the compression tests the longitudinal and the transverse strains were plotted in the same figure. This showed that the transverse strains are close to half the longitudinal strains. This means that HDPE does not experience any significant change in volume and the material is considered an isochoric material.

A further study of this thesis would be to implement a viscoelastic effect into the material model in LS – Dyna. In addition there could have been performed a thorough calibration instead of the partial recalibration performed in this thesis.

7. Reference

- [1] SIMONA - Product Information PE-HWU/HWST, 1995
- [2] M. Polanco-Loria, A.H. Clausen, T. Berstad and O.S. Hopperstad – A constitutive model for thermoplastics intended for structural applications, 2009
- [3] J. Rosler, H. Harders and M. Baker – Mechanical Behaviour of Engineering Materials, 2006
- [4] A.H. Clausen, M Polanco-Loria, MT Hovden, M Haugen, OS Hopperstad - "Experimental and numerical study of HDPE and PVC at different loading conditions", In preparation for possible journal publication (2012).
- [5] A.H. Clausen, M. Polanco-Loria, T. Berstad and O.S. Hopperstad – A constitutive model for thermoplastics with some applications, 2011
- [6] Hovden M.T. – Tests and numerical simulations of polymer components, Master Thesis 2010.
- [7] A. H. Clausen – Geometry of tensile specimen.
- [8]] R.F. Moura, A.H. Clausen, E. Fagerholt, M. Alves, M. Langseth – Impact on HDPE and PVC – Experimental tests and numerical simulations, 2010
- [9] O. S. Hopperstad and T. Børvik – Lecture Notes TKT4135 Mechanics of materials, 2012
- [10] A. H. Clausen – Personal communication
- [11] Livermore Software Technology Corporation (LSTC) – LS – Dyna Keyword manual Volume1. Version 971, 2007.
- [12] K. M. Mathisen – Lecture Notes, Non-Linear Finite element analysis. Lecture 9 – Solution of the Nonlinear Dynamic Equilibrium Equations.
- [13] Y. Ling – Uniaxial True Stress – Strain after Necking, 1996
- [14] M. Andersen – Personal communication
- [15] LS – Dyna support: <http://www.dynasupport.com/tutorial/ls-dyna-users-guide/contact-modeling-in-ls-dyna>.
- [16] matbase.com – friction coefficient of HDPE.

Appendix A

Tensile testing

The tensile tests were performed in the laboratory at NTNU in February 2012. The material Polyethylene (HDPE) was delivered by a German company called SIMONA.

The uniaxial tensile tests are presented with key data and pictures. The test results of the force – displacement curve, stress – strain curve and longitudinal versus transverse strains are illustrated for each tensile test performed. The geometri of the tensile specimen is illustrated below.

The most essential key data is given as:

w_0 – initial width, [mm]

t_0 – initial thickness, [mm]

$\dot{\epsilon}$ - nominal strain rate, [s^{-1}]

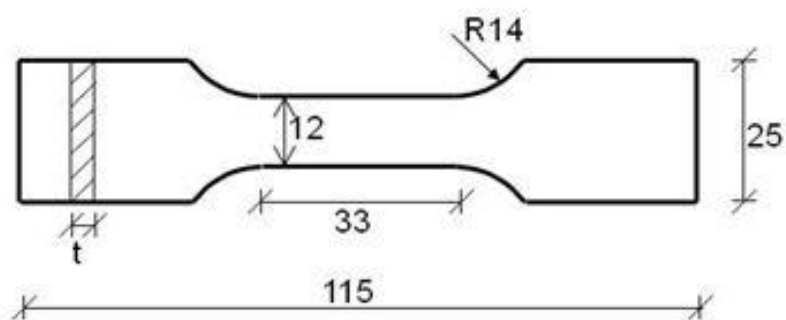
v – velocity, [mm/s]

F_{max} – Maximum force, [N]

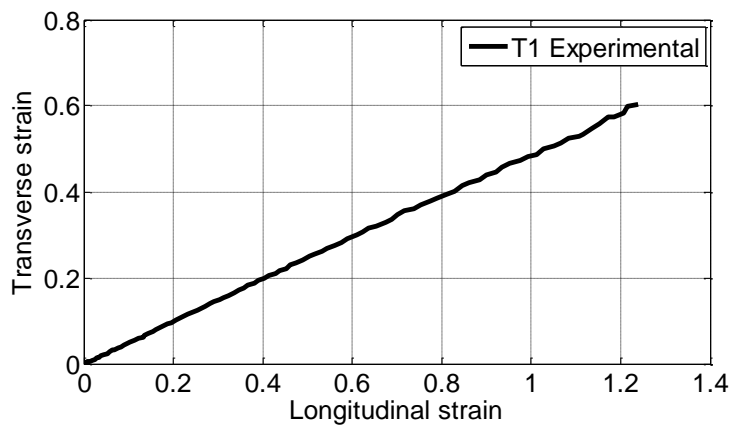
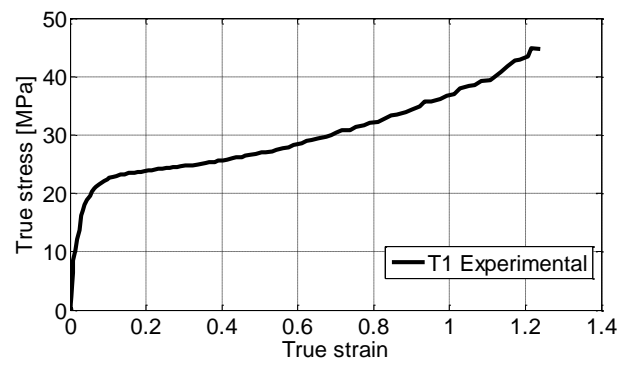
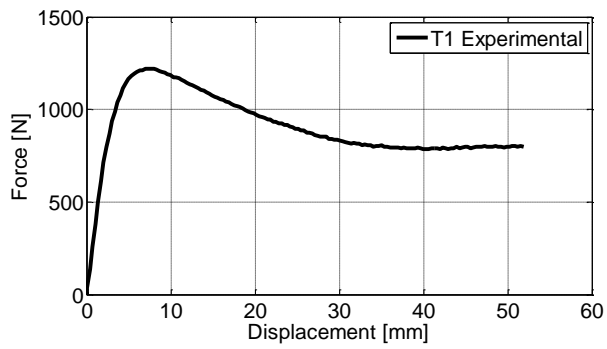
σ_y – yield stress, [MPa]

Δ_{max} – Maximum displacement, [mm]

v – contraction ratio

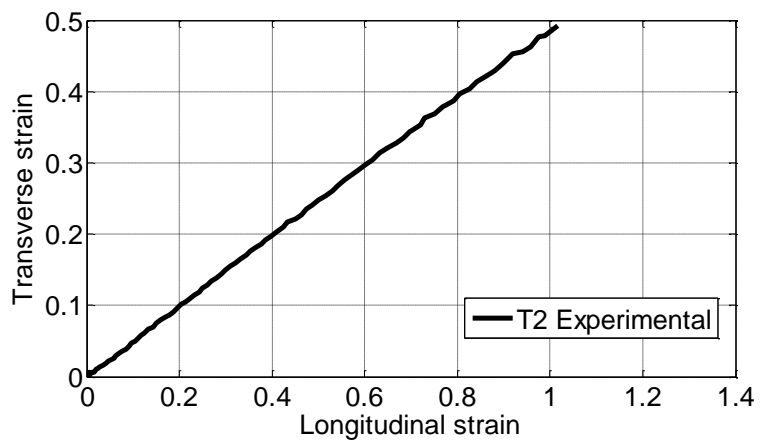
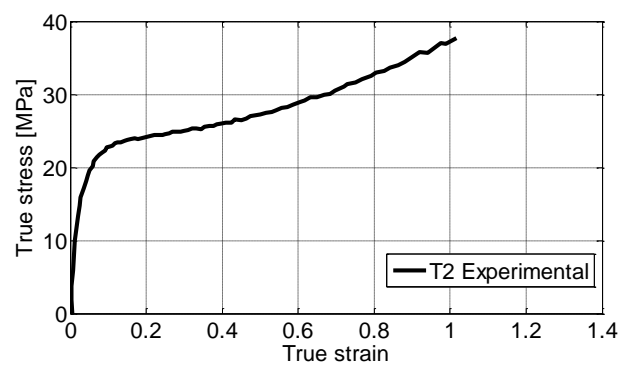
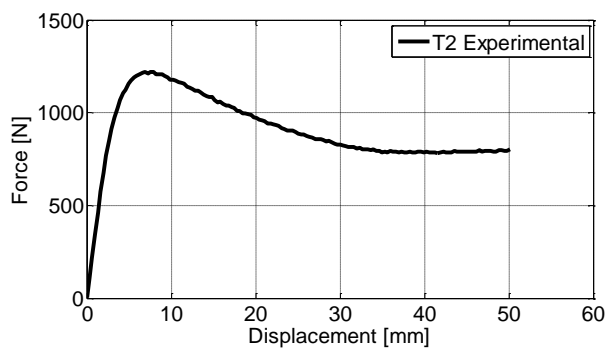


Tensile test T1



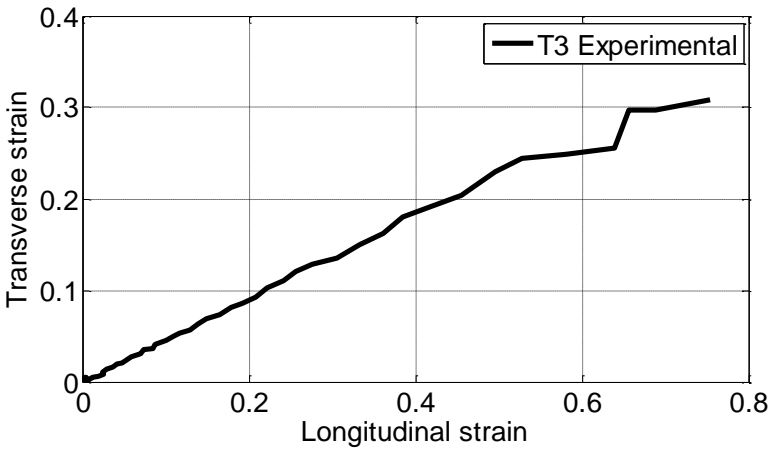
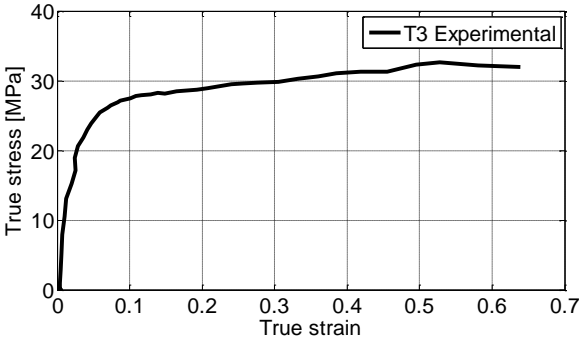
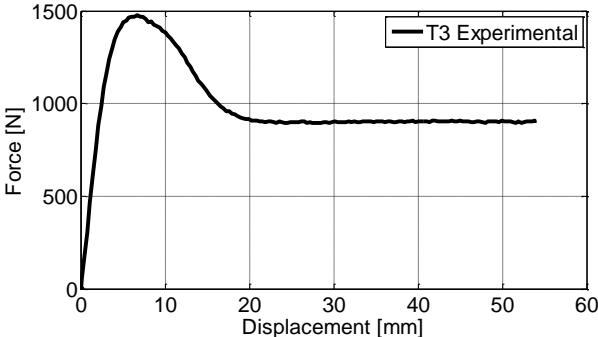
w_0 [mm]	t_0 [mm]	$\dot{\epsilon}$ [s^{-1}]	v [mm/s]	F_{max} [N]	σ_Y [MPa]	Δ_{max} [mm]	ν
12.00	4.91	10^{-3}	0.033	1218	22.7	51.85	0.49

Tensile test T2



b_0 [mm]	t_0 [mm]	$\dot{\epsilon}$ [s^{-1}]	V [mm/s]	F_{max} [N]	σ_Y [MPa]	Δ_{max} [mm]	ν
12.0	4.90	10^{-3}	0.033	1218	22.9	50.14	0.49

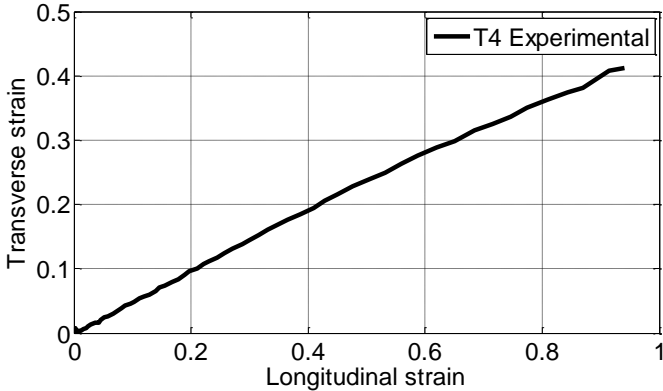
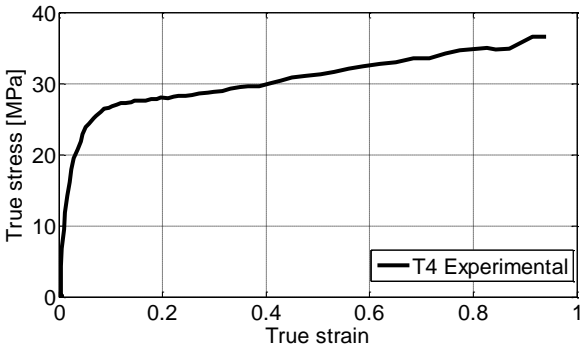
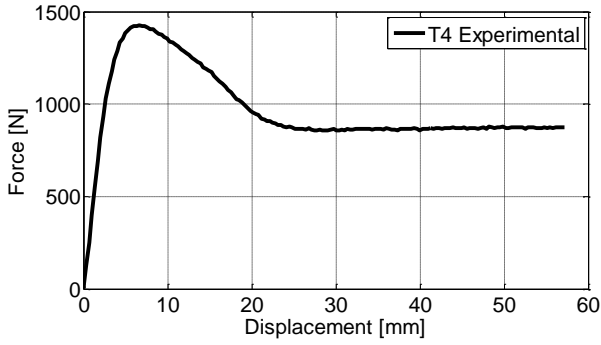
Tensile test T3



b_0 [mm]	t_0 [mm]	$\dot{\epsilon}$ [s^{-1}]	V [mm/s]	F_{max} [N]	σ_Y [MPa]	Δ_{max} [mm]	ν
11.94	4.91	10^{-2}	0.33	1475	27.8	53.85	0.45

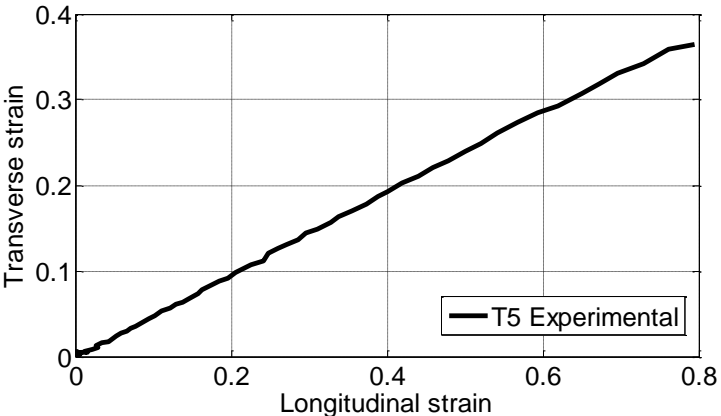
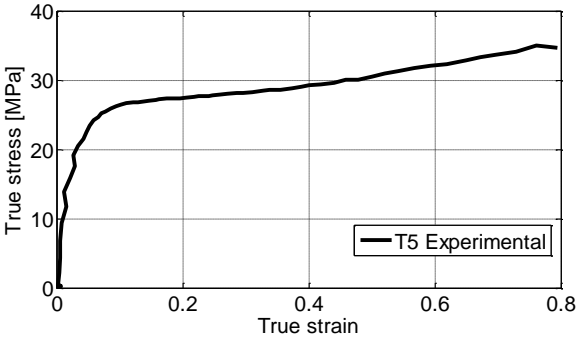
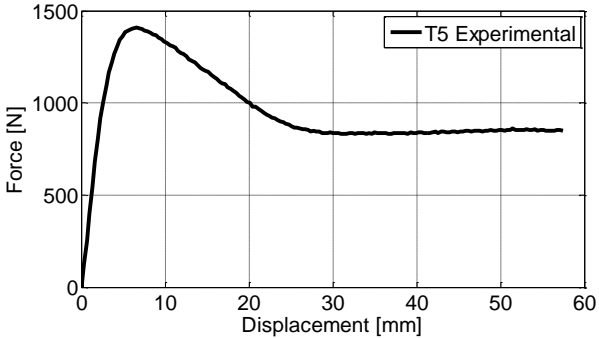
Comments: The contraction ratio is seen to be slightly lower for this test.

Tensile test T4



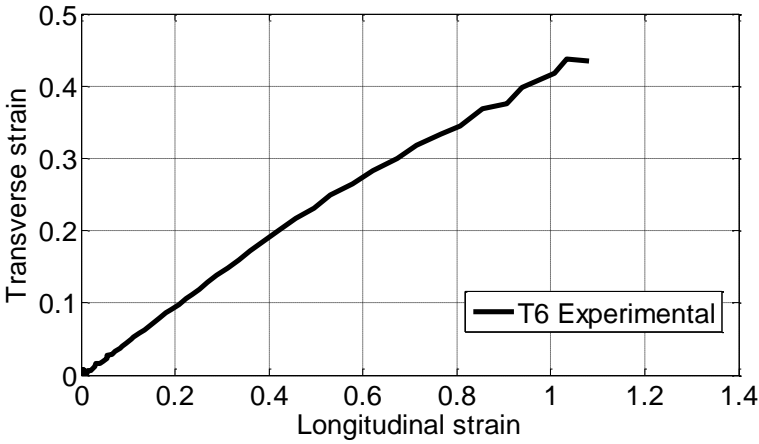
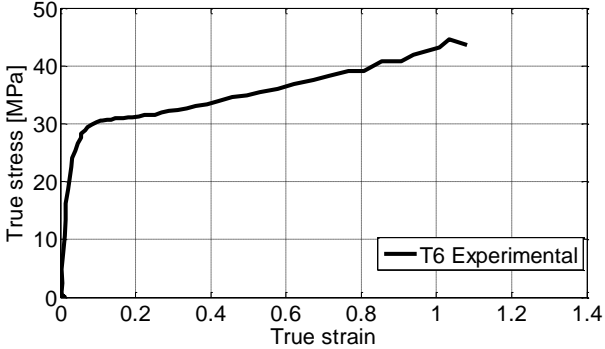
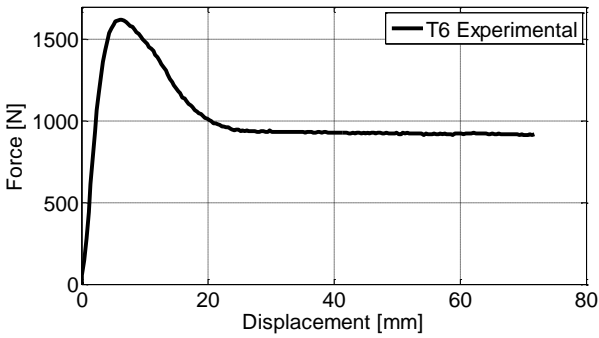
b_0 [mm]	t_0 [mm]	$\dot{\epsilon}$ [s^{-1}]	V [mm/s]	F_{max} [N]	σ_Y [MPa]	Δ_{max} [mm]	ν
11.96	4.90	10^{-2}	0.33	1425	26.6	57.13	0.48

Tensile test T5



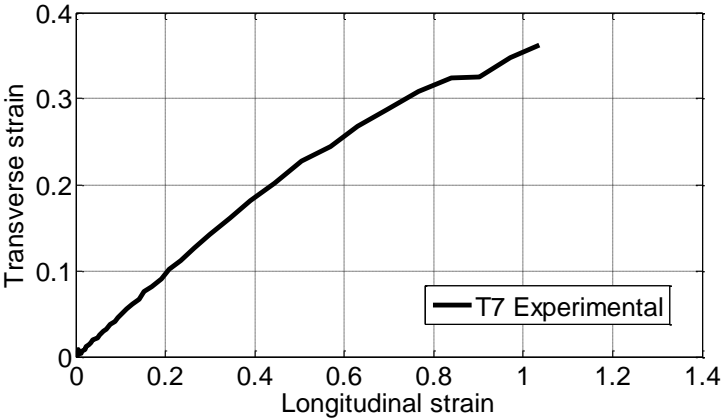
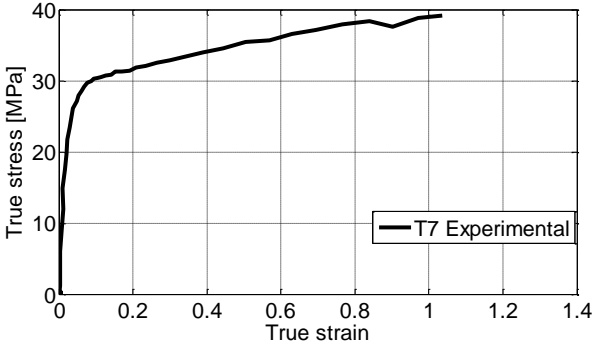
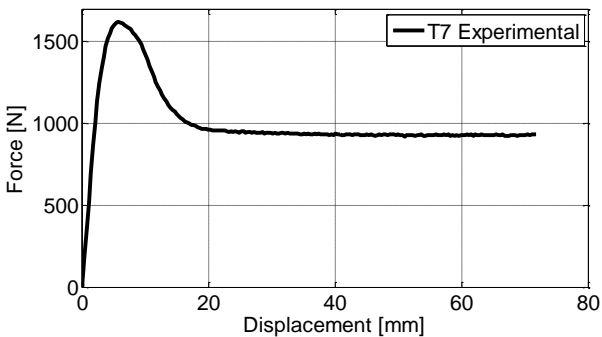
b_0 [mm]	t_0 [mm]	$\dot{\epsilon}$ [s^{-1}]	V [mm/s]	F_{max} [N]	σ_V [MPa]	Δ_{max} [mm]	ν
11.96	4.90	10^{-2}	0.33	1409	26.6	57.42	0.48

Tensile test T6



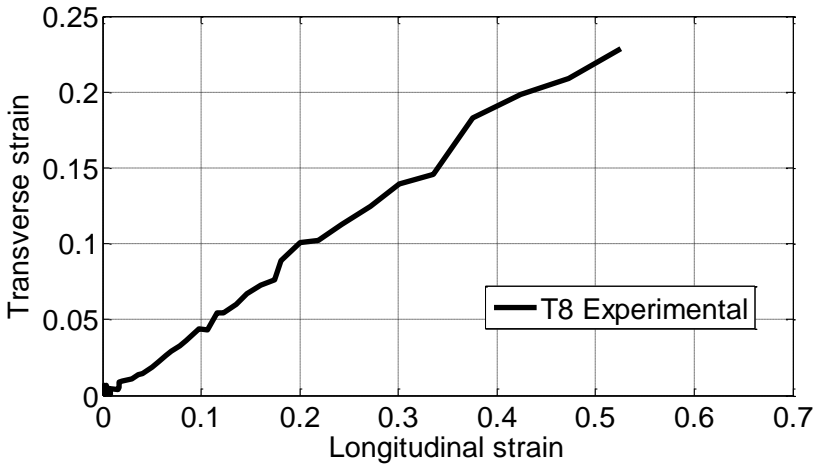
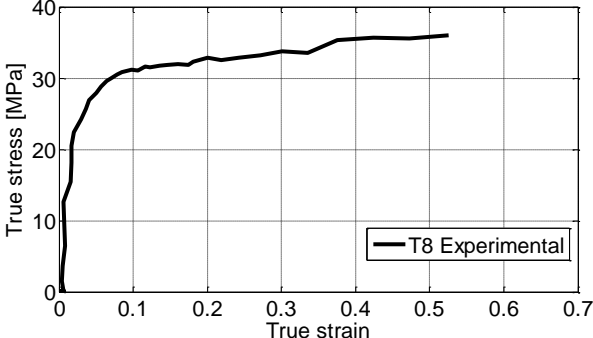
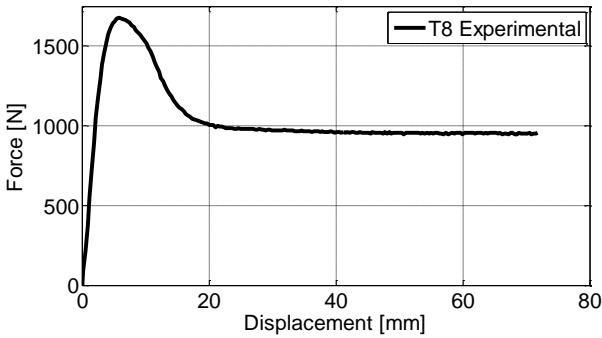
b_0 [mm]	t_0 [mm]	$\dot{\epsilon}$ [s^{-1}]	V [mm/s]	F_{max} [N]	σ_Y [MPa]	Δ_{max} [mm]	ν
11.95	4.89	10^{-1}	3.3	1619	30.2	71.76	0.47

Tensile test T7



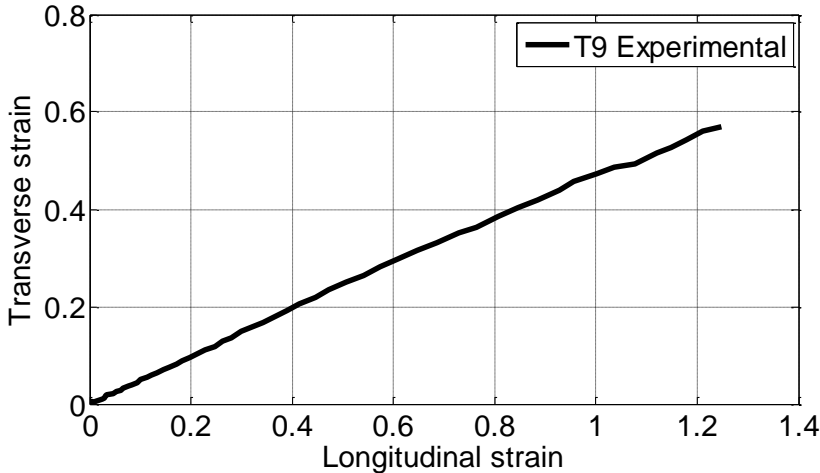
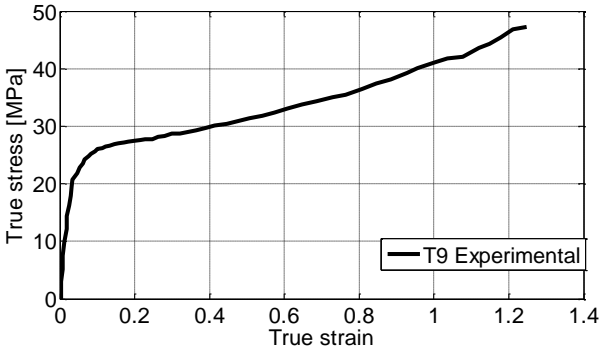
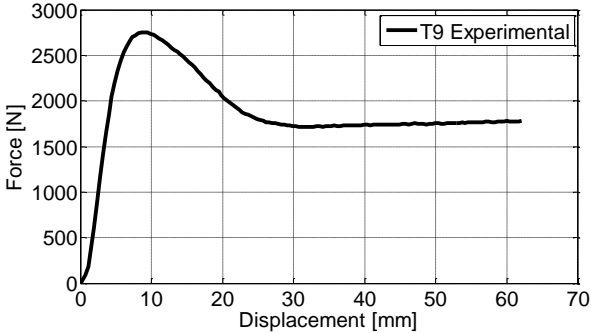
b_0 [mm]	t_0 [mm]	$\dot{\epsilon}$ [s^{-1}]	v [mm/s]	F_{max} [N]	σ_Y [MPa]	Δ_{max} [mm]	ν
11.95	4.91	10^{-1}	3.3	1621	29.9	71.77	0.49

Tensile test T8



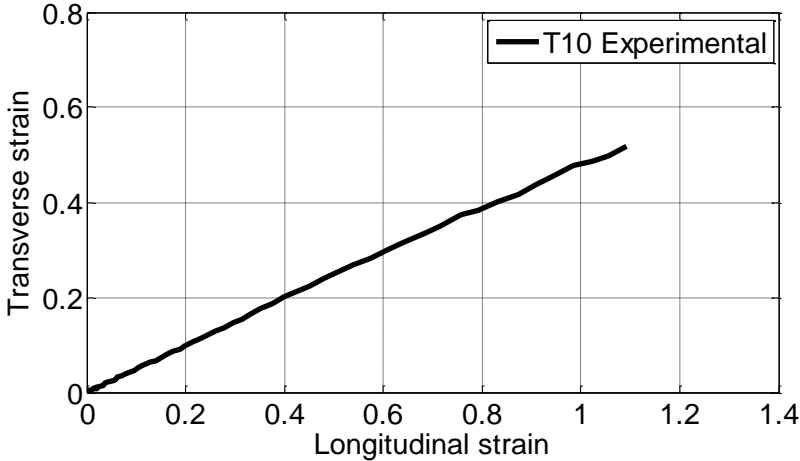
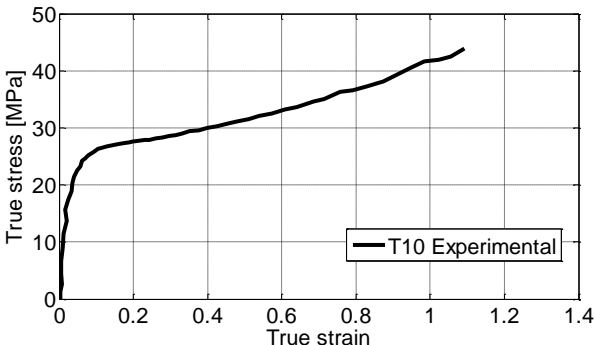
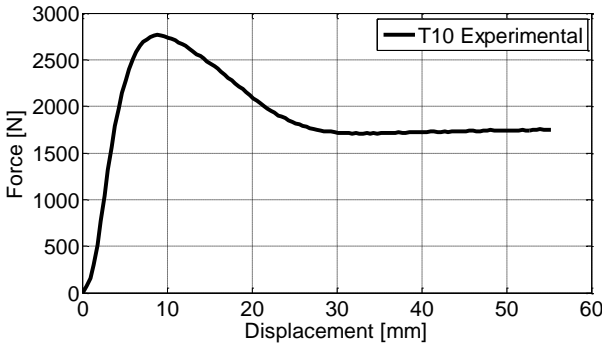
b_0 [mm]	t_0 [mm]	$\dot{\epsilon}$ [s^{-1}]	V [mm/s]	F_{max} [N]	σ_Y [MPa]	Δ_{max} [mm]	ν
11.95	4.90	10^{-1}	3.3	1677	30.9	71.52	0.42

Tensile test T9



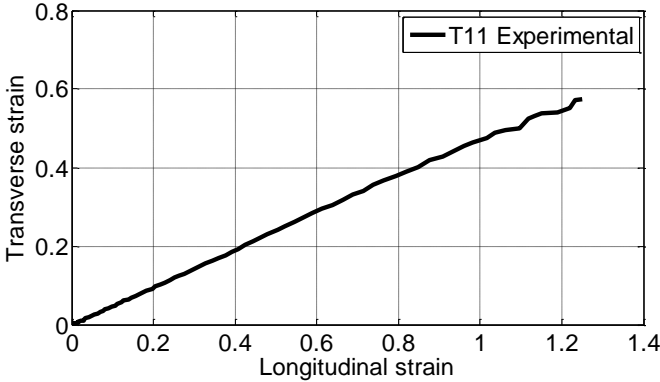
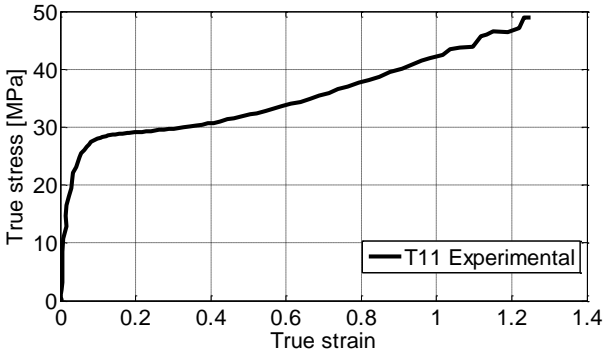
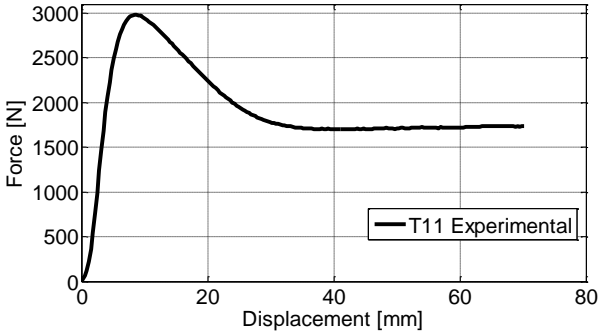
b_0 [mm]	t_0 [mm]	$\dot{\epsilon}$ [s^{-1}]	V [mm/s]	F_{max} [N]	σ_y [MPa]	Δ_{max} [mm]	ν
11.97	9.76	$10^{-2.5}$	0.1443	2750	26.2	62.05	0.48

Tensile test T10



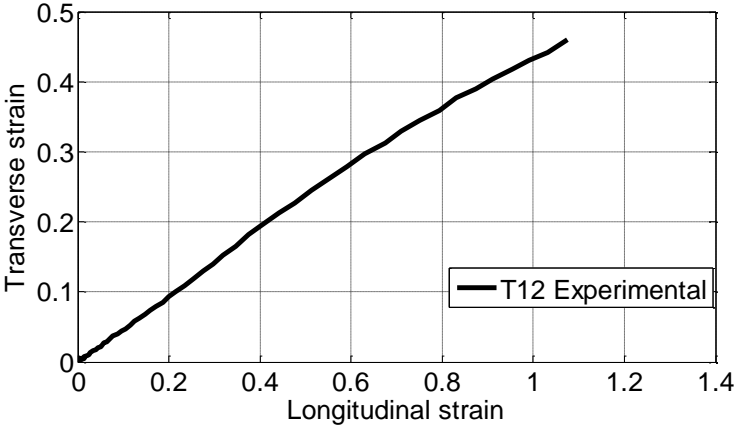
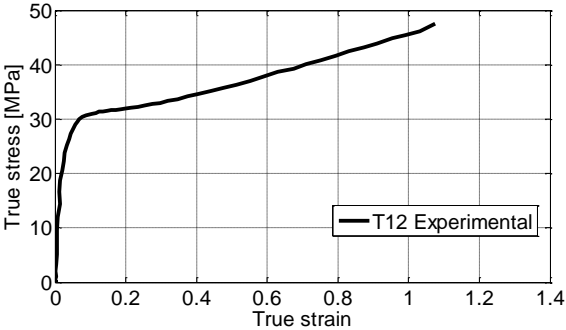
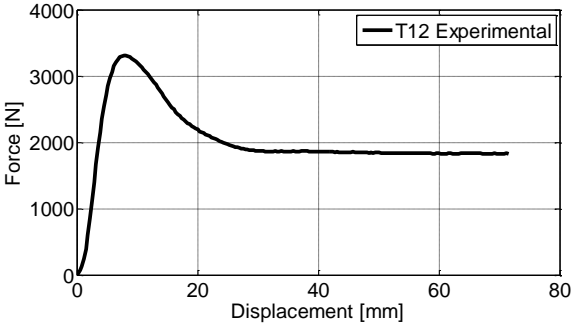
b_0 [mm]	t_0 [mm]	$\dot{\epsilon}$ [s^{-1}]	V [mm/s]	F_{max} [N]	σ_Y [MPa]	Δ_{max} [mm]	ν
11.95	9.76	$10^{-2.5}$	0.1443	2767	26.5	55.22	0.50

Tensile test T11



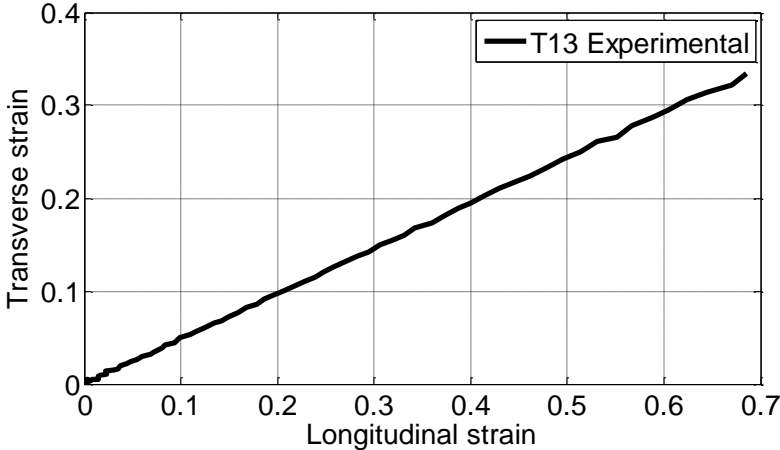
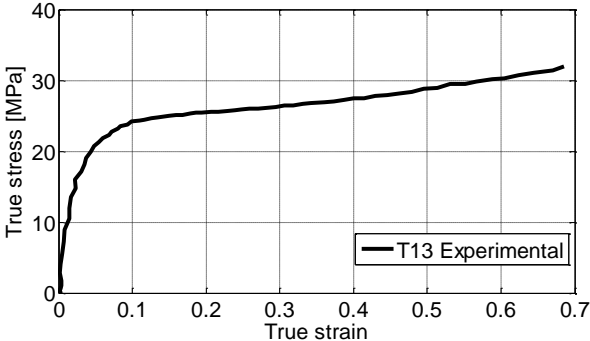
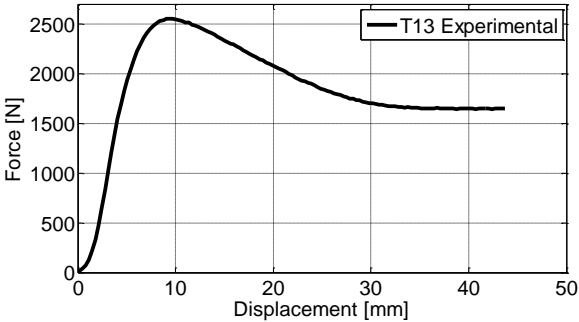
w_0 [mm]	t_0 [mm]	$\dot{\epsilon}$ [s^{-1}]	V [mm/s]	F_{max} [N]	σ_Y [MPa]	Δ_{max} [mm]	ν
11.96	9.76	10^{-2}	0.33	2985	28.0	70.13	0.48

Tensile test T12



w_0 [mm]	t_0 [mm]	$\dot{\epsilon}$ [s^{-1}]	V [mm/s]	F_{max} [N]	σ_Y [MPa]	Δ_{max} [mm]	ν
11.97	9.76	10^{-1}	3.3	3307	30.5	71.49	0.47

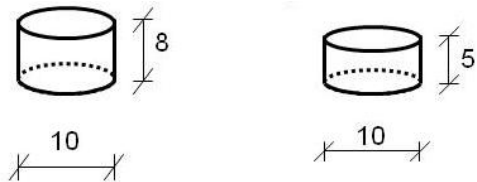
Tensile test T13



w_0 [mm]	t_0 [mm]	$\dot{\epsilon}$ [s^{-1}]	V [mm/s]	F_{max} [N]	σ_Y [MPa]	Δ_{max} [mm]	ν
11.96	9.76	10^{-3}	0.033	2552	24.2	43.7	0.49

Compression tests

The compression tests were performed in the laboratory at NTNU in February. The compression specimen was extruded in two different directions. The first four were extruded in the yz - direction and had a height of 8mm. The fifth test was extruded in the xy - direction and had a height of 5 mm. The geometry of the test specimens are illustrated below.



The results represented herein are the force – displacement curves, true stress – strain curves and the transversal strains versus the longitudinal strains. In addition the most important key data is given as

h_0 – initial height, [mm]

d_0 – initial diameter, [mm]

$\dot{\epsilon}$ - nominal strain rate, [s^{-1}]

v – velocity, [mm/s]

F_{max} – maximum force, [N]

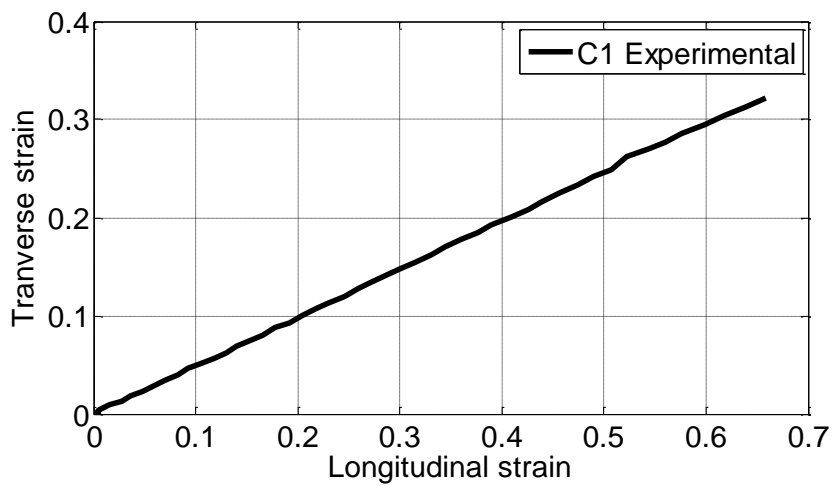
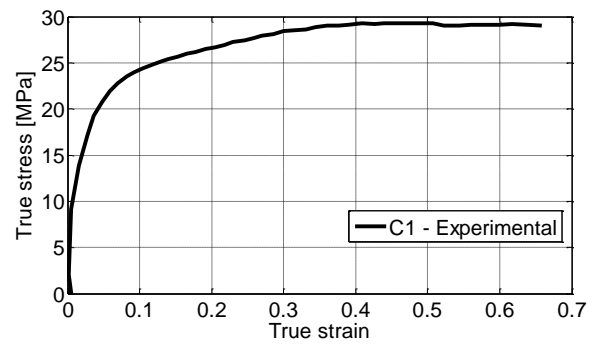
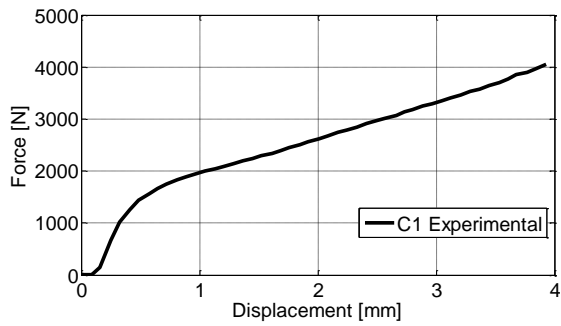
σ_y – yield stress, [MPa]

Δ_{max} – maximum displacement, [mm]

ν – contraction ratio

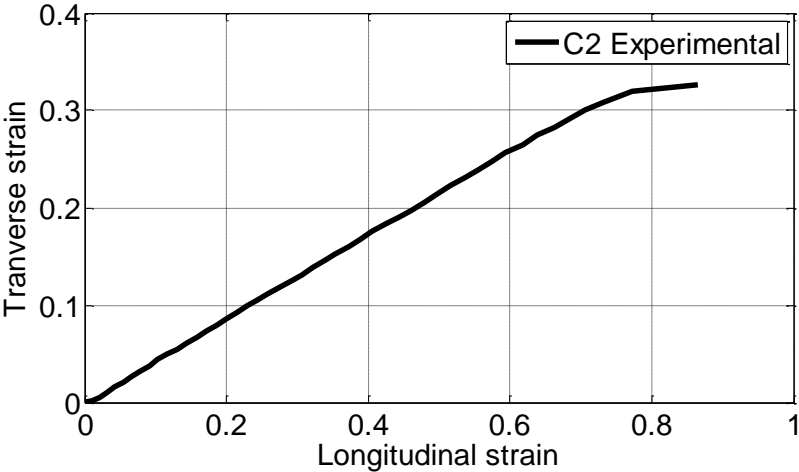
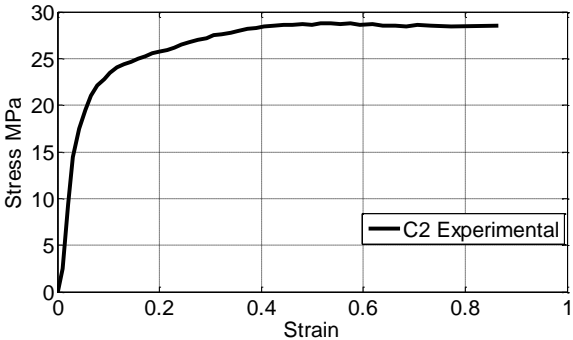
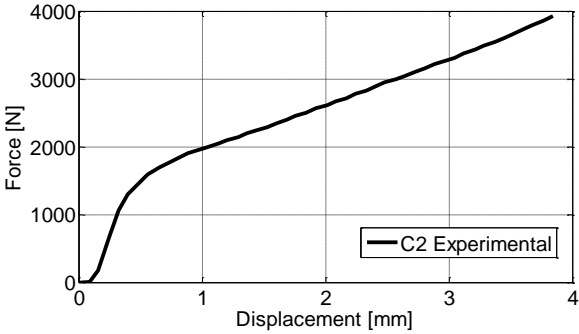


Compression test C1



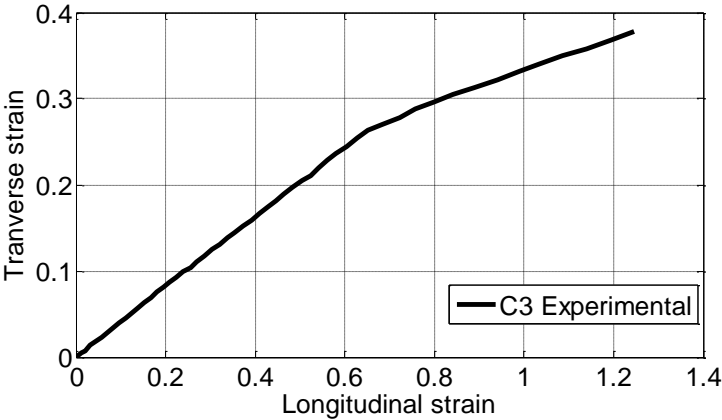
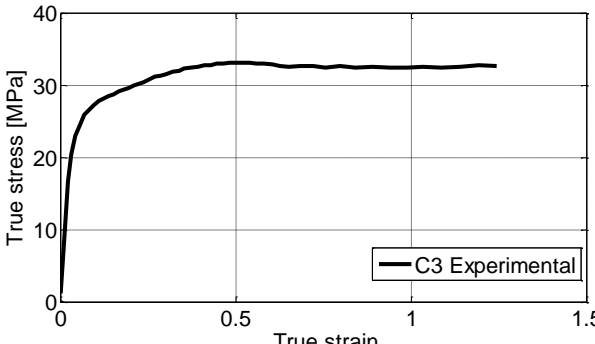
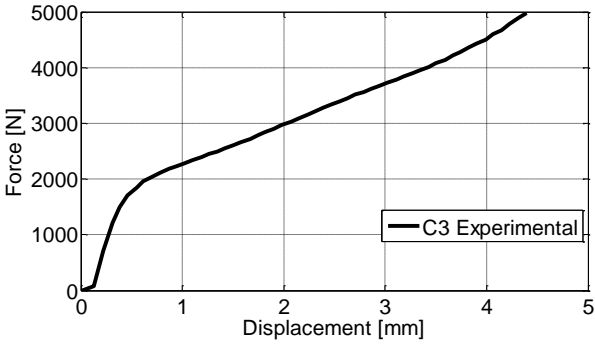
h_0 [mm]	d_0 [mm]	$\dot{\epsilon}$ [s^{-1}]	v [mm/s]	F_{max} [N]	σ_Y [MPa]	Δ_{max} [mm]	ν
8.02	9.56	10^{-3}	0.008	4048	25.1	3.93	0.49

Compression test C2



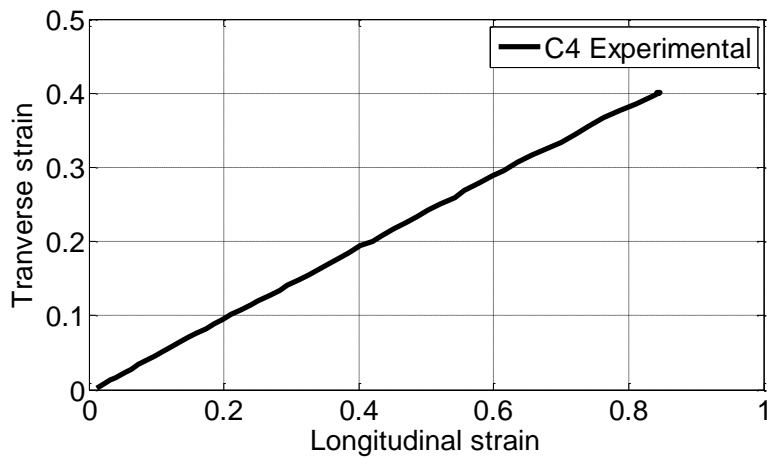
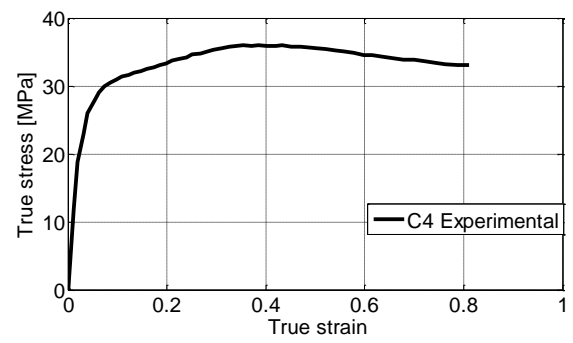
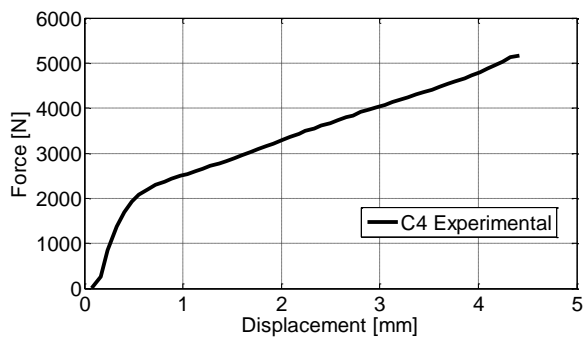
h_0 [mm]	d_0 [mm]	$\dot{\epsilon}$ [s^{-1}]	V [mm/s]	F_{max} [N]	σ_Y [MPa]	Δ_{max} [mm]	ν
8.01	9.55	10^{-3}	0.008	3925	24.3	3.84	0.43

Compression test C3



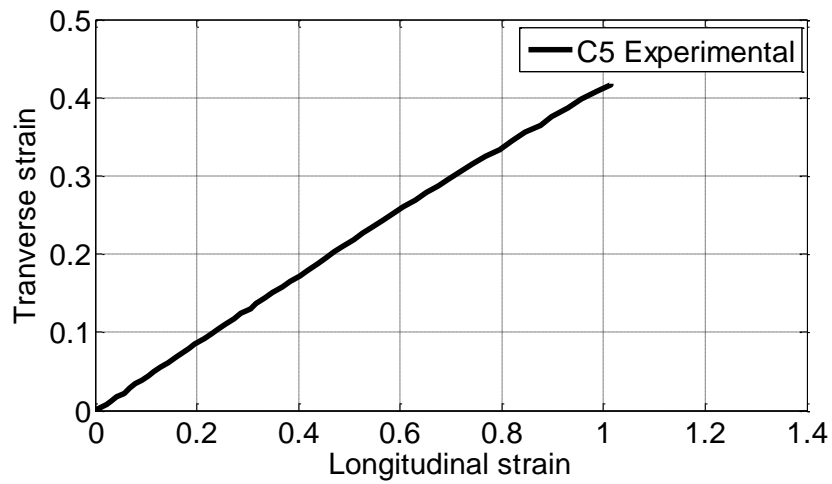
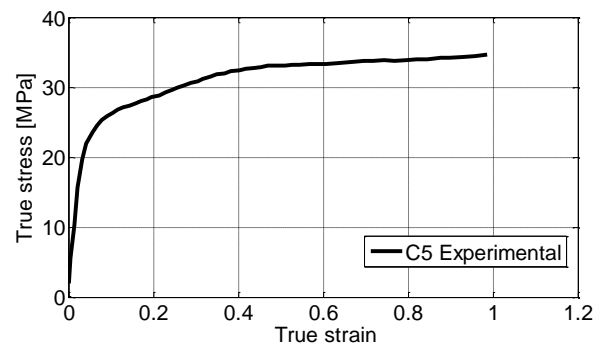
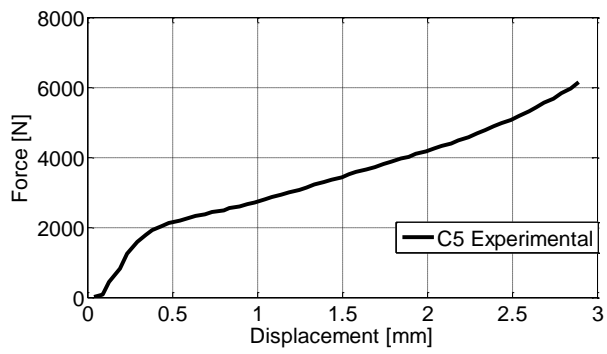
h_0 [mm]	d_0 [mm]	$\dot{\epsilon}$ [s^{-1}]	V [mm/s]	F_{max} [N]	σ_Y [MPa]	Δ_{max} [mm]	ν
8.02	9.55	10^{-2}	0.08	4978	28.0	4.39	0.42

Compression test C4



h_0 [mm]	d_0 [mm]	$\dot{\epsilon}$ [s^{-1}]	V [mm/s]	F_{max} [N]	σ_Y [MPa]	Δ_{max} [mm]	ν
8.02	9.55	10^{-1}	0.8	5167	31.2	4.42	0.48

Compression test C5



h_0 [mm]	d_0 [mm]	$\dot{\epsilon}$ [s^{-1}]	V [mm/s]	F_{max} [N]	σ_Y [MPa]	Δ_{max} [mm]	ν
4.94	9.99	10^{-2}	0.05	6157	27.0	2.89	0.43

Plate with a hole testing

The plate with a hole tests were performed in the beginning of march in the laboratory at NTNU. The plates were made from the 2000 x 1000 mm sheets that were delivered by the German company SIMONA.

The results of the change in diameter, thickness and the width of the lateral faces are illustrated as well as the force – displacement curves for each test performed. In addition some key data is provided.

Key data:

$w_{1,0}$ – initial width of lateral face 1

$d_{y,0}$ – initial diameter in the y – direction

$w_{2,0}$ – initial width of lateral face 2

v – velocity, [mm/s]

t_0 – initial thickness

F_{\max} – maximum load

$d_{x,0}$ – initial diameter in the x – direction

Δ_{\max} – maximum displacement

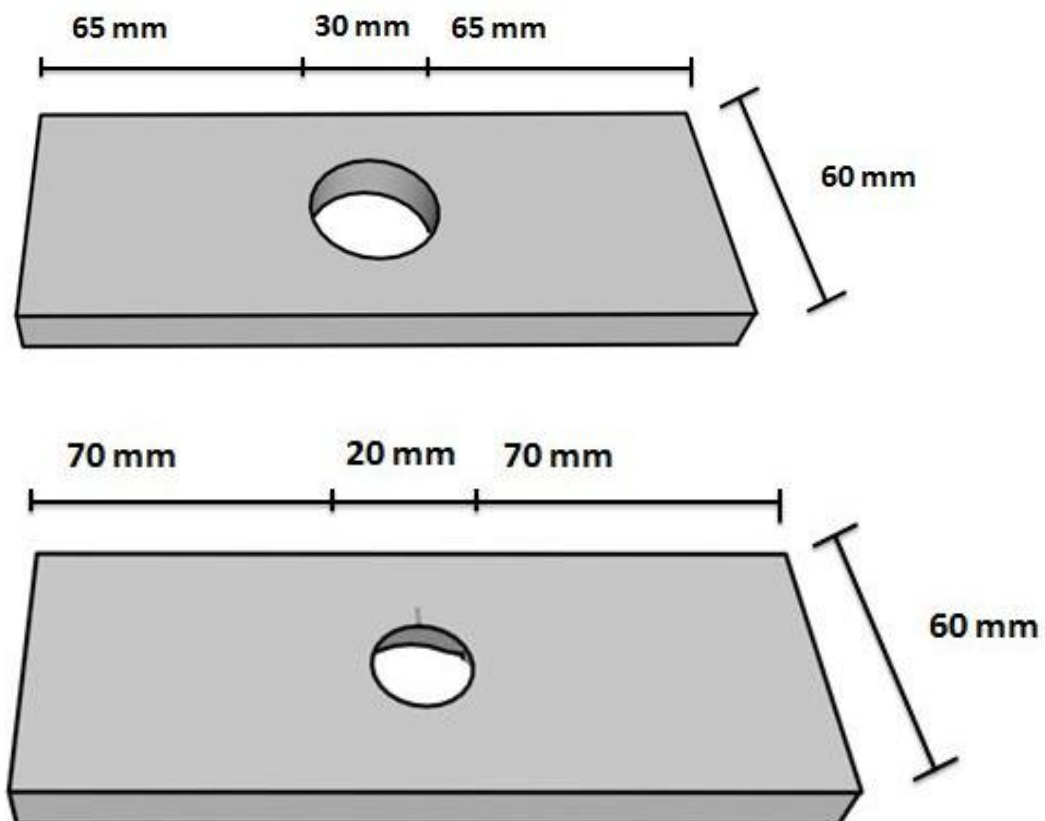
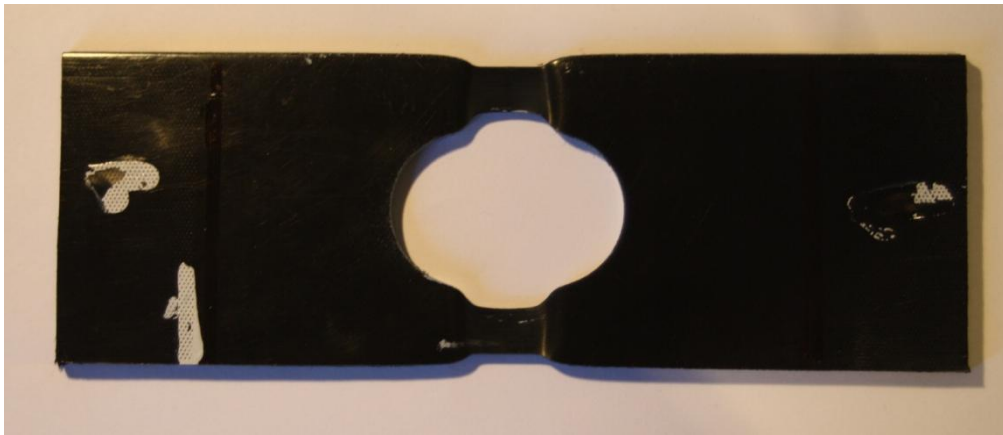
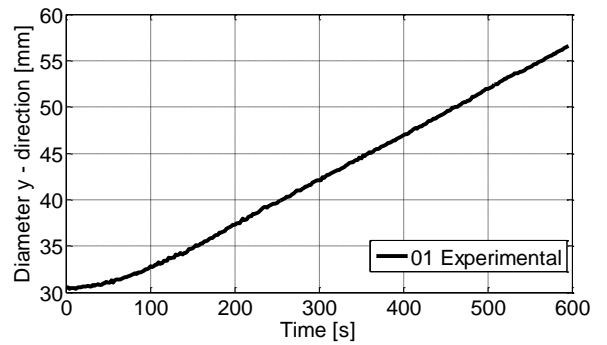
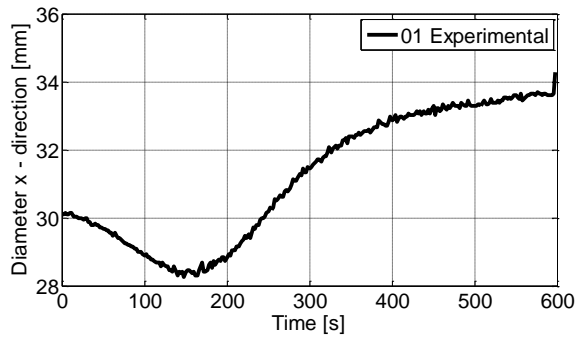
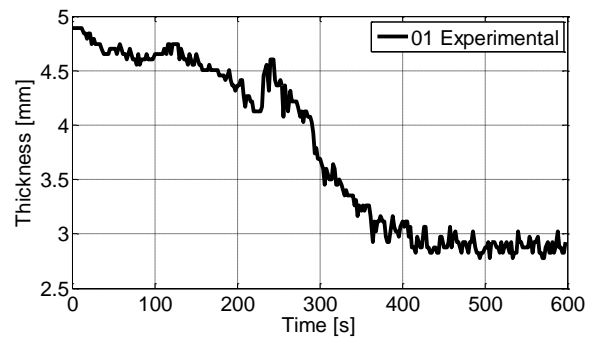
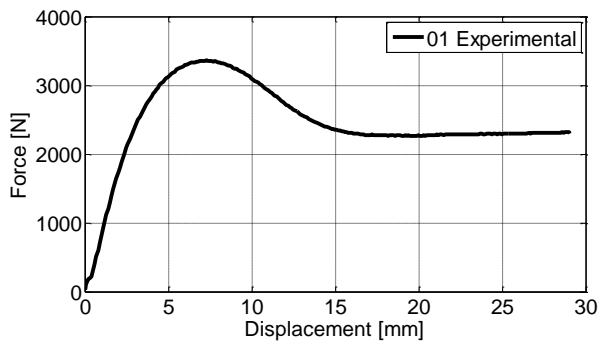
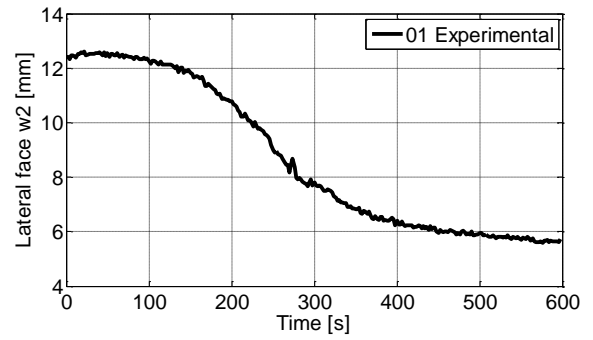
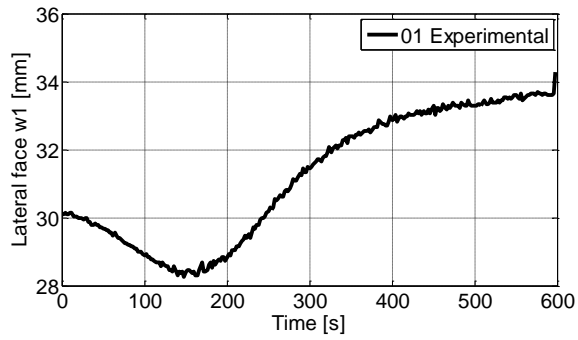


Plate with a hole, test 01



$w_{1,0}$ [mm]	$w_{2,0}$ [mm]	t_0 [mm]	$d_{x,0}$ [mm]	$d_{y,0}$ [mm]	v [mm/s]	F_{max} [N]	Δ_{max} [mm]
15.69	15.29	4.89	30.09	30	0.05	3361	29.06

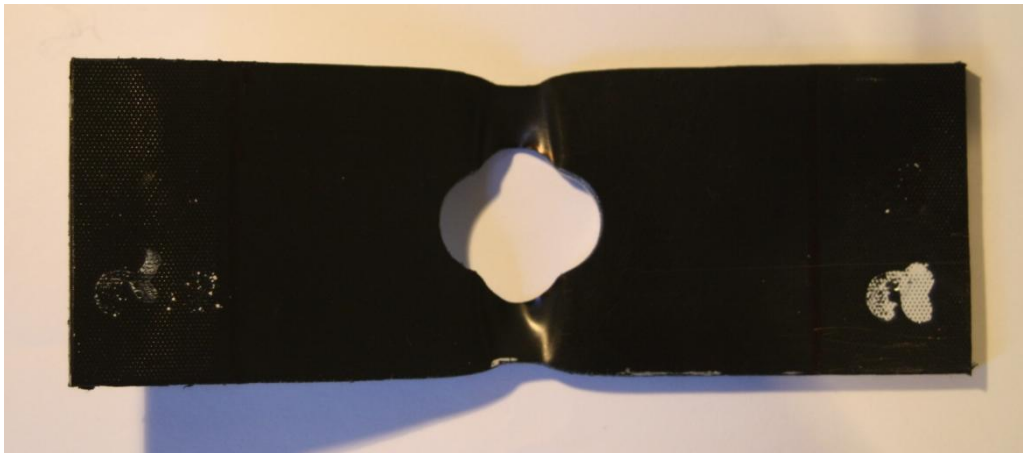




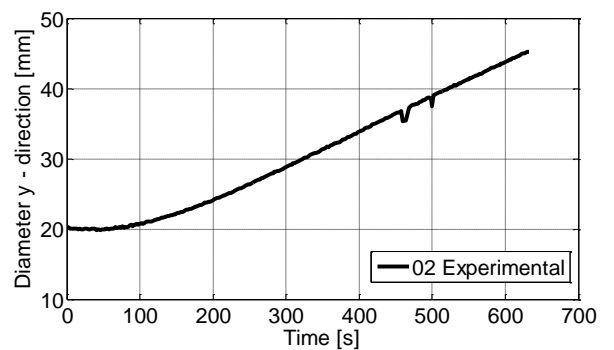
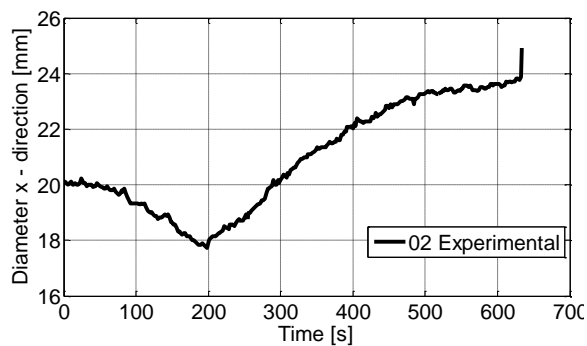
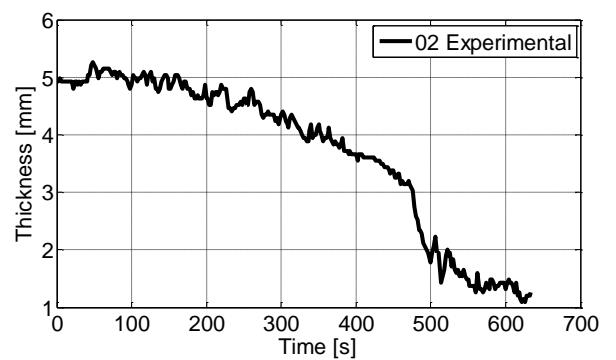
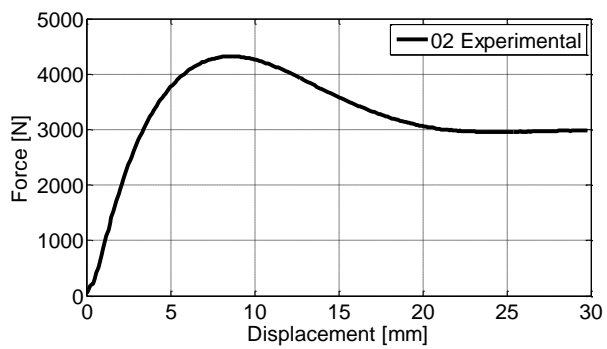
Comments:

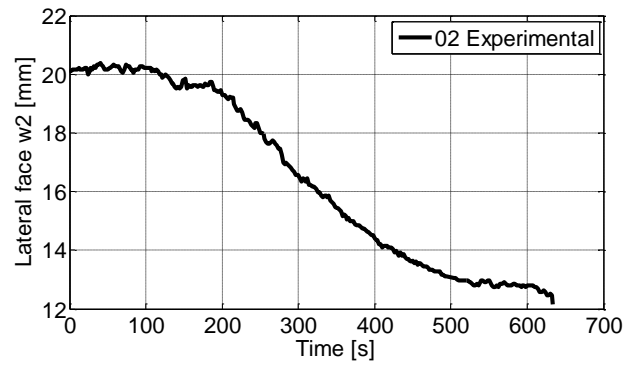
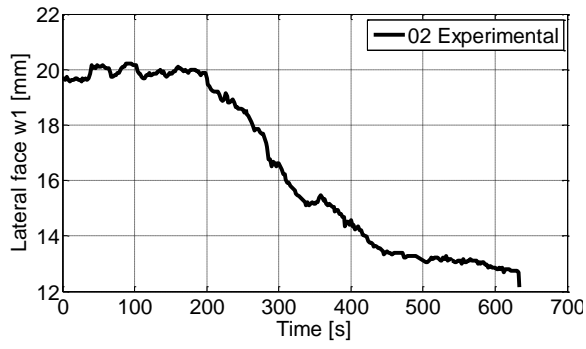
- Lateral face w_2 is incorrect due to poor quality of the pictures taken.
- The diameter in the y – direction was not measured before testing, and therefore value of the diameter is given as approximately 30 mm in the table.

Plate with a hole, test 02



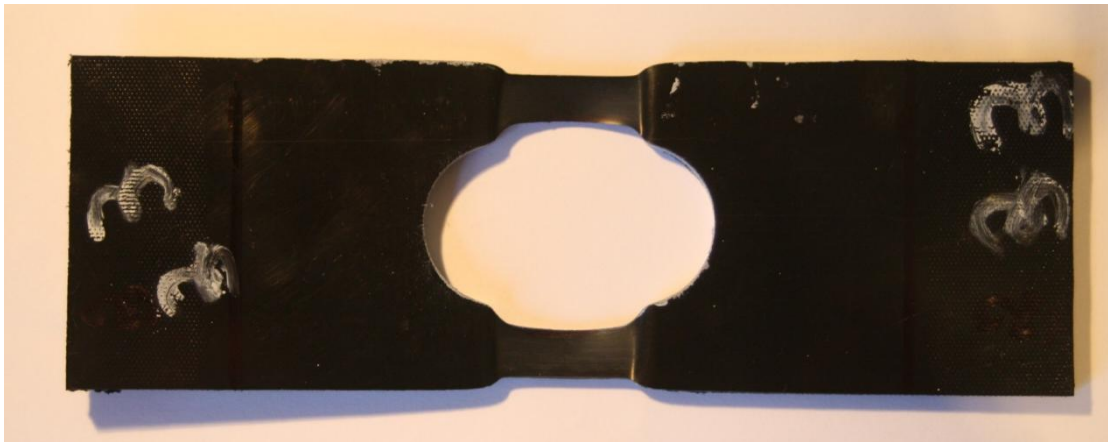
$w_{1,0}$ [mm]	$w_{2,0}$ [mm]	t_0 [mm]	$d_{x,0}$ [mm]	$d_{y,0}$ [mm]	v [mm/s]	F_{max} [N]	Δ_{max} [mm]
20.21	20.16	4.92	20.06	20	0.05	4321	29.79



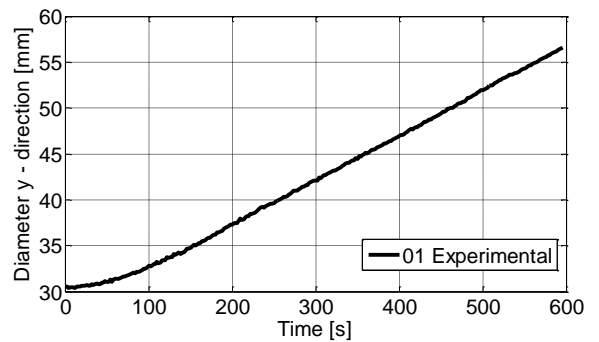
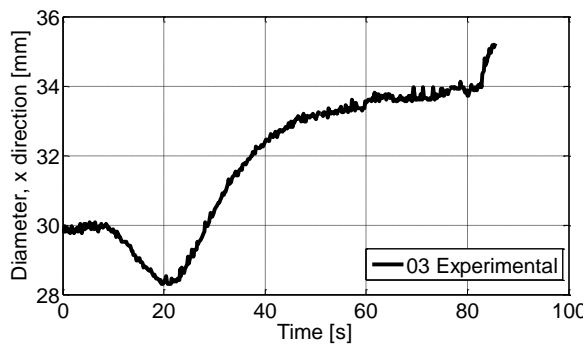
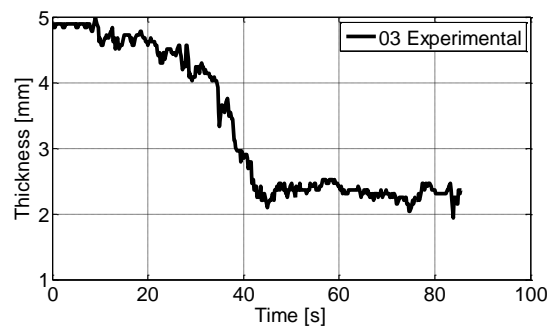
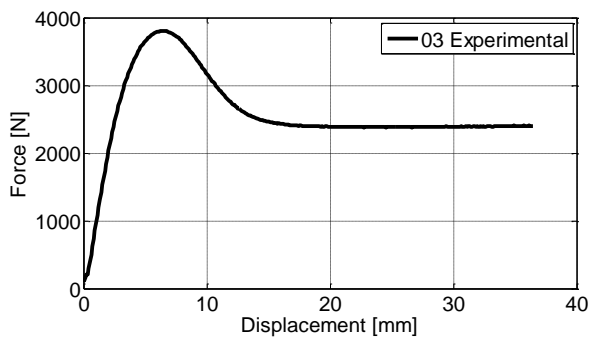


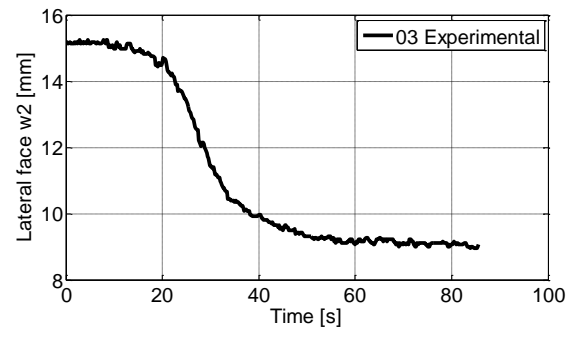
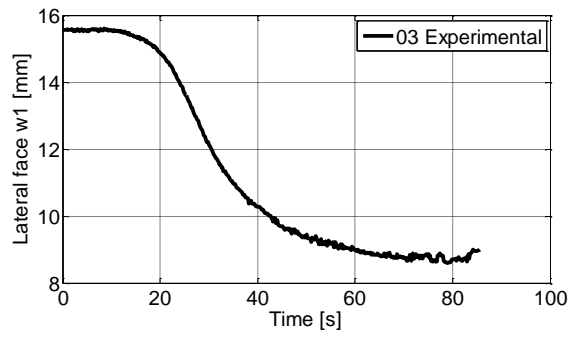
Comments: The diameter in the y – direction was not measured before testing and is therefore given as an approximately value of 20 mm.

Plate with a hole, test 03



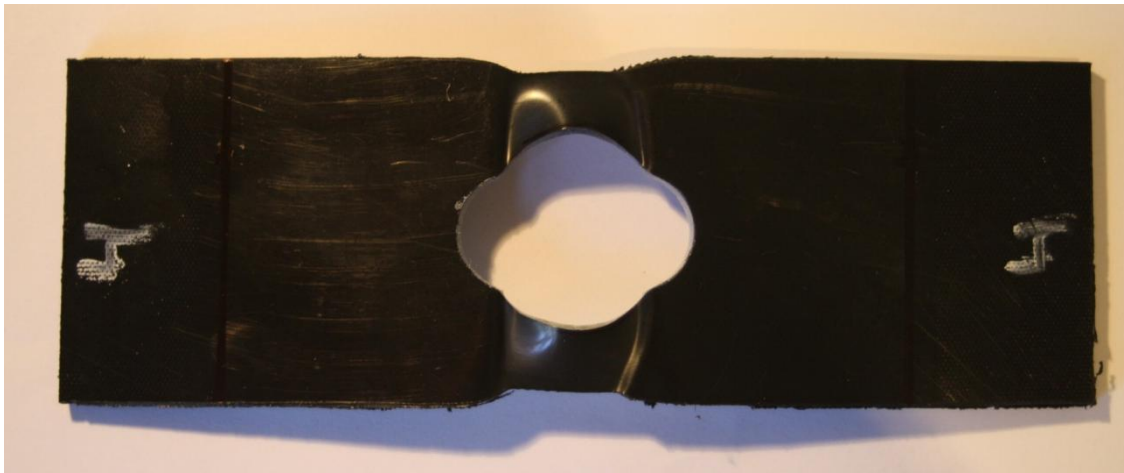
$w_{1,0}$ [mm]	$w_{2,0}$ [mm]	t_0 [mm]	$d_{x,0}$ [mm]	$d_{y,0}$ [mm]	v [mm/s]	F_{max} [N]	Δ_{max} [mm]
15.56	15.12	4.89	29.87	30 mm	0.5	3806	36.42



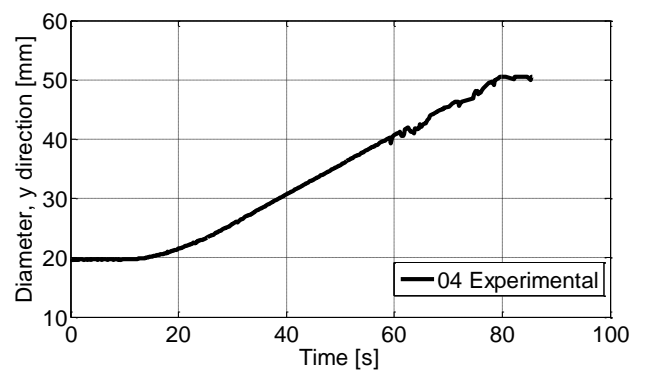
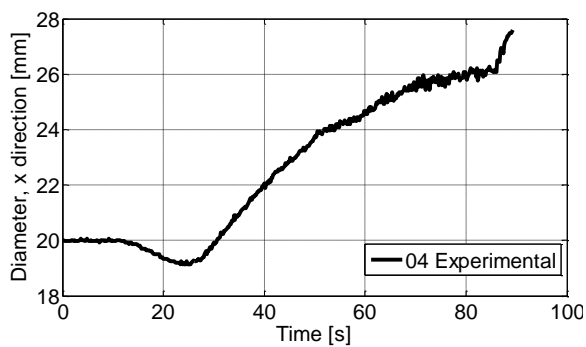
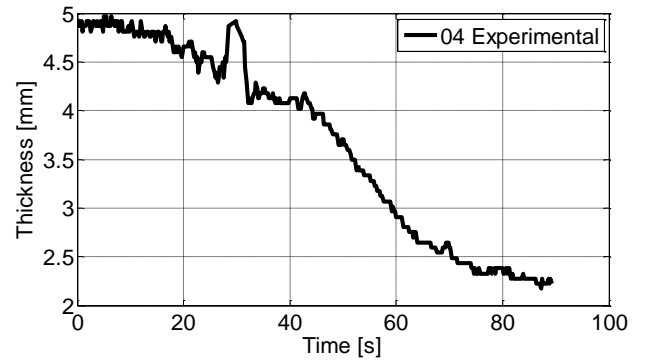
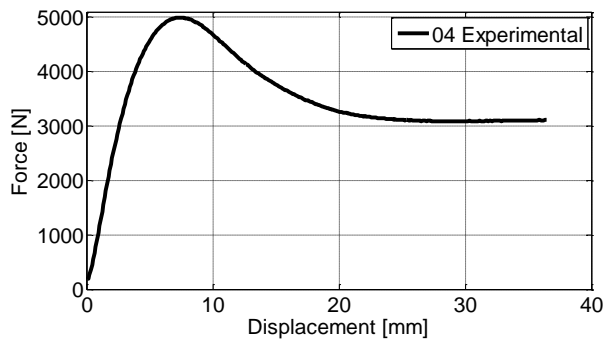


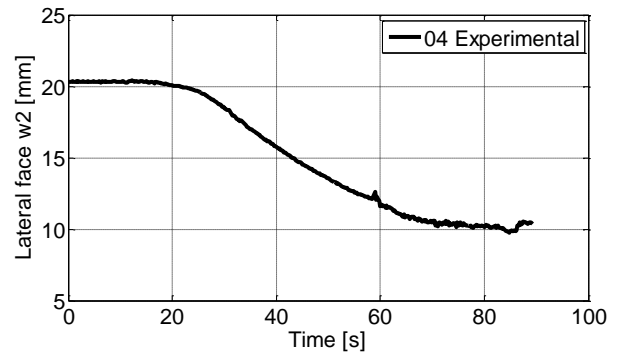
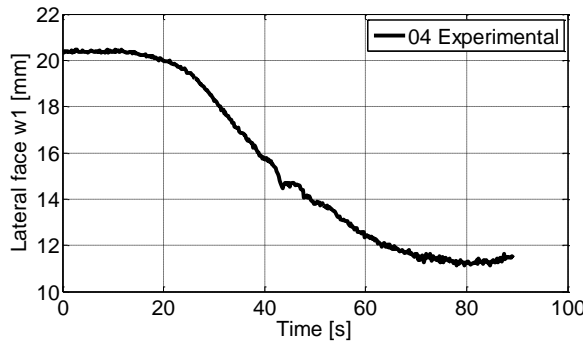
Comments: The diameter in the y – direction was not measured before testing and is given as an approximately value of 30 mm.

Plate with a hole, test 04



$w_{1,0}$ [mm]	$w_{2,0}$ [mm]	t_0 [mm]	$d_{x,0}$ [mm]	$d_{y,0}$ [mm]	v [mm/s]	F_{max} [N]	Δ_{max} [mm]
20.33	20.11	4.92	20.02	20	0.05	4999	36.44





Comments: The diameter in the y – direction was not measured before the test and is therefore given an approximate value of 20 mm.

Drop tower testing

The drop tower machine Instron CEAST 9350 had never been used before, and was first tried out in the end of April when the impact tests were performed. The test specimen was a 100 mm x 100 mm plate of thickness 5 mm made from the extruded sheets delivered by the manufacturer SIMONA.

The test results that are given are the force – displacement curve of all six of the impacts tests performed. In addition some essential key data is given as

v – velocity, [mm/s]

W – weight applied during testing, [kg]

t_0 – initial thickness

H – fall height of the shaft, [m]

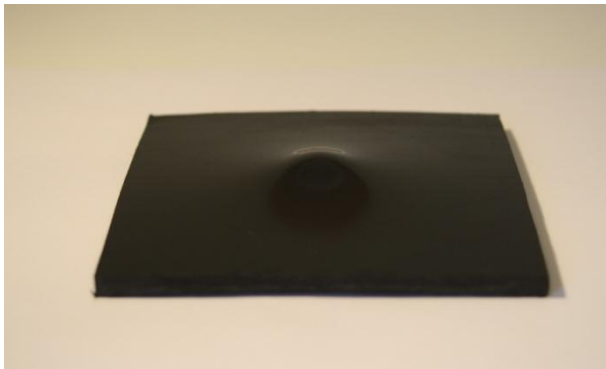
E_p – potential energy, [J]

F_{\max} – maximum force, [N]

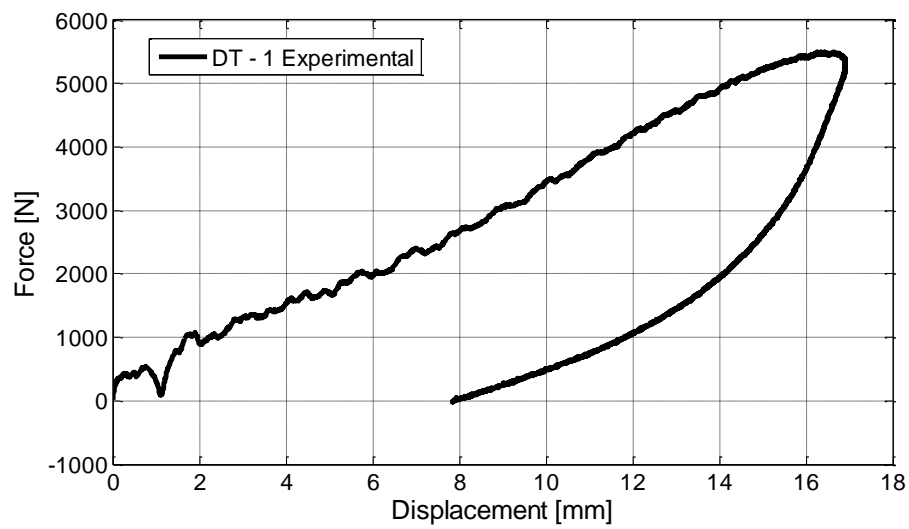
Δ_{\max} – maximum displacement, [mm]



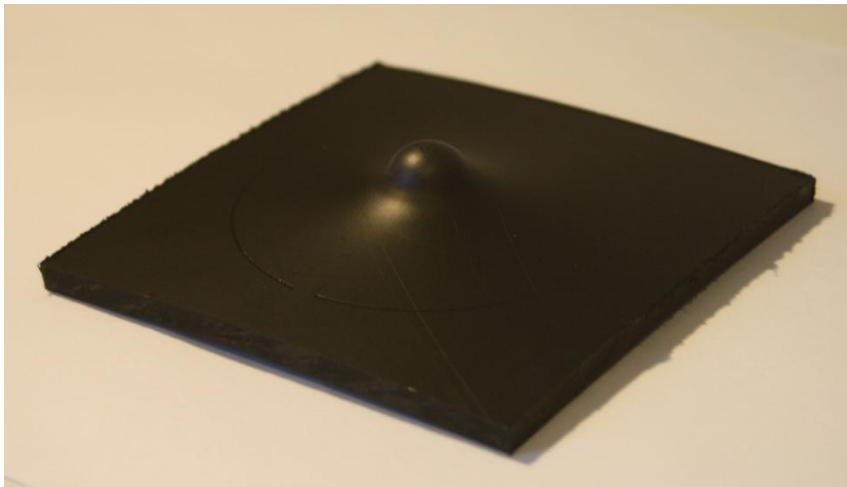
Impact test, DT -1



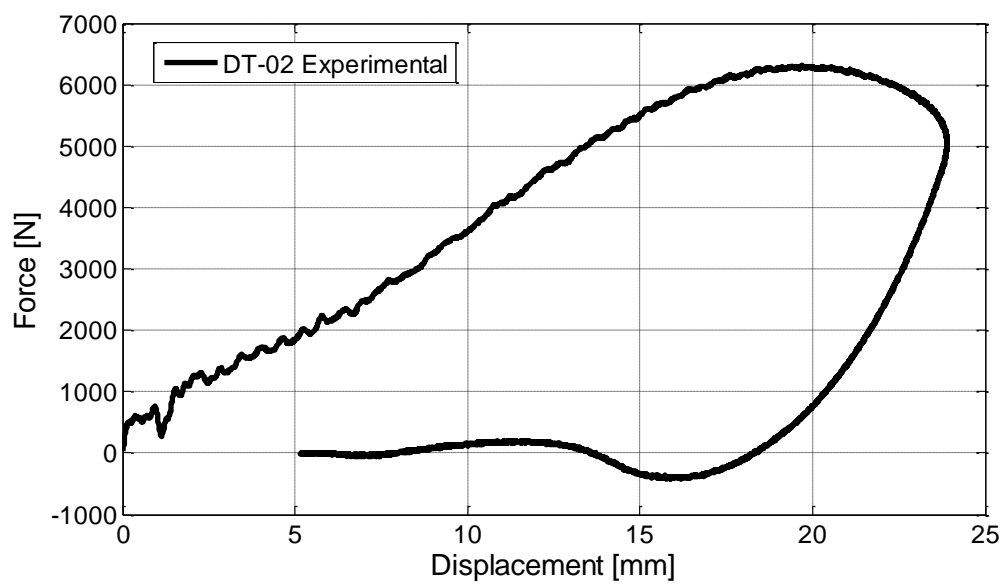
v [mm/s]	W [kg]	t_0 [mm]	H [m]	E_p [J]	F_{max} [N]	Δ_{max}
4400	5.045	4.91	1	50	5499	16.92



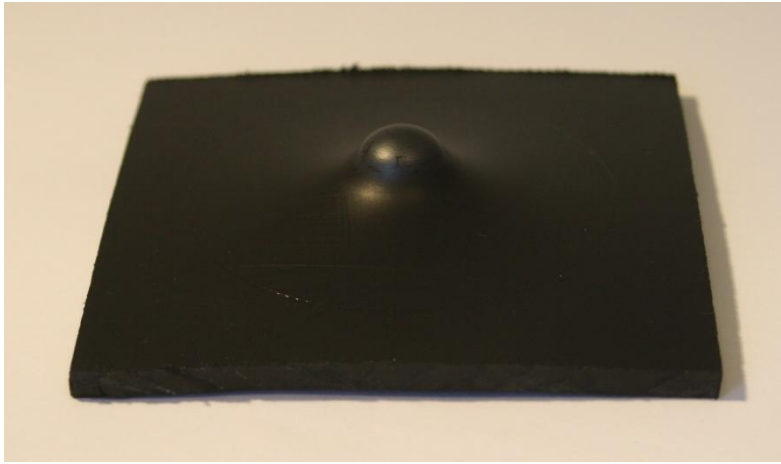
Impact test, DT - 2



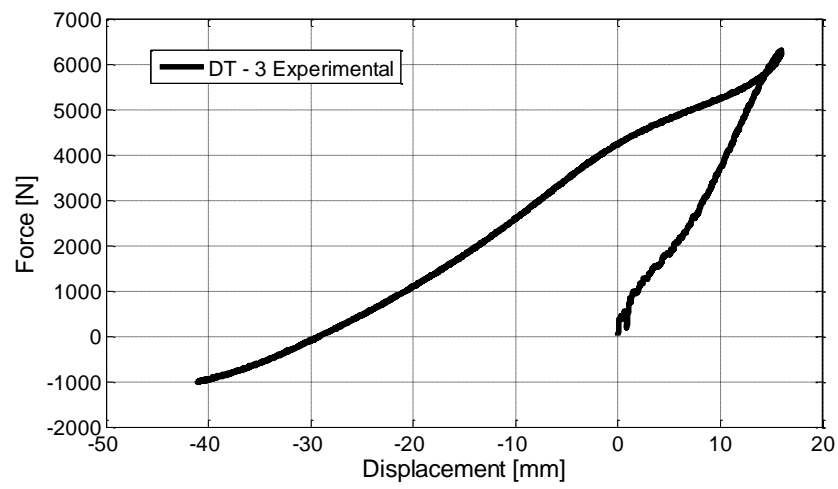
v [mm/s]	Mass [kg]	t_0 [mm]	Fall Height [m]	E_p [J]	F_{max} [N]	Δ_{max}
6263	5.045	4.90	2	100	6303	23.89



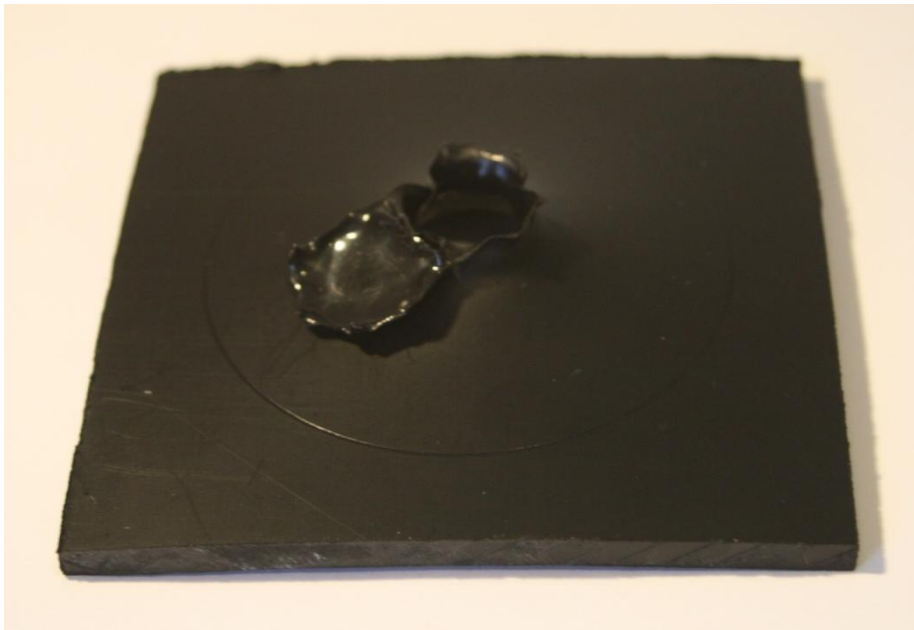
Impact test, DT - 3



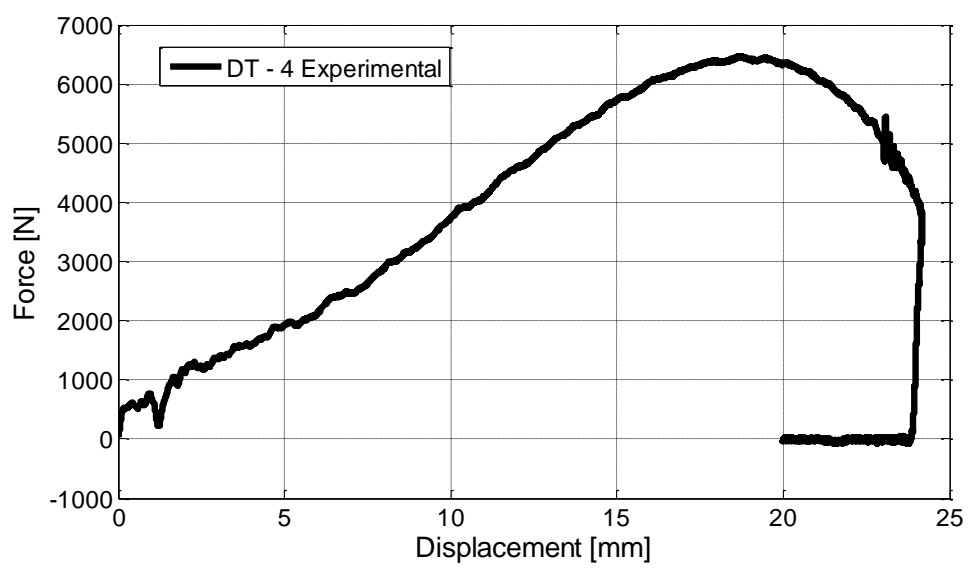
v [mm/s]	Mass [kg]	t ₀ [mm]	Fall Height [m]	E _p [J]	F _{max} [N]	Δ _{max}
4400	10.045	4.90	1	100	6276	15.95



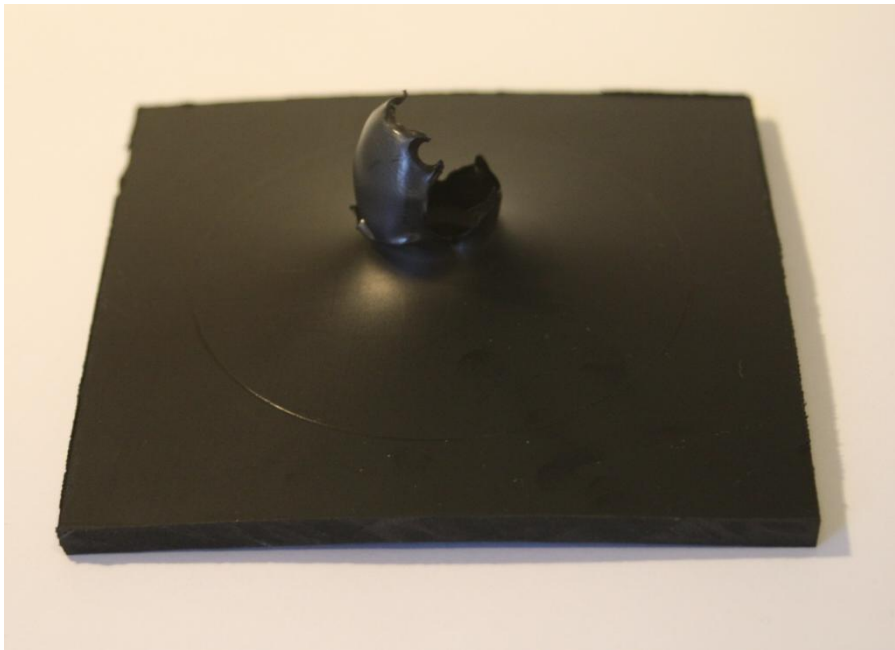
Drop tower, test 4



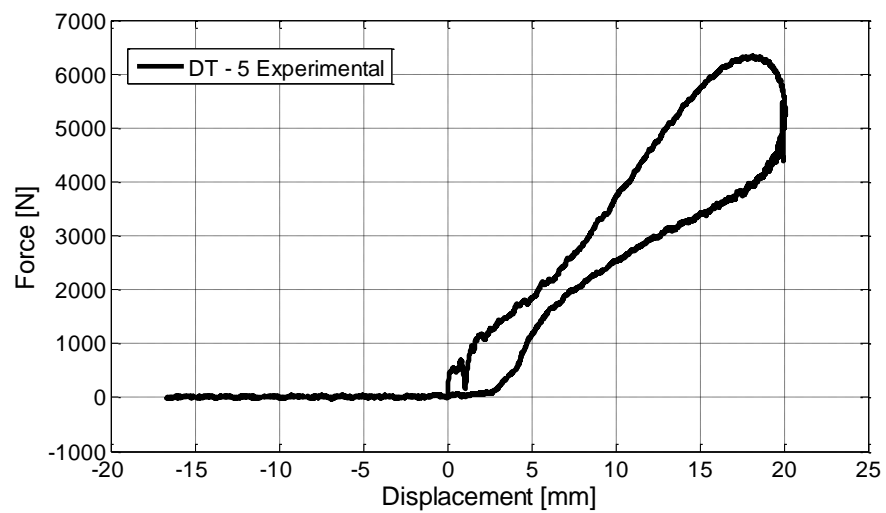
v [mm/s]	Mass [kg]	t_0 [mm]	Fall Height [m]	E_p [J]	F_{max} [N]	Δ_{max}
6263	10.045	4.90	2	200	6469	24.17



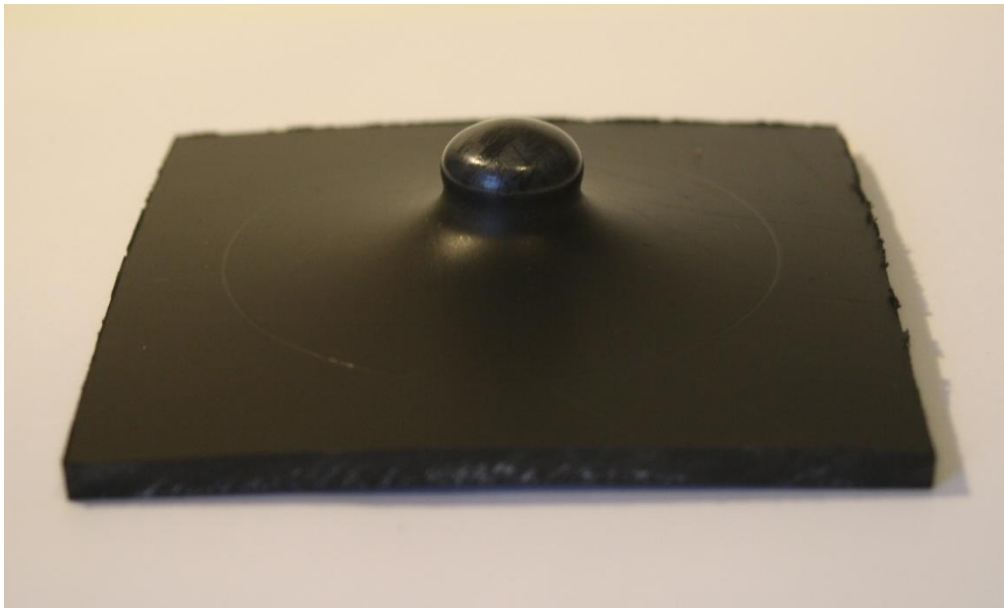
Drop tower test 5



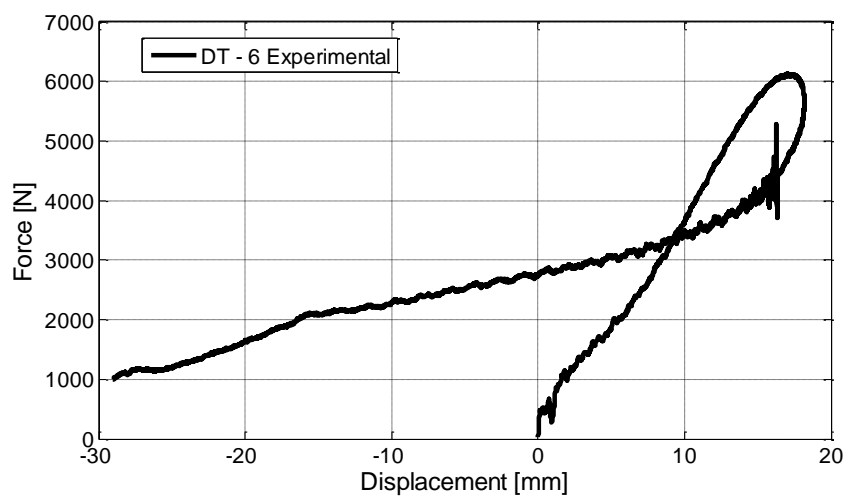
v [mm/s]	Mass [kg]	t_0 [mm]	Fall Height [m]	E_p [J]	F_{max} [N]	Δ_{max}
5400	10.045	4.90	1.5	150	6336	20.06



Drop tower test 6



v [mm/s]	Mass [kg]	t_0 [mm]	Fall Height [m]	E_p [J]	F_{max} [N]	Δ_{max}
4850	10.045	4.90	1.2	120	6114	18.17



Appendix B

Matlab script

This script finds the average strains in the necking area. The image is used to see where the largest strains can be obtained. The script is used for the tensile tests.

```
pic=elnmaxi085;
x=11;
y=60;
elnmaxi(1,1)=0;

for i = y-20:y+20
    n=1;
    for j = x-10:x+10
        elnmaxi_teller(n)=(pic(i,j));
        n=n+1;
    end
    ave_elnmaxi(i)=mean(elnmaxi_teller);
end

k = max(ave_elnmaxi)
```

This script is used to evaluate the strains, and gives the average strains in each picture taken during the testing as long as the mesh in 7D holds. The strains are given in a vector, and are applied to the tensile tests.

```
ant=112; % Number of pictures
y=57;
x=11;

elnmaxi(1)=0;
elnmini(1)=0;

for i=1:ant-1
    teller=1;
    for k=1:10
        (sprintf('elnmaxi%.3d(y,%d)',i,k))
        elnmaxi_skritt(teller)=(eval([sprintf('elnmaxi%.3d(y,%d)',i,(x-
10/2)+k)]));
        elnmini_skritt(teller)=(eval([sprintf('elnmini%.3d(y,%d)',i,(x-
10/2)+k)]));

        teller=teller+1;
    end
    elnmaxi(i+1)=mean(elnmaxi_skritt);
    elnmini(i+1)=mean(elnmini_skritt);
end
```

This script gives the height and the diameter of the compression specimens. The pictures are inverted to black and white pictures, white = 1, and black = 0. By summing up the values the diameter and the height is obtained.

```
% compression test
% HDPE-C1

ant_images = 50;
files = dir('HDPE-C1*');

for i = 1:1

image = imread(files(i).name);
  BW = im2bw(image,0.4);           % inverte the pictures in a
                                   % grayscale of 0.4
  V = 1-BW;
  imshow(BW);

row_first_nonzero = find(BW(:,1),1,'first'); % Gives the location of where
%                                           % the first value is.
row_last_nonzero = find(BW(:,1),1,'last');   % Gives the location of the
%                                           % where the last value is.

  row_diameter(i) = round(row_first_nonzero + (row_last_nonzero -
row_first_nonzero)/2); % Finner raden midt i teststykket

  col_first_nonzero = find(V(row_diameter(i),:),1,'first');
col_last_nonzero = find(V(row_diameter(i),:),1,'last');

  height_pixels(i) = row_last_nonzero - row_first_nonzero;
diameter_pixels(i) = col_last_nonzero - col_first_nonzero;

end

height_pixels = transpose(height_pixels);
diameter_pixels = transpose(diameter_pixels);

The diameter and the height are obtained in pixels.
```

This script gives the displacement of the first row in each matrix, and put them into a new matrix containing the first row of displacements for each picture taken during the plate with a hole test.

```
ant = 93;
dy(1)=0;
y = 1;
x = 1;

for i = 1:ant-1
    p = 1;
    for k = 1:113
        row(i,p) = eval(sprintf('dy%.3d(y,%d)',i,k));    % i = ant bilder,
    k = x verdi,
        p = p+1;
    end
    matrix(i,:) = row(i,:);
end

%All_first_rows = matrix();
```

This script gives the average strains in lateral face w2. Though the deformations were too large, and the strains were not possible to contract, this script was only used for test 1.

```
%% Plate with diameter 30 mm, test 01.
```

```
pic = dy112;

x = 26;
y = 50;
elnmaxi(1,1)=0;

for i = x-4:x+3
    n = 1;
    for j = y-6:y+5
        elnmaxi_teller(n)=pic(j,i);
        n = n+1;
    end
    ave_elnmaxi(i)= mean(elnmaxi_teller);
end
k = max(ave_elnmaxi)
```

This script is used to get the strains from the plate with a hole. Though this script was only used for test 1 as the strains were not possible to extract due to large deformations.

```
ant = 212;
y = 49;
x = 28;

elnmaxi(1) = 0;
elnmini(1) = 0;

for i = 1:ant
    n = 1;
    for k = 1:10
        elnmaxi_skritt(n) = eval(sprintf('elnmaxi%.3d((y-10/2)+k,%d)',i,k));
        elnmini_skritt(n) = eval(sprintf('elnmini%.3d((y-10/2)+k,%d)',i,x));
        n = n+1;
    end
    elnmaxi(i+1) = mean(elnmaxi_skritt);
    elnmini(i+1) = mean(elnmini_skritt);
end
```

```
longitudinal_strain = elnmaxi';
transverse_strain = elnmini';
This script gives diameter in x and y directions and both the lateral
faces.
```

```
% HDPE-01. Test av plate med stort hull.
clear all
clc
```

```
ant_images = 300;
files = dir('HDPE-01*');
```

```
for i = 1:ant_images

    image = imread(files(i).name);
    BW = im2bw(image,0.2);
    V = 1-BW;
    %    imshow(V)

    col_first_nonzero(i) = find(BW(463,:),1,'first');
    col_last_nonzero(i) = find(BW(463,:),1,'last');
    Plate_center = round(col_first_nonzero + (col_last_nonzero -
col_first_nonzero)/2);

    length_diameter_Y(i) = sum(V(463:end,1248));

    row_last_nonzero(i) = find(V(:,1248),1,'last');
    row_first_nonzero(i) = row_last_nonzero(i) - length_diameter_Y(i);
    mid_point(i) = round(row_first_nonzero(i) + (row_last_nonzero(i) -
row_first_nonzero(i))/2);
    length_diameter_X(i) = sum(V(mid_point(i),830:1650));

    length_side1(i) = sum(V(mid_point(i),1:830));
    length_side2(i) = sum(V(mid_point(i),1650:2448));
```

```

    Half_width_image(i) = length(V)/2;
    Length_b2(i) = Half_width_image(i) - length_side1(i) -
(length_diameter_X(i)/2);
    Length_b1(i) = Half_width_image(i) - length_side2(i) -
(length_diameter_X(i)/2);
end

```

```

Dx = transpose(length_diameter_X);
Dy = transpose(length_diameter_Y);
b1 = transpose(Length_b1);
b2 = transpose(Length_b2);

```

This script gives the thickness of the plate with a hole tests. The images is converted into black and white pictures, and the contrast gives the thickness of the specimens.

```

clear all
clc

```

```

ant_images = 300;
files = dir('HDPE-01*')

```

```

for i = 1:ant_images
    image = imread(files(i).name);
    BW = im2bw(image,0.2);
    V = 1-BW;

```

```

    col_first_nonzero(i) = find(V(1025,:),1,'first');
    col_last_nonzero(i) = find(V(1025,:),1,'last');

```

```

    thickness(i) = sum(V(1025,1134:1315));

```

```

end

```

```

t = transpose(thickness);

```